January 2018

Morphological And Genetic Analysis Of Embryo Specific Mutants In Maize

Dale Cletus Brunelle

MORPHOLOGICAL AND GENETIC ANALYSIS OF EMBRYO SPECIFIC
MUTANTS IN MAIZE

by

Dale Cletus Brunelle
Bachelor of Science, University of North Dakota, 2009
Master of Science, University of North Dakota, 2011

A Dissertation

Submitted to the Graduate Faculty

of the

University of North Dakota
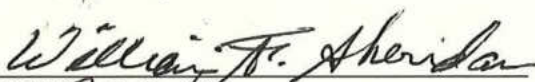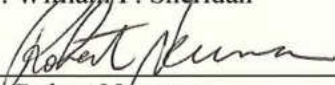
in partial fulfillment of the requirements

for the degree of

Doctor of Philosophy
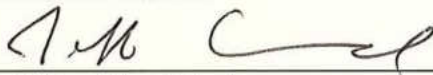
Grand Forks, North Dakota
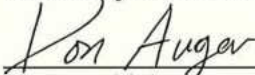
December
2018
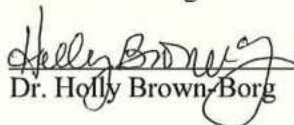
This dissertation, submitted by Dale C. Brunelle in partial fulfillment of the requirements for the Degree of Doctor of Philosophy from the University of North Dakota, has been read by the Faculty Advisory Committee underwhom the work has been done and is hereby approved.

_____
Dr. William F. Sheridan

_____
Dr. Robert Newman

_____
Dr. Jeffrey Carmichael

_____
Dr. Donald Auger

_____
Dr. Holly Brown-Borg

This dissertation is being submitted by the appointed advisory committee as having met all of the requirements of the School of Graduate Studies at the University of North Dakota and is hereby approved.

_____
Grant McGimpsey
Dean of the School of Graduate Studies

December 5, 2018
_____
Date

ii

PERMISSION

Title- Morphological and Genetic Analysis of Embryo Specific Mutants in Maize

Department Biology

Degree Doctor of Philosophy

In presenting this dissertation in partial fulfillment of the requirements for a graduate degree from the University of North Dakota, I agree that the library of this University shall make it freely available for inspection. I further agree that permission for extensive copying for scholarly purposes may be granted by the professor who supervised my dissertation work or, in his absence, by the Chairperson of the department or the dean of the School of Graduate Studies. It is understood that any copying or publication or other use of this dissertation or part thereof for financial gain shall not be allowed without my written permission. It is also understood that due recognition shall be given to me and to the University of North Dakota in any scholarly use which may be made of any material in my dissertation.

Dale C. Brunelle
December 06, 2018

TABLE OF CONTENTS

LIST OF TABLES

LIST OF FIGURES

ACKNOWLEDGMENTS

Dedicated to my mom, grandma and family

ABSTRACT

The maize zygote normally develops over approximately 45-days into a mature

embryo comprised of five or six leaf primordia and several root primordia. The

developing embryo passes through the proembryo, transition, coleoptilar and stage 1

(first leaf primordium) morphogenetic stages followed by the iterative formation of

additional leaf primordia during stages 2 through 6 according to Abbe and Stein (1954).

Using ethyl methanesulfonate (EMS) treatment of maize pollen from W22 inbreed we

have produced lethal *embryo specific* (*emb*) mutants that have no obvious effects on

endosperm development except for some reduction in kernel size in some cases. Thirteen

emb mutants were selected for further study. Ten mature kernels that exhibited the *emb*

phenotype were dissected for morphological analysis. Eight of the *embryo specific*

mutants had their development blocked at the transition to coleoptilar stage. One *embryo*

specific mutant had its development blocked from the proembryo stage to the coleoptilar

stage. Two *embryo specific* mutants were blocked from the coleoptilar stage to stage 1 or

later. Two *embryo specific* mutants were blocked from the coleoptilar stage to beyond

stage 1. Germination tests of 25 kernels samples containing mutant embryos revealed

that almost all had zero germination although some did germinate albino seedlings from

both normal and mutant kernels. The use of EMS resulted in 30 self-pollinated ears out

of 238 producing *emb* phenotype which is a frequency of 12.6%. The abundance of

EMS-induced mutations blocked early in embryo development suggest an abundance of

genes acting during this period to regulate the changing patterns of signaling molecules

that underlie the cellular changes occurring during the proembryo and coleoptile stages. In order to further understand embryo development, 10 fluorescent protein constructs were evaluated in normal developing embryos from the proembryo stage to stage 1. Additionally, 11 fluorescent protein constructs were crossed with the *emb* mutant lines to later evaluate how the mutations affect expression patterns as compared to the normal embryos. Two of the constructs involved with auxin transport, PIN1, and auxin inducible tissue expression, DR5, were more thoroughly evaluated. The work performed here is foundational to understanding the genes involved in embryogenesis and will aid in developing a systems biology for embryogenesis.

CHAPTER I

INTRODUCTION

Maize

Corn or maize (*Zea mays*) has recently become the most productive crop in the world producing more than 1 billion tons of crop in both 2013 and 2014 (Flint-Garcia, 2017). It is used as food for humans and livestock, as well as for non-edible commodities like plastic and ethanol. As the world population increases and climate change effects environmental conditions, the need for maize to be able to grow in harsh or new environments will also increase (Tigchelaara *et al.*2018). In this aspect, maize has a history of people selectively breeding it to grow in new environments since its domestication in what is now central Mexico. Early selective breeding from the Natives of North and South America allowed for maize to increase its range from what is now southern Canada to the southern Chile (Flint-Garcia, 2017; Ramirez-Cabral *et al.*, 2017). With the arrival of the Europeans, maize has again expanded its range to every continent, except Antarica (Ramirez-Cabral *et al.* 2017).

In addition, the first cultivators of maize are believed to have domesticated maize from teosinte although the two plants seem very different (Flint-Garcia, 2017). Morphologically teosinte is a plant with many lateral branches each ending with a tassel, while maize has one main stock that ends in a tassel, but no lateral branches (Doebley *et al.*, 1990). The ears of teosinte also differ remarkably from maize. Teosinte ears are

smaller, have two ranks of cupules, a single spikelet, hard outer glumes and are able to shatter which is to release its kernels. In contrast, maize has four or more ranks of cupules, paired spikelet, soft outer glooms, and they are unable to shatter therefore the kernels remain on the ear (Doebley, *et al.¸* 1990). These remarkable changes are thought to be the result of a difference in alleles in five master genes, which then affect up to 1000 other genes (Flint-Garcia, 2017).

In 2009 the maize genome was reported to be 2.3 gigabase containing around 32,000 genes in 10 chromosomes (Schnable *et al.*, 2009).   In order to further expand the range of growing conditions and environments in which maize can germinate and grow, it is imported to understand the function and identity of the genes. The genes involved in embryogenesis may aid in this goal, since during embryogenesis in maize the shoot apical meristem, root apical meristem, the scutellum and six leaf primordia (Randoph, 1936) are produce and form an embryo which is like a miniature plant. As of now the genes involved in embryogenesis are not well known and many of them will need to be discovered before a systems biological approach can be established for maize embryogenesis.

This research aims to produce *embryo specific* (*emb*) mutants using ethyl methanesulphonate in a W22 inbreed. These mutants are recessive embryo lethal, which have little or no effect on endosperm development (Clark and Sheridan, 1991). Germination test will be performed to determine germination and kernels will be scored to determine single gene mendelian inheritance. Each *embryo specific* mutant will have the extent of development to both characterize the phenotype generated by the mutation and to aid in identifying candidates for alleleism tests. Identification of alleles will also

aid in gene identification in future research. In addition, the *emb* which was generated in a W22 inbred will be crossed into the B73 inbred line for propagation and future analysis in gene identification. Finally, fluorescent protein constructs of 12 proteins involved in embryogenesis or meristem development will be evaluated in normal embryos to form a baseline set of expression patterns for embryogenesis. These 12 fluorescent protein constructs will also be crossed into the *emb* lines for future evaluation of the effect the mutation has on the expression pattern of each fluorescent protein construct.

Normal Kernel Development

Double Fertilization

Zea mays reproduces by double fertilization. The coat of the pollen grain contains and produces proteins that are required to penetrate the silk and produce the pollen tube (Vollbrecht and Evans, 2017). The pollen tube penetrates the silks and grows in one of two transmitting tracks of the silk, after which the two sperm cells exit the pollen grain and enter the pollen tube. Chemical signals guide the pollen tube growth toward the ovary, with the two sperm cells following behind the tip of the growing tube. (Vollbrecht and Evans, 2017). The pollen tube grows between cells in the micropyle and ruptures when it enters the embryo sac releasing the two sperm: one of the sperm fuses with the egg cell to form the embryo and the second sperm fuses with the two polar nuclei to form the primary endosperm nucleus (Kiesselbach, 1949).

Proembryo Stage

Embryo development begins with an asymmetric first cell division of the zygote between 28 to 40 hours after fertilization. The apical cell is smaller, and the basal cell is noticeably larger. This is the beginning of the proembryo stage. These cells go through further cell divisions, but the growth patterns and cell shape are irregular; only the orientation of smaller cells being apical to the larger basal cells is maintained (Figure 1-a). (Kiesselback, 1949; Randoph, 1936). The apical cells go through more cell divisions and become the embryo proper, while the basal cells become the suspensor and with each cell division both apical and basal cells are reduced in size. The proembryo stage typically proceeds to 8-10 days after pollination (DAP) and develops into a club like shape (Figure 1-b) (Randolph, 1936; Sheridan and Clark, 2017). In the late proembryo stage the peripheral cells of the embryo develop both anticlinal and periclinal walls allowing for both anticlinal and periclinal cell division. In contrast, the rest of the cells in the embryo are dividing randomly and are small isodiametric cells (Figure1-c). (Randolph, 1936; Vernoud, 2005; Sherdian and Clark, 2017).

Transition Stage

The beginning of the transition stage, 10-12 DAP, is marked by the anticlinal division of apical cells of the embryo proper advancing down the exterior of the embryo toward the suspensor producing an epidermal layer of cells, the protoderm (Randolph, 1936). Concurrently cells in the subapical area divide and produce cells with cell walls that are at right angles to the original embryonic axis. There is a shift from cells differentiating on a vertical axis as seen in the proembryo to cells differentiating on an oblique axis indicative of the mature embryo (Randolph, 1936). As the transition stage

continues to develop it is marked by the further differentiation of the cells at the anterior face of the embryo undergoing rapid division, eventually producing a lateral protuberance; These cells have a dense protoplasm and comprise a triangular section of meristematic cells that extend into the center of the embryo proper (Figure 1-d; Figure 2-trans) (Randolph, 1936; Abbe and Stein, 1954). As a result of the change from random division of cells to the development of the triangular meristematic cells extending to the anterior face of the embryo, the radial symmetry of the proembryo is changed into a bilateral symmetry of the transition stage which is through the midline sagittal plane of the embryo (Randolph, 1936; Vernoud, 2005). In the late transition stage, the meristematic cells which were triangular in shape change in polarity to an oblique orientation in reference to the embryo's longitudinal axis (Figure 1-e). The meristematic cells form a lateral structure which is the shoot-root axis of differentiation for subsequent stages of development (Randolph, 1936; Vernoud, 2005; Sherdian and Clark, 2017). While the shoot-root axis is developing, the embryo shows additional upward growth in the apical portion of the embryo, lateral growth in the embryo above the suspensor and enlargement along the posterior side of the embryo above the suspensor. The embryo morphologically changs from a club like shape to a distorted triangular shape indicative of the early coleoptilar stage (Randolph, 1936; Vernoud, 2005).

Coleoptilar Stage

The coleoptilar stage, 12-14 DAP, is marked by the meristematic cells dividing into an upper anterior portion and lower posterior portion. The upper anterior portion develops into the shoot apical meristem (SAM) and the coleoptile primordium. The coleoptile primordium forms on the face of the scutellum above the SAM and nearly

encircles it, which is then called the coleoptilar ring. The lower posterior portion of meristematic cells will become the coleorhiza and root apical meristem (RAM). The suspensor has an increase in growth becoming more prominent. Further growth of the apical and dorsal regions differentiates into the scutellum with lateral growth causing the scutellum to flatten out. Elongated cells, originating from between the SAM and RAM, extend to the scutellum and will become vascular tissue supplying the scutellum (Figure 1-f; Figure 2-col; Figure 3-a) (Randolph, 1936; Abbe and Stein, 1954; Vernoud, 2005; Sheridan and Clark, 2017).

Stage 1

The next six stages of development are named for the iterative formation of subsequent leaves; six leaves in total (Abbe and Stein, 1954). Figure 2 shows the sagittal view and the frontal view of development through the transition stage, coleoptilar stage, and Stages 1 through 6. Also, Figure 3 shows the coleoptilar stage and stages 1 through 4 in a transverse cross section through the SAM. Stage 1, about 14-18 DAP, is marked by the development of the first leaf primordium (Figure 2-1; Figure 3-b). It originates on the lower face of the SAM, opposite the coleoptile and diametrically opposite the scutellum. The first leaf primordium develops laterally to surround the back of the SAM and is encompassed by the coleoptile. The scutellum continues to enlarge as described earlier and has developed a scutellar groove in which the embryo protrudes slightly (Randolph, 1936; Abbe and Stein, 1954).

Stage 2

Stage 2, about 18-22 DAP, starts when the second leaf primordium develops on the face of the SAM opposite the first leaf primordium, encircles the SAM and is surrounded by both the first leaf primordium and the coleoptile (Figure 2-2; Figure 3-c). The coleoptile has almost completely surrounded the leaf primordia and SAM leaving only a small pore, termed the coleoptilar stage pore which is visible on the anterior face of the embryo. The scutellum has enlarged further but has rounded out to be more ovate when viewing the anterior. The embryo proper when viewed from the anterior is an elongated structure that extends from the suspensor to the center of the scutellum and is situated in the scutellar groove. The suspensor stops growing and Randolph states that it "persists apparently as a nonfunctional and unimportant part of the maturing embryo" (Abbe and Stein, 1954; Randolph, 1936).

Stage 3

Stage 3, 22-28 DAP, the first two leaves continue to grow, and the third leaf primordium forms opposite the second leaf primordium increasing the size of the embryo proper (Figure 2-Stage 3; Figure 3-d). Three distinct regions can be seen on the anterior face of the embryo proper and is even more evident in sagittal sections. The coleoptile is a nearly cylindrical structure at the top of the embryo proper and at its lower region there is a coleoptilar node. Below the coleoptilar node is the scutellar node, which is a flatter structure and is directly connected to the scutellum. The coleorhiza, a nearly cylindrical structure, is directly below the scutellar node and in cross section the RAM is clearly recognizable. In the frontal view, the edge of the scuteller groove borders the embryonic axis (Abbe and Stein, 1954).

Stage 4

Stage 4, 28-37 DAP, is marked by the development of the fourth leaf primordium, with the embryo proper extending closer to the top of the scutellum (Figure 2-4; Figure 3-e). The scutellum appears elliptical to ovate in shape as viewed anteriorly and the edges of the scutellar groove have encroached onto the embryo proper from both sides near the scutellar node region. Both the coleoptile and coleorhiza are flatter on the anterior face. The mesocotyl is now visible between the coleoptilar node and the scutellar node.

Stage 5 and Stage 6

Stage five (37-50 DAP), and stage six, (beyond 51 DAP) develop their additional leaf primordia and slightly increase in size, but no new structures develop. However, the edge of the scutellar groove has further encroached onto he embryonic axis but does not cover the very top portion and the very bottom portion. (Figure 2-5 and 2-6) (Abbe and Stein, 1954).

Defective Kernel Research

Early Defective Maize Kernel Research

Defective maize kernels have been reported by investigators since the first years of maize research. D.G. Jones (1920) reported on defective maize kernels he observed which he termed defective seeds. Three years later M.Demeric (1923) reported on defective maize kernels which he termed germless seeds. P.C. Manglesdorf (1923)

reported on defective maize kernels, which he believed were the same type as reported by D.G. Jones and referred to them as defective seeds.

In 1926, Manglesdorf also assembled a more comprehensive report in which he stated that many scientists have reported seeds with defects since the Jones report and mentioned that each report used a different term to describe these defective seed (Mangelsdorf, 1926). The mutations that he was reporting on appeared in a variety of inbred lines. One line produced four defective kernel phenotypes. The first two occurred after 13 generations of inbreeding in two sister strains and then again four generations later, from a third sister strain, two more defective kernel mutants appeared. These observations lead Mangelsdorf to conclude that "germinal changes do occur" in maize as has been reported in *Drosophila* (Mangelsdorf, 1926). The report focused on 14 defective seed mutants whose phenotypes segregated as a ratio of 3 normal:1 mutant; indicating a single gene recessive genotype. These mutants were designated "*de*" with a subscript number 1-14; the higher numbers showing a more severe defective phenotype. His discussion noted that the pericarp and nucellus didn't show any developmental problems, which is due to its maternal origins. Both endosperm and starch grain formation showed a decreased mass and slowed formation in those seeds with a more severe defective phenotype (de_{14}) than those of the less severe defective phenotypes (de_1). The aleurone layer only formed in the defective seed mutants ranging from de_1 to de_{10}, but not those ranging from de$_{11}$ to de_{15}. Embryo development was correlated with the endosperm development. The more severely defective seeds (de_{14}) showed hardly any embryo development, while those less severe defective seeds (de_1) showed development of the coleoptile, scutellum, and primordial leaf formations, but also abnormal growth.

The one exception being *de₄*, which didn't have an embryo and Mangelsdorf considered it akin to Demerec's "germless" seeds (Demeric, 1923; Mangelsdorf, 1926). In one experiment to determine the rate of growth and overall seed weight of the defective seeds compared to normal seeds, Mangelsdorf crossed the defective seed inbred lines with a different "unrelated stock". Mangelsdorf noted that morphology of some of the defective seeds was changed and in one case, *de₂*, to such a degree as to be unrecognizable. In Mangelsdorf's report the defective seed mutants included those that didn't germinate and those that did germinate, it wouldn't be Neuffer and Sheridan (1980), and Sheridan and Neuffer (1980) that the defective seed phenotypes would be categorized more specifically.

The First Large Screening for Defective Kernel Mutants

The reports of Neuffer and Sheridan were centered around what they termed "defective kernel" mutants which they stated were the same type as those reported by Jones (1920) and Mangelsdorf (1923,1926). Defective kernel mutant is a more generalized term that includes kernels whose embryo and endosperm are affected. Both dominant (eight kernels) and recessive (855 kernels) kernel mutants were found in their mutant populations, but they reported on the recessive kernel mutants in these reports (Neuffer and Sheridan,1980). The defective kernel mutants are then divided into 4 types:

- Type 1-both endosperm and embryo are affected, and embryo is not viable: 646 mutants

- Type 2- both endosperm and embryo are affected, but embryo is viable which produces a seedling with a mutant phenotype. Most of these died as

seedlings and included phenotypes of white, yellow and yellow-green

plants among other types. A few gree to maturity: 59 mutants

- Type 3- the endosperm is only affected and therefor produces a normal

  seedling. Many of these were allelic to known mutants: 147 mutants

- Type 4- the embryo is only affected and expressed as germless kernels.

  These kernels were mostly found in the progeny of some of the 855

  receive mutants which had already been classified as type 1, 2 or 3; with

  only three found in the original 855.

The defective kernel mutants were generated by treating pollen with ethyl

methanesulfonate (EMS) and applying the pollen to the silks of normal ears. The

subsequent kernels were planted and both the 3461 plants and 3172 selfed ears that were

produced were screened for heritable changes. Recessive kernel mutants accounted for

855 of 2457 recessive mutants found on the selfed ears. All mutants were labeled with the

capital letter "E" followed by a number, starting with 1. Any additional mutants that

appeared in subsequent generations were labeled with the addition of a letter "A", "B",

and so forth (Neuffer and Sheridan, 1980).

A chromosome mapping experiment was performed for 396 kernel mutants using

18 B-A translocations, all except 7S and 8S, which allowed for coverage of 85% of the

genome. They were able to find the chromosome location for 165 mutants, which were

located on all arms except 6S (Neuffer and Sheridan, 1980). These results indicated that

genes for defective kernel mutants are scattered throughout the genome.

A subset of 19 mutants were then evaluated for endosperm-embryo interactions,

using materials which contained both the B-A translocation and the defective kernel

mutants. Three types of kernels were produced by selfing the plants: hypoploid mutant embryo/hyperploid nonmutant endosperm; hyperploid nonmutant embryos/hypoploid mutant endosperm; and normal embryo/ normal endosperm. They determined that those kernels with mutant endosperm and nonmutant embryos produced normal seedlings except for two cases; *E1122a* and *E1315A*. This indicated that for most of these cases the mutant endosperm does not affect the nonmutant embryo. The nonmutant embryo did affect the mutant endosperm in 10 cases: 3 nonmutant embryos helped the mutant endosperm; and 7 depleted the mutant endosperm. In those cases with a mutant embryo and normal endosperm, 14 of the 19 indicated that the normal endosperm did not help the mutant embryo. The remaining 5 helped the embryo develop a visually normal phenotype, although the subsequent growth was only normal in two mutants, one of which developed normal in the concordant mutant (Neuffer and Sheridan, 1980).

Information including kernel phenotype, viability or seedling phenotype, and chromosome arm location was reported for 196 kernel mutants, which included two proline-1 mutants (Neuffer and Sheridan, 1980). In Sheridan and Neuffer (1980), 150 of those mutants which had "easily distinguishable defective endosperms, displayed segregation patterns on mature ears, and had nonviable embryos or lethal seedling phenotypes in their original genetic background." were further studied in morphological and embryo culture experiments.

The morphological analysis included *timing of mutant expression*, *phenotype of the immature kernel mutants*, *phenotype of immature mutant embryos*, and *developmental stage of immature mutant embryos*. As with Mangeldorf's observations, the mutant kernels lagged behind in development compared to the normal kernels. It was noted that

embryo development was further behind than endosperm development. The data presented was relative to the endosperm development and showed that as early as 11 days after pollination (DAP) some mutants were noticeably behind in development; by 17 DAP all but 127 of the 150 embryos showed developmental retardation.   These mutants showing an earlier delay in development had common phenotypic appearance and were described as "being smaller, lighter colored and more translucent in appearance" than normal kernels of the same ear. The later developing kernel were closer to normal kernels in phenotype and consisted of two general types: A collapsed mature kernel phenotype that had a swollen appearance but lacked a solid endosperm; and kernels whose endosperm were smaller, but solid and appeared either colorless or pigmented (Sheridan and Neuffer, 1980). The immature embryos were analyzed by comparing normal embryo weight to mutant embryo weight which resulted in an average mutant embryo weight of 27% of normal embryos.   Also, most of the mutant embryos were less than 2/3 the size of the normal embryos.

The development stage reached by 106 of the immature mutant embryos was presented and evaluated using Abbe and Stein's standard (Abbe and Stein, 1954; Sheridan and Neuffer, 1980). The results had 13 in early proembryo stage or unknown, three transition stage, four coleoptilar stage, 27 Stage 1, 30 Stage 2, 26 Stage 3, and three Stage 4 or later. Additional histological studies confirmed that 20 of the mutant embryos were either blocked in development before stage 1 or degenerated. The other 130 mutant embryos developed to stage 1 and later. Even though these mutants develop to stage1 and later, most of the mutant kernels are lethal. This prompted additional research in which 102 of the mutants that developed to stage1 were cultured to determine if they are

autotrophs and could be rescued (Sheridan and Neuffer, 1980). The embryos from these mutants were grown on either basal medium, enriched medium, basal medium lacking ammonium nitrate or enriched medium lacking ammonium nitrate. The basal medium was made using 4% sucrose, .08% agar and mineral salts of Murashige and Skoog (1962) which included ammonium nitrate. The enriched medium was made by adding 20 amino acids, eight vitamins, and six nucleic acid bases to the basal meduium. Twenty-one of the mutants showed little to no growth on any medium. The remaining kernels grew into small plants less than 5cm tall or larger plants greater than 5cm with 60% of the 102 kernel mutants producing plants over 5cm. Since many of these mutants are lethal under normal growing conditions, it was stated that loss of viability must happen during the later stages of development (Sheridan and Neuffer, 1980). In evaluating the response of each mutant growing in different media, there were four general results: 1) those plants that grew better on enriched medium compared to basal medium; 2) those plants that grew significantly better in basal medium, compared to enriched medium, must be sensitive to the additives that inhibited growth; 3)those plants that grew better in basal medium and enriched medium which were free of ammonium nitrate, therefore must be sensitive to the ammonium nitrate; 4) and those that grew best only on basal medium with no ammonium nitrate; which they believed must need a significant lower amount of nitrate to keep from becoming toxic (Sheridan and Neuffer,1980).

These results indicated that ten of the defective kernel mutants could possibly be auxotrophs. Nine grew best on enriched medium with ammonium nitrate and one on enriched medium with no ammonium nitrate. One of these ten, E1121, was discovered to be allelic to a proline-requiring mutant *pro-1*(Sheridan and Neuffer, 1980).

The developmental profiles of the defective kernel mutants were further elucidated in several follow up papers (Clark and Sheridan, 1986; Sheridan and Thornstenson, 1986; Clark and Sheridan, 1988).   The embryo mutants *E1113A* and *E1428* were designated *dek22* and *dek23,* respectively. Each of these defective kernel mutants were examined at 4, 8, 10, 12, 16, 25, and 37 DAP; and at maturity by sectioning the kernels into 15 micron thick sections. Development was blocked at transition stage for *dek22* and at an abnormal coleoptilar stage for *dek23*. It was reported that the mutants lagged behind normal kernel development with embryo development exhibiting a more prominent lag than endosperm development. It was observed that the embryo is retarded in growth as early as 8 DAP for *dek22* and 12DAP for *dek23*. The *dek22* mutant develop to the transition stage by 16DAP and remains there with further development limited to the enlargement of cells and vacuolization. The *dek23* mutant develops to an abnormal coleoptilar stage at 12DAP although there is no shoot apical meristem or coleoptilar ring; but both the scutellum and root apical meristem continue to proliferate up to maturity. Necrosis of at the site of the SAM is also observed in *dek23* at 12DAP and "spread, more or less, throughout the embryo" (Clark and Sheridan, 1986).   The endosperm of *dek22* is severely collapsed in contrast to *dek23*, which maintained an abundant endosperm with a collapsed crown.

 In experiments using kernels with mutant embryos for either *dek22* or *dek23* with genetically normal endosperms, termed nonconcordant, both *dek22* and *dek23* embryos of nonconcordant kernel displayed identical morphology to that of the concordant *dek22* and *dek23* embryos. This indicated that both mutated genes were not dependent on any

interaction with the endosperm to produce the mutant embryo phenotype (Clark and Sheridan, 1986).

Additional research with the embryo lethal mutants *bno*-747B, ptd*-1130,* cp*-1418, and *rgh*-1210*, which fail to produce leaf primordia, and *fl*-1253B*, which does produce leaf primordia (Sheridan and Thornstenson, 1986; Clark and Sheridan, 1988) supported and expanded the information obtained from the studies of *dek22* and *dek23*. All of these mutations affect both the embryo and endosperm, with the embryo retarded in development earlier than the endosperm. Development is blocked in transition stage for *ptd*-1130,* cp*-1418, *rgh*-1210*, while *bno*-747B* is blocked during coleoptilar stage and *fl*-1253B* is variably blocked from coleoptilar stage to stage 2. Similar to *dek22* cells enlarge and vacuolize in *ptd*-1130,* bno*-747B, and *rgh*-1210* as the kernels mature, however *cp*-1418* and *fl*-1253B* show no abnormal cell enlargement like *dek23*. Necrosis was observed in *ptd*-1130*, *rgh*-1210*, and *fl*-1253B* which was also seen in *dek23*. In contrast to *dek22* and *dek23*, irregular cell growth in both the aleurone and embryo is seen in *rgh*-1210*, *fl*-1253B*, *ptd*-1130*, and *bno*-747B* (Sheridan and Thornstenson, 1986; Clark and Sheridan, 1988).

The Second Large Screening for Defective Kernel Mutants

Identification of more *dek* mutants was reported by Scanlon *et al*. (1994) isolating 63 mutations from a *Mutator* stock that was produced by 1978 (Robertson, 1978). They observed many different phenotypes, but specifically mentioned two types which were more common than most: those with reduced endosperm size (ren) and those with an empty pericarp (emp). The ren mutants almost always contained a small embryo, but the emp mutants usually didn't contain an embryo (Scanlon *et al.,* 1994). As with previous

studies, chromosome arm location was performed with B-A translocations, but also with

the *waxy*-marked translocations or by allelism testing with other mapped mutants with

similar phenotypes. A total of 53 of the 63 mutants were mapped to 15 out of the 20

chromosome arms.

The allelism tests also included testing those mutants that were mapped to the

same chromosome arm with each other and with previously identified *dek* mutants that

were mapped to the same arm. Alleles for already known mutants were found, along with

alleles for new *dek* loci within the 63 mutations; 20 mutations with two or more alleles in

all (Scanlon *et al.,* 1994). Alleles of several mutations showed phenotypic variations.

The alleles for the gene *brn1* designated *brn1-R* and *brn1-307* displayed both variation in

kernel phenotype and germination. The alleles for *dek25* designated *dek25-R*, *dek-1566*

are homozygous lethal, but *dek25-2410* displayed 10% germination which were seedling

lethal. All three alleles for *dek25* showed the same kernel phenotype. The alleles for

dek5 showed differences in inheritance and alleles for *su1* displayed more wrinkling and

translucence in the kernel (Scanlon *et al.,* 1994).

Current Defective Kernel Mutant Gene Identification

The generation of *dek* mutants from EMS, and *Mutator*-transposons discussed

above along with other studies produced materials to further understand *dek* mutants.

Finding the gene's location was greatly helped by the use of the *Mutator* stocks, since the

DNA sequence of these transposons is known and genes that have been found are

exclusively from these types of stocks. A majority of the reports presented below on dek

mutants indicate that most of the *dek* mutants examined are in nuclear genes which code

for proteins that are similar in function and are involved with the mitochondria, and possibly plastids.

The *dek1* mutant, which is active in aleurone development and embryonic axial pattern formation, was found to code for 2,159 amino acid (a.a.) protein (Becraft, 2002; Lid, 2002). The protein contains an extracellular loop, 21 transmembrane regions and a cysteine proteinase domain that shares high homology with domain II and domain III of m-calpain. The calpain superfamily is found mainly in animals and *dek1* is the only known calpain gene in plants. These genes are cytosolic enzymes, which are activated by Ca^{2+} and are part of signal transduction pathways (Lid, 2002).

The mutant *emp6* affects the basal endosperm transfer layer and arrests embryo development at late transition to early coleoptilar stage (Chettoor *et al.*, 2015). The gene codes for 408 amino acids. that is a putative plant organelle RNA recognition (PORR) protein that is targeted to the mitochondria. The PORR proteins bind to organellar RNA and function in regulation or processing (Chettoor *et al.*, 2015).

The pentatricopeptide repeat (PPR) family is highly represented in *dek* mutants. It is one of the largest families of proteins in plants and is characterized by multiple repeats of a degenerate 35-amino acid motif with hydrophobic and hydrophilic residues (Small and Peeters, 2000; Hottori *et al*., 2004). These proteins are involved in regulation of posttranscriptional processes in organelles (Lurin et al., 2004). Each of the PPR proteins which were identified because of *dek* mutants and briefly described in the following paragraph are targeted to the mitochondria and abolish the C to U editing at specific sites of the target RNA transcripts (Guitierrea-Marcos *et al.*, 2007; Liu *et al.*,

2013; Li *et al.*, 2014; Sun *et al.*, 2015; Xiu *et al.*, 2016; Qi *et al.*, 2017; Chen *et al.*, 2017; Yang *et al.*, 2017).

One of the first described is *empty pericarp4* which was localized to the mitochondria. It appears to regulate a subset of mitochondria genes, since microarray and RNA gel blots reveal low transcript levels compared to wildtype (Guitierrea-Marcos *et al.*, 2007). The *dek* mutant *emp5*, which is blocked in development in the transition stage, encodes for a protein that edits mitochondrial gene transcripts at10 sites in four genes: *nad9*(complex I), *cox3*(complex IV), *rpl16* and *rps12*(both ribosomal proteins) (Liu *et al.*, 2013). A *dek* mutant *small kernel 1*, which is blocked in development from the coleoptilar stage to Stage 1, encodes a protein that edits the *nad7* RNA, which is a subunit of NADH dehydrogenase complex I in mitochondria (Li *et al.*, 2014). Another mutant *emp7*, blocked in development in the transition stage, fails to edit the *ccmF$_N$* transcript which encodes for a subunit of cytochrome c synthetase in the mitochondria. This results in defects in the assembly of complex III (Sun *et al.*, 2015). The *emp16* mutants are blocked at the transition stage and fail in *cis*-splicing the mitochondrial *nad2* intron 4. This results in an inability of complex I to assemble (Xiu *et al.*, 2016). The *dek2* mutant results in a reduced splicing efficiency of *nad1* intron 1; this results in a "functional reduction of complex I" (Qi *et al.*, 2017). The *dek35* mutant affects the splicing of RNA for *nad4*, which is a subunit in complex I NADH dehydrogenase. Additionally, NAD7 was also decreased in *dek35* mutant embryos (Chen *et al.*, 2017). The defective kernel mutant, *emp9*, affects the RNA editing of *ccmB-43* which is a "component of the ATP-binding cassette transporter and essential for cytochrome *c* maturation." (Yang *et al.*, 2017). The 30S ribosomal subunit is also affected since *rps4-*

335 is not properly spliced in *emp9* mutants. Therefore, *emp9* mutants show a disruption in complex III, along with lesser effects on complex I and V (Yang *et al.*, 2017).

Embryo Specific Mutants

First Screening for Embryo Specific Mutants

A group of mutations effecting maize kernels in which the endosperm is normal, but the embryo is stopped in development is named *embryo-specific* mutants (*emb).* Since these mutations only effect the embryo, they are in genes that may be essential for embryogenesis (Clark and Sheridan, 1991). The first major study to examine *emb* mutations reported on 51 mutants which were found in the Robertson's *Mutator* stock (Clark and Sheridan, 1991; Sheridan and Clark, 1993).

The 51 *emb* mutants were tested for segregation ratios, lethality, chromosome arm location, and developmental profiles. The segregation ratios were reported to range from 19% to 29% for 37 of the mutants, which are not significantly different from the expected 3:1 ratio for one gene mendelian inheritance. The other 12 showed significantly lower segregation ratios with reductions ranging from 10% to 18%; two *emb*s were not tested. The use of B-A translocations stocks uncovered the chromosome arm location for 25 out of the 45 *emb*s tested, however the B-A translocation stocks only represented 40% of the genome (Clark and Sheridan, 1991). The lethality of the *emb*s was determined through germination tests, between 25 to 100 kernel mutants for each mutant, which resulted in just seven of the mutants able to germinate at high enough frequency to not be considered embryonic lethal (Clark and Sheridan, 1991; Sheridan and Clark, 1993). The

development profiles of all 51 *emb* mutants were categorized into three groups based on major developmental events previously discussed: proembryo-transition, 11 mutants; late transition-stage 1, 29 mutants; and stage 2-stage 6, 10 mutants (Clark and Sheridan, 1991; Sheridan and Clark, 1993).

Clark and Sheridan concluded that the *emb* phenotype can be produced by many loci. This is because the mutation frequency was relatively high with a mutation rate of 51 out of 1000 gametes tested. The B-A chromosome tests indicate that the loci are throughout the genome. The variety of the mutants being blocked at stages from proembryo to Stage 6 point to a large group of genes associated with the *emb* phenotype. Clark and Sheridan also concluded that the *emb* loci are essential for embryo development because the *emb*s were arrested in development before maturity and because of the *emb*s failure to germinate (Clark and Sheridan, 1991; Sheridan and Clark, 1993).

Clark and Sheridan reported that the *emb* loci are fundamentally involved in morphogenesis. The 51 *emb* mutants displayed a variety of morphology, which indicate a range of developmental events. Those 10 *emb* mutants blocked in the pro-embryo to transition stage are likely involved in pattern formations affecting the "setting a part of the embryo proper and suspensor" and seven of 10 *emb* mutants failed to develop an embryo proper or were necrotic. These mutations may be in genes responsible for the change to asymmetric cell division of the proembryo at either: the first transverse cell division of the zygote; or the cell divisions which produce the embryo proper and suspensor (Sheridan and Clark, 1993). The 28 *emb* mutants blocked at the late transition to stage 1 may be involved in embryonic axis formation. Three of the mutants had the SAM or the coleoptile appear in a different location. Eleven of them blocked SAM

formation, but still produced a scutellum (Sheridan and Clark, 1993). The 13 *emb* mutant

embryos classified as being in the stage 2 to stage 6 group developed an embryonic axis.

However, there was a variety of phenotypes of embryonic axis and scutellum formation

(Sheridan and Clark, 1993).

Although these mutations were categorized into three developmental groups, the

data presented indicate a more complex situation. Among the three developmental

groups studied, 15 *emb* mutations had individual embryos with earlier or later stage of

development than their group classification and only 14 out of the 51 *emb* mutations were

blocked at a single stage of development as described by Abbe and Stein (1954).   Also,

scutellum formation was affected by many of the mutations in all stages of development

with misshapen scutellum or abnormal cell proliferations, and two even displayed a

reduced scutellum size. There were two mutations affecting the coleoptile: one in an

abnormal location and the other it's elongation (Clark and Sheridan, 1991; Sheridan and

Clark, 1993).

Reports for Select Defective Kernel Mutants

In order to better understand the *emb* mutants a further study was undertaken to

better classify five out of the 51 *emb* mutants: *emb-8516*, *emb-8522*, *emb-8535, emb-

8543*, and *emb-8547* (Heckel *et al.*, 1999).   Each of these mutants are blocked in

development before the coleoptilar stage and may be in genes involved with pattern

formation of the embryo. All five *emb* mutants were tested and found to be non-allelic

through a combination of complementation tests and B-A chromosome tests.

Developmental profiles were taken at 9DAP and 16DAP as opposed to at maturity, as

reported earlier. The development profiles were performed on 20 kernels from five sister

plants for each mutant and they reported that the phenotype was homogenous between kernels from the same ear and between sister plants (Heckel *et al.*, 1999).

The two mutants, *emb-8543* and *emb8547*, resemble wild-type embryos which have stopped in development at the pro-embryo stage for both 9 DAP and 16 DAP, in contrast to transition stage at maturity (Clark and Sheridan, 1991; Heckel *et al.*, 1999). However, it was noted that *emb-8547* may be a different mutation, since the phenotype is slightly different from those reported by Clark and Sheridan (1991). Also, the B-A chromosome tests for chromosome arm location give different results, 4L in the 1991 report and 6L in the 1999 report.

The mutants *emb-8522*, *emb-8535*, and *emb-8516* displayed abnormal development which didn't resemble development of normal embryos. It was reported that at maturity *emb-8522* was blocked at mid-transition stage, emb-*8535* was blocked from late proembryo to early coleoptilar stage, and *emb-8516* was blocked at proembryo to early transition stage (Clark and Sheridan, 1991; Sheridan and Clark, 1993). Cytological sections revealed that both *emb-8522* and *emb-8535* cells showed no differentiation into an embryo proper and suspensor, but rather resembled a tubular structure (Heckel *et al.*, 1999). The cells were large and didn't resemble either cells of the embryo proper or suspensor, implying that neither cell type is a default in development. These *emb* mutations may be in genes which are involved in the formation of the embryo proper and suspensor. The *emb-8516* was initially described as being blocked at proembryo to early transition stage with occurrences of necrosis in the embryo proper at maturity (Sheridan and Clark, 1993). At 9DAP and 16 DAP it was observed that two

embryo-like structures were developing from the suspensor. This may indicate that this gene is involved in suspensor identity (Heckel *et al.*, 1999).

Four of the 51 *emb* mutants were phenotypically analyzed using confocal microscopy: *emb-8518*, *emb-8521*, *emb-8537*, and *emb-8542*. Additionally, three fluorescent protein expression patterns were analyzed in these mutants: *Lipid transfer protein* 2(*LTP2*), *Zea mays Outer Cell layer* 1(*ZmOCL1*), and *Knotted* 1(*Kn1*). *LTP2* is a protoderm marker, *ZmOCL1* is a epidermal marker, and *Kn1* is a SAM marker (Elster *al*., 2000). Two of the mutants arrested development in the proembryo to transition stage, *emb-8521* and *emb-8518.* This is evident by the lack of expression of *Kn1* in either of the *emb*s. In *emb-8521* development stopped in the pro-embryo stage and cell growth has restricted to apical-basal division. The protodermal layer was not fully established and *LPT2* expression was present in some cells, which looked morphologically like protoderm cells. Additionally, large cells protruded into the protodermal layer. (Elster *al*., 2000) In *emb-8518* expression of *LPT2* is seen in all cells of the protoderm layer and no protrusions of large cells into the layer is present. This indicates that *emb-8518* is further along in development than *emb-8521.* Expression of *ZmOCL1* is normally seen in all cells of the embryo proper in early embryo development and becomes restricted to the L1 layer during the transition stage. In both *emb-8521* and *emb-8518*, the *ZmOCL1* expression is present throughout the embryo proper. These results indicated that radial patterning may be dependent on two steps; the first involving expression of *LTP2* in the protoderm and the second involving *ZmOCL1* expression being lost in the embryo proper cells except the protoderm layer (Elster *al*., 2000).

The other two mutants, *emb-8537* and *emb-8542*, developed to the coleoptilar stage or later. They both showed a restriction of expression for *ZmOCL1* to the protoderm layer that continued as the transition stage embryo transitioned into the coleoptilar stage. During this transition, radial symmetry changes to a bilateral symmetry (Elster *al*., 2000). Both *emb*s also show expression for *Kn1* at the correct position in the embryo, but the cells have "lost some meristematic character" (Elster *et al.*, 2000). Since these mutants also fail to germinate, it is evident that the SAM is not fully developed in these mutants (Elster *et al.*, 2000). In reference to *emb-8537* it was shown that if a SAM develops, true leaves can develop absent of a coleoptile, indicating that coleoptilar stage development may be separate from SAM development. Additionally, in *emb-8537 LTP2* is expressed in the coleoptile and scutellum outer layer, but not the L1 layer of the SAM and leaf primordia which may indicate that the coleoptile is an appendix of the scutellum (Elster *et al.*, 2000).

Another study analyzed four *emb* mutants of which two were found to be allelic and all of them were blocked at late proembryo stage or transition stage. The allelic pair *emb*-7191 and *emb* 7917 were renamed *emb-7919-1* and *emb-7919-*2, respectively; and only one allele was used in each of the follow up experiments. All of the *emb*s failed to form a embryonic axis or scutellum, and had a radial symmetry (Consonni *et al.*, 2003). The *embs* were observed to have abnormal cell growth at 15-19 DAP, which lead to the disappearance of an identifiable suspensor with continued uncontrolled cell growth by 32 DAP. The proliferation of cells in the suspensor was examined by use of the TUNEL method which identify cell undergone programmed cell death (PCD) (Giuliani *et al.*, 2002). Normal developing embryos, at 14 DAP, have cells in "the scutellum surrounding

the shoot primordium and in the coleoptile" undergoing PCD; the cells in the suspensor at

14DAP also were positive for undergoing PCD. No PCD was detected in the *emb* seeds

at 14 DAP in either the embryo proper or suspensor (Consonni *et al.*, 2003). These

results lead Conosoni *et al* to state that if PCD is involved in the morphology of tissues

and organs, that there might be a mechanism for PCD to not be initiated in the three *emb*

mutants represented by: *emb-7182; emb-7192;* and *emb-7191-1*(or its allele *emb-7191-2*).

This would explain why there is uncontrolled cell growth and why there were no cells

undergoing PCD (Consonni *et al.*, 2003).

Consonii *et al* also performed some embryo rescue experiments. Between 12 to

18 DAP embryos from *emb-7191-1*, *emb-7182*, and *emb-7192* were collected and

cultured on basic MS medium for 15 days. Growth and development were retarded for

each of the mutants, but each was able to yield individuals which were able to grow to

seedlings. In *emb-7191-1* and *emb-7182* the seedlings were albino. The seedlings of

emb-7192 were able to be rescued and germinated normally (Consonii *et al.*, 2003).

These results lead the researchers to speculate albino seedling are the result of either: a

SAM that is unable to produce a " functional photosynthetic apparatus"; or the SAM was

formed through organogenesis from cell have lost the "competence to differentiate

functional chloroplasts" (Consonii *et al.*, 2003).

Current Embryo Specific Mutant Gene Identification

Multiple studies have identified that the genes, which when mutated produce the

emb phenotype, are involved with plastids. An embryo specific mutant called *lethal*

embryo 1(*lem1*) which aborts before transition stage is in a gene that encodes for the

plastid 30S ribosomal protein S9. It was found to have a nuclear localizing signal (NLS) domain, which had not been previously reported (Ma and Dooner, 2004). A second mutant originally reported in the 51 *emb*s of Clark and Sheridan (1991) and identified as *emb-8516* was located to the gene *ZmPRPL35-1* by its *Mutator* transposon. It likely encodes for a L35 protein that is part of the 50S ribosome in plastids (Magnard *et al.*, 2004). The mutant *emb-8522* was the first pentatricopeptide repeat (PPR)gene associated with a maize embryo-lethal phenotype. Both chloroplast development and vegetative growth are effected by *emb-8522*. It was demonstrated that the phenotype of this *emb* is dependent on the genetic background; in the R-scm2 and A188 background the *emb* is lethal, however in the B73 background the 80% of ears segregating for the mutants gave "rise to albino seedlings" (Sosso *et al.*, 2012). In another study involving *emb* mutants, it was discovered that *emb16* is an allele of the *WHIRLY1* (*WHY1*) gene. Two previously found mutants of *WHY1* gene resulted in albino seedling, as opposed to *emb16* causing embryo development to stop at the transition stage (Zhang *et al.*, 2013). They found that the genetic background effected the phenotype expressed by *emb16*. The *WHY1* gene is involved in chloroplast biogenesis and may be required for thylakoid membrane formation (Zhang *et al.*, 2013). The *emb12* mutation has been found to be in a gene that encodes the plastid initiation factor 3. However, it also negatively affects the expression of rRNAs and ribosome assembly in plastids (Shen *et al.*, 2013). The *emb14* mutation affects a gene whose product is targeted to the plastids. The gene encodes for a cGTPase and is functionally equivalent to the Arabidopsis gene *AtNOA1* and shares similarities with *YqeH* in prokaryotes. *YqeH* is important in 30S ribosomal subunit maturation and binds to "30S in a GTP/GDP dependent manner".

Fluorescent Protein Fusion Constructs.

Fluorescent Protein Tagging

The high-throughput technique termed fluorescent tagging of full-length proteins (FTFLP) was developed in *A. thaliana* to analyze the expression patterns and subcellular location of proteins (Tain *et al.*, 2004).   Previous techniques used to examine expression in cells and tissues involved antibodies, a reporter or an antigenic tag. These techniques are labor intensive, and the use of green fluorescent protein (GFP) had been shown to be faster, but it was shown that fusions of GFP to the N or C terminal has caused proteins to become non-functional (Tain *et al.*, 2004). However, if the fluorescent protein gene sequence is placed internally in the target protein sequence, then the target protein remains functional and can be localized to its known destination (Sedbrook *et al.*, 2002).

The FTFLP technique uses the strategy of inserting a fluorescent protein in between signal sequences of a protein of interest to study expression patterns and localization (Tain *et al.,* 2004). The fluorescent reporter needs to be stable within the cell when exposed to different physiological condition, such as pH. Second, insertion should not affect posttranslational modifications, targeting signals, or protein conformation. Third, the expression of the tagged protein should occur from its native regulatory sequence in order to detect its developmental and tissue-specific regulation (Tain *et al.*, 2004).

A polymerase chain reaction (PCR) protocol was developed to insert a yellow fluorescent (YFP) or cyan fluorescent protein (CFP) DNA sequence into the target protein sequence. In over 93% of the cases tested the insertion was 30 base pairs

upstream from the stop codon (Tain *et al.*, 2004). The selected gene was first amplified

using two sets of primers. Primers P1 and P2 were for one section and P3 and P4 for the

second sections. P1 and P4 were also complementary to a Gateway primer at the tail

ends. P2 and P3 were also complementary to the YFP or CFP. The YFP or CFP also

contained coding sequences that allowed them to be amplified in the first round of PCR.

The second round of PCR, called triple template PCR or TT-PCR, involved amplification

of all three fragments and resulted in overlapping templates. This leads to the YFP or

CFP being inserted into the gene sequence and then the entire sequence being amplified

by the Gateway primers (Tain *et al.*, 2004). Each of these YFP or CFP tagged genes

were then cloned and transferred into agrobacterium and used to transform plants (Tain *et

al.*, 2004).

Each of the constructs for each gene includes: a maximum of 3kb of the DNA

sequence upstream from the start codon; the DNA sequence 1 kb downstream of the stop

codon; the 5´UTR; the promotor sequence; the coding region with introns; and the 3´

UTR (Tain *et al.*, 2004). The gene sequence with the fluorescent protein inserted was

transferred into an Agrobacterium binary vector in which the T-DNA has its promotor

removed. In addition, they constructed a second binary destination vector with a

tetramerized Cauliflower mosaic virus 35S enhancer inserted to augment the expression

of genes with weak promoters. In order to demonstrate that proteins targeted to different

locations in the cell were not disrupted by the addition of the fluorescent protein into their

structure, proteins with known expression locations were used for proof of concept:

peroxisome, tonoplast membrane, plasma membrane, cell wall, plasmodesmata,

cytoskeletal elements, nuclear membrane, proplastids, nuclear targeting, *and cytosolic*

localization (Tain *et al.*, 2004).   The expression of the genes with a tagged fluorescent protein was compared between those with only the genes promotor to those with the promotor and 35S enhancer. The location of the cell signal for all the constructs tested with the 35S enhancer sequence was the same as those without the 35S enhancer. However, for some proteins the signal was stronger in the constructs with the 35S enhancer sequence (Tain *et al.*, 2004).

The work with the FTFLP technique in *A. thaliana* was expanded into *Zea mays* (Mohanty *et al.*, 2009). In the maize protocol they not only used the YFP and CFP, but also red fluorescent proteins (RFP). These fluorescent proteins were inserted into the full genomic sequence including the regulatory regions with the aim of the entire sequence being limited in size from 8 to 9 kb. The genes chosen for the initial 40 constructs were those with robust predicted functions based on evidence from localizations studies with antibody or expression data. As with the *A. thaliana*, genes whose proteins localized to the full range of subcellular locations were used. It was also noted that a quarter of the genes selected were requested from researchers in the maize community. The rest of the genes were selected using multiple databases. The first database was The Institute for Genomic Research (TIGR) maize databased in which 2,500 Assembled *Zea mays* (AZM's) that were greater than 5kb and also 300 TIGR maize BAC sequences were evaluated (Mohanty *et al.*, 2009). An AZM is a consensus sequence which was determined by comparing multiple sequences and grouping those with similarities into group clusters (http://maize.jcvi.org/release5.0/azm5.shtml).   The Fgenesh database allowed for the prediction of genes from a genomic sequence and PSORT (protein sorting tool) was used to predict subcellular location. (Mohanty *et al.*, 2009). Finally, GenBank,

Maize Assembled Genomic Island sequences, and MaizeGDB were used to find additional gene sequences. Initially 40 proteins were tagged, and the seeds have been made available for use. Additional proteins have been tagged since then and all fluorescent protein constructs can be requested from the web site at http://maize.jcvi.org/tigr-scripts/maize/cellgenomics/seed_request.pl (Mohanty *et al.*, 2009).

Expression Profiles of Protein Fusion Constructs.

In my dissertation research project twelve fluorescent protein constructs were used in evaluating both normal embryo development and *emb* embryo development. They are described in the next sections and summarized in Table 1.

pin1

PINFORMED1 is a member of the auxin efflux transporter family and is localized in the plasma membrane; initially found in Arabidopsis, it has three maize orthologues named *ZmPIN1a*, *ZmPIN1b*, and *ZmPIN1c* (Carraro *et al.*, 2006; Gallavotti *et al.*, 2008). It has been shown to accumulate in the L1 layer of axillary meristems and the inflorescent meristem in maize. It is found at areas of vascularization. ZmPIN1 is polarly localized, upregulated in areas where auxin response maxima form and at areas of primordia emergence; and it is broadly expressed throughout the maize plant (Gallavotti *et al.*, 2008). PIN1 expression has been looked at in embryogenesis in two reports. A report by Forestan *et al.* (2010) described PIN1 expression from the proembryo stage to stage 6, while a report by Chen *et al.* (2014) reported on PIN1 in early embryogenesis for proembryo stage to late transition stage.

The Forestean *et al.*(2010) determined the distribution of ZmPIN1 during embryogenesis initially by immunolocalization and also using fluorescent proteins (Forestan *et al.*, 2010). The proembryo stage embryo showed expression in the interior cells of the embryo proper, indicating that auxin is first produced and exported from these initial cells. As the protoderm formed ZmPIN1 was detected in the anticlinal membranes of the protoderm cells that were differentiating which indicated movement of auxin to the upper tip of the embryo (Forestan *et al.*, 2010). The transition stage embryo showed expression at the adaxial surface where the SAM would appear and at the top of the scutellum. The coleoptilar stage embryo showed expression in the coleptile, "the vasculature of the scutellum, the inner tissue of the SAM and the initials of the RAM." (Forestan *et al.*, 2010).   The next six embryo stages involving the sequential development of leaf primordia showed expression in the corpus of the SAM of the primordia, the vasculature of the differentiated leaves, in the coleorhiza of the RAM, and inthe seminal root primordia (Forestan *et al.*, 2010).

Chen *et al.* (2014) reported that first expression of PIN1 was in the apical cells of the embryo proper, which they state indicates that auxin in brought into the embryo from surrounding tissue. The early transition stage embryos have expression in the basal membranes of the cells of the apical portion of the embryo proper. The late transition stage embryos show expression just below the apical part of the scutellum down to near the basal part of the embryo proper (Chen *et al*, 2014).

dr5

A synthetic auxin response element called DR5 was created from the *GH3* gene in soybeans (Ulmasov *et al.*, 1997). The *GH3* gene has multiple auxin response elements (AuxRE) in an auxin-response promotor of where each can function independent of each other. The *GH3* promotor has AuxRE that consist of a TGTCTC element and a coupling element; both are required to confer auxin responsiveness (Liu *et al.*, 1994; Ulmasov *et al.*,1995). DR5 is the nomenclature assigned to a site directed mutation at the 5' end in the D1-4 composite AuxRE of the *GH3* promoter which resulted in auxin induced transcription factor binding to AuxRE stronger than the natural occuring AuxRE (Ulmasov *et al.*, 1995). A synthetic DR5 reporter for auxin was produced by fusing seven tandem repeats of the DR5 upstream from a cauliflower mosaic virus 35S promoter-β-glucuronidase (GUS) reporter gene. In comparison to a similar synthetic construct using the natural D1-4 AuxRE which was induced 5 fold by the presence of 25 µM 1-naphthalene acetic acid, the DR5 synthetic construct was induced 25 to 50 fold (Ulmasov *et al.*, 1997). DR5 is detected on the axial surface of the embryo in transition stage, but not interiorly (Chen et al. 2014); DR5 is first detected in the embryo on the apical portion of the embryo in late transition stage (Chen et al., 2014).

tcs

A synthetic reporter to report cytokinin activity was developed and named Two Component Signaling Sensor (TCS) (Muller and Sheen, 2008). Cytokinin signaling is done using a multi-step two component circuity dependent on histidine and aspartate phosphorylay using an A-type and B-type response regulator. The A-type regulator represses signaling via negative feedback; and the B-type response regulator mediate

33

transcriptional activation in response to phosphorylay signaling (Muller and Sheen, 2008). The synthetic TCS has **a** concatemerized B-type Arabidopsis response regulator binding motifs and a minimal 35S promoter. TCS was tested to and was able to phosphorlay output caused by the three known cytokinin receptors and relayed to any of the response regulators tested (Muller and Sheen, 2008).

TCS was reported to be expressed in the late transition stage at the tip and adaxial surface of the scutellum and the initiation site of the SAM. (Chen *et al.*, 2014). The signal was still localized to these cells in the coleoptilar stage, but at a stronger expression (Chen *et al.* 2014). In Arabidopsis, TCS first appears in the hypophysis at the 16-cell stage (Muller and Sheen, 2008). By late globular stage the signal is only retained in the apical cells of the hypophysis. At the heart stage, expression was seen near the shoot stem-cell primordium (Muller and Sheen, 2008).

wus

WUSHEL (WUS) is a transcription factor first described in Arabadopsis and has two orthologues in maize: *ZmWUS1* and *ZmWUS2* (Nardman and Werr, 2006). There are two putative domains that have been identified: one homeodomain and the other an acidic amino acid cluster. The acid cluster allows WUS to be a transcription regulator (Mayer et al. 1998). WUS is known to regulate over 100 genes involving inhibition of auxin signaling and cell division to cytokinin signaling and meristem maintenance in Arabadopsis. A major interaction is in a feedback loop with *CLAVATA3 (CLV3)*, a secretory signaling peptide. The *CLV3-WUS* feedback loop was first shown to also contain *CLAVATA1(CLV1)*, a putative receptor kinase transmembrane protein; and *WUS* aids in the fine tuning of *CLV1* transcription (Busch *et al.,* 2010). The description of the

CLV-WUS feedback loop began with only the *CLV3*, *CLV1* and *WUS* genes (Busch *et al.,* 2010) as being a part of meristem maintenance, but since then two new signaling pathways have been discovered. The entire workings of the CLV-WUS feedback loop are only just being understood.

In Arabidopsis, *WUS* can be detected at the 16-cell stage in embryo development and stays confined to the center of the shoot meristem throughout embryo development (Mayer *et al.*, 1998). However, in maize, the two orthologues are differentially expressed. The *ZmWUS2* gene is expressed in the first leaf primordia in cells flanking the apex. In sectioning it was seen that expression extended to leaf primordium which have detached from the shoot apex and is seen in lateral leaf domains with the greatest expression at the marginal tip and continued expression in P2/P3 leaves. In contrast *ZmWUS1*, is first detected below the emerging coleoptile. It is initially expressed in the L1 layer, but then expression extends to deeper layers. Expression then stops when the second primordial leaf emerges and only shows up again in post germination (Nardman and Werr, 2006). In this research only the *ZmWUS1* gene was available for expression analysis.

abphyll 1

Abphyll 1 is an A-type cytokinin-induced response regulator, which has also been identified as the *Zea mays* response regulator 3(*ZmRR3*) (Guilini *et al.*, 2004). It acts by regulating cytokinin signaling in the SAM using a negative feedback loop. It controls phyllotactic patterning by limiting the space available for leaf primordia to develop at the apex of the SAM (Jackson and Hake, 1999; Guilini *et al.*, 2004). It is first detected in the

transition stage at the site of SAM formation. Expression continued in the SAM during the coleoptilar stage and was still being expressed in the SAM during stage 1 (Guilini *et al.*, 2004).

bes1

Brassinoid Insensitive-EMS-Suppressor 1 (*BES1*) in Arabidopsis is a homologue to *BZR1* in Arabidopsis and was found to be the same gene as *BZR2* (Yin *et al.*, 2002; Wang *et al.*, 2002). Expression of *BES1* is localized to the nucleus and cytoplasm in hypocotyls cells with stronger nuclear localization in elongating cells. The addition of brassinolide increased the localization of BES1 to the nucleus (Yin *et al.*, 2002). The *BZR1* gene that encodes for a nuclear protein which is a positive regulator of the Brassinoid signaling pathway. In Arabadopsis *BZR1* has a role in growth responses induced by brassinoids and regulates brassinoid biosynthesis and its expression is correlated with growing stems and cells undergoing elongation (Wang *et al.*, 2002). Both genes are involved in the brassinosteroid pathway, although the genes they target in the nucleus may not be the same group of genes (Yin *et al.*, 2002). The genes involved in the Brassinoid signaling pathway have been found to contain "high confidence homologs" in maize. A search of the maize genome for a *BES1/BZR1* homolog found a candidate with a 50% identity and 62% similarity to Arabidopsis *BES1*; additionally, the rice homolog *OsBZR1* shared 78% identity and 82% similarity (Kir *et al.*, 2015).

his1

The H1 histone or linker histone is ubiquitously found in eukaryotes, along with four other histones (Razafimaharatra *et al.*, 1991). The H1 histone is not part of the

nucleosome, which is comprised of the four other histones. H1 histone is a general

repressor of gene expression, although it has been shown to be a "control element" for

transcription in maize for some genes (Razafimaharatra *et al.*, 1991). The H1 histone is

positioned outside of the nucleosome and can organize inter-nucleosomal linker DNA

and stabilize higher order chromatin structures (Kotlinski *et al.*, 2016). The H1 histone

consists of three domains. The central hydrophobic globular region is responsible for

interactions with the internucleosomal DNA. The N-terminal domain is used to position

the H1 histone in respect to the nucleosome. The C-terminal domain allows for the

formation of higher order chromatin structure (Razafimaharatra *et al.*, 1991). Expression

of Histone1 using mRNA in a Northern blot has been shown to occur in meristematic

tissue, but also in tissue undergoing elongation. There is no H1 expression in fully

formed organs (Razafirmaharatra *et al.*, 1991).

rab17

The maize abscisic acid responsive *RAB17* is a gene that is a part of the RAB

(Ras-like in rat brain) branch of the RAS superfamily and was first found in epitheialial

cells in mouse tissue (Lutcke *et al.*, 1993; Bhuin and Roy, 2014). RAB proteins are

GTPase/GTP binding proteins which are found in organisms ranging from yeast to

humans. They are associated with exocytic and endocytic organelles on the cytoplasmic

face and with transport vesicles between these compartments (Bhuin and Roy, 2014).

Rab17 in particular has been localized to the apical recycling endosomes that "facilitate

transcytic transport to the apical and basolateral plasma membranes (Bhuin and Roy,

2014). The expression of Rab17, using in situ hybridization, during maize embryo

development was found to be expressed in all embryo cell types in both the nucleus and

cytoplasm starting at 22 DAP (Goday *et al.*, 1994). The initial area where expression of Rab17 could be found was in the leaf primordia and radicle, although a weak hybridization was seen throughout the embryonic axis. The scutellum showed very low expression or none. By 30 to 40 DAP Rab17 was detected in the "embryo axis organs" and scutellum. In the embryonic axis the "prevalent accumulation" was in the embryonic radicle cortex, metaxylem cells in the central core, leaf primordia, coleoptile and provascular elements. The scutellum showed hybridization in the procambium strands and surface epidermal cells (Goday *et al.*, 1994).

pyabby

The *yabby14* gene is involved in leaf development. In maize embryo development it is restricted to the three adaxial tiers of cells and may be involved in adaxial/abaxial patterning (Juarez *et al.*, 2004). Expression is broader in the first leaf primordia and becomes restricted in older leaf primordia. In older leaf primordia expression is near the margin throughout the adaxial domain, but the expression is restricted to the central layer of ground tissue in the rest of the leaf (Jaurez *et al.*, 2004). Either *yabby14* is restricted to the adaxial/abaxial boundary in developing leaves or it is limited to "less determined cells" in the primordium (Juarez *et al.*, 2004)

prk

The *PHOSPHORIBULOKINASE* gene (*PRK)* encodes a chloroplast localized kinase which is only involved in the Calvin Cycle (Hariharan *et al.*, 1998).   It catalysis the reaction in which Ru5P and adenosine triphosphate (ATP) are converted into ribulose-1, 5-biphosphate and adenosine diphosphate (Hariharan *et al.*, 1998).   Research

in *A. thaliana* indicate that *PRK* is kinetically activated by light and regulated under the circadian clock. *PRK* is down regulated during senescence and also regulated by the accumulation of reduced thioredoxins and metabolite in the stroma of chloroplasts (Marri *et al.*, 2004). PRK forms a supramolecular complex with several other proteins in the chloroplasts (Marri *et al.*, 2004). The expression of PRK and other genes that form this complex are inhibited by sucrose in the presences of light. There were no RNA transcripts found in the roots and low levels were found in flowers and siliques (Marri *et al.*, 2004). In maize the *ZmPRK* gene is expressed in the bundle sheath cells where the Calvin-cycle occurs (Sawers *et al.,* 2007).

mre11b

The *Mre11* gene was first discovered in *Saccharomyces cereviciea* and has two maize orthologues: *Mre11B* or *ZmMre11B* and *Mre11A* or *ZmMre11A* (Waterworth *et al.*, 2007; Samanic *et al.*, 2013). The *Mre11* gene is found in archaebacteria, bacteria and eukaryotes (Borde, 2007). It has been shown in *A. thaliana*, other plants and animals that MRE forms a complex with two other proteins: Rad50 and NBS1 (Borde, 2007). This complex is involved in double stranded breaks by making single stranded overhangs. The MRE11 protein possesses three functions: endonuclease, exonuclease, and helicase actives (Sidhu *et al.*, 2017). In maize it has been shown that ZmNBS1 protein interacts with ZmMre11A protein, but not with ZmMre11B protein (Waterworth *et al*., 2007). However, ZmMre11B and ZmMre11A interact with each other in a yeast two-hybrid system. (Altun, 2008). Although the exact function of ZmMre11B is not known, it is found in the nucleus of actively dividing cells and is developmentally regulated (Altun,

2008).   It has also been found that ZmMre11B is under positive selection and is found in a genome region which has undergone a selective sweep (Sidhu *et al.*, 2017).

zmperi

The *Perianthia* (*PAN*) gene in *A. thaliana* encodes for a bZIP transcription factor (Chuang *et al.*, 1999). The protein coded for by *PAN* contains a basic region for binding to DNA and contains a region consisting of a leucine zipper which mediates homo- and heterodimerization. A sequence analysis indicated that *PAN* is a TGACGT/C-binding protein with an amino-terminal bZip domain and a C-terminus enriched with glutamine and acidic amino acids (Chuang *et al.*, 1999).   An immunohistochemical analysis of *PAN* expression determined that its protein is localized in floral and vegetative tissues. It has been found in apical meristems, young leaf primordia, the whorls of the floral organ, developing petals, stamens and ovules (Chuang *et al.*, 1999).

CHAPTER II

MATERIALS AND METHODS

Genetic and Morphological Methods

Mutant Production by EMS Treatment

Mutations were produced by applying Ethyl methanesufonate (EMS) treated W22 pollen onto the silks of B73 ears. The pollen parent source was the W22 inbred converted to the homozygous *R1-scm2* purple stock provided by James Birchler or was a W22 inbred stock converted to a homozygous *r1-scm3* yellow kernel stock originally provided by Thomas Brutnell. The ear parent was an inbred B73 line that was a colorless yellow stock and is homozygous recessive for both *C1* and *R1* loci, which was provided by Thomas Brutnell. The following items are used to perform this procedure:

- Three 50 ml squeezable plastic bottles with caps.

- Three additional caps modified by making a whole in the center and securely inserting a 250 µl disposable pipette tip with the tip trimmed.

- 100 ml mineral oil.

- Fine mesh kitchen strainer and wax paper.

- 10 ml graduated cylinder.

- Hooded safety overalls, safety goggles and latex gloves.

- Knife to trim back ears.

- Lawson Shoot bags, Lawson tassel bags, and Lawson pollination bags.

- Caution tape.

The day prior to treatment a knife was used to cut back husks of 150 ears, above the tip of the growing ear of B73 stock and the ear shoot bags replaced. Lawson tassel bags were put over the tassels of 20-30 W22 stock plants. One-hundred fifty Lawson pollination bags were dated for the following day.

On the day of the pollinations B73 ears were examined by lifting their shoot bags to determine that the silks had regrown to at least 1cm of length. Three people were involved in the operation of this procedure. In the Field Research Lab one person, wearing goggles and latex gloves, added 33 µl of EMS to 100ml of mineral oil (Neuffer, 1994). This suspension was stirred and then divided evenly into the 50ml bottles. Pollen from the tassels of 7 to 10 W22 plants was collected by the other two people and brought into the lab. The pollen was poured through the fine mesh kitchen strainer onto wax paper to remove anthers and additional debris. About 7 cm^3 of pollen was measured into a 10 ml graduated cylinder and then added to one of the EMS/mineral oil solutions in the 50ml bottles. A timer was set for 35 minutes for the first bottle. This procedure was repeated for the other two bottles, with timers set to 45 and 55 minutes. One person was assigned to shake the bottles intermittently until pollination.   The other two people set up a portable table in the field near the B73 plants that were being pollinated. The dated Lawson pollination bags, and latex gloves were put on the table. As the time neared for the first pollination, those two people performing the pollinations put on the hooded overalls, latex gloves, and goggles. The pollination team is divided into the first person, who is applying the EMS/mineral oil/W22 pollen solution; and the second person, who

42

will follow and staple the dated Lawson pollination bags over the treated ears.   The

person intermittently shaking the three 50 ml bottles with the EMS/mineral oil/W22

pollen solution relocates to the table in the field along with the timers with the help of the

other two people. At the beeping of the first timer, the cover of the 35-minute bottle is

replace with the 250 µl pipette modified cover. The pipette was cut to allow for an

increased flow rate of the solution. The first pollination team member takes the 50 ml

bottle solution and goes to the first plant to be pollinated. The shoot bag is removed, and

the mineral oil solution is added to the top of the silks, about 0.5 to 0.6 ml per ear. The

shoot bag is not replaced, and the first team member moves onto the next cutback ear.

The second team member then puts a dated Lawson pollination bag over the pollinated

ears and staples it securely to the stem of the plant. About 45 to 50 ears are pollinated in

5-10 minutes. The same procedure is repeated with the 45-minute and 55-minute bottles.

After pollinations were complete a yellow caution tape was put around the experimental

area and the materials exposed to EMS were put into a black plastic bag and disposed of.

The next day the dated Lawson pollination bags were replaced with Lawson pollination

bags dated and labeled with the female and male parents by a team member. The dated

Lawson pollination bags were put into a black plastic bag and disposed of. No one

entered the EMS treated area until harvest.

Screening for Embryo Specific Mutants

At harvest the ears were collected and husked, dried in their pollination bags on a

forced-air dryer and then transported to the seed storage repository. Each ear was labeled

with the pedigree of the parents on a cardboard tag that is attached to the cob with a

parcel hook. The ears that showed a 20-30% seed set were selected as source ears for

possibly having mutations only affecting embryo development. In addition, ears that showed some kernels containing colorless yellow sectors on a purple aleurone background were also selected as suggested by M. Gerald Neuffer.

Fifteen kernels were removed from the middle section of selected ears and were planted in the experimental field in Grand Forks, North Dakota or on Molokai, Hawaii. At maturity (time of flowering), the plants were self-pollinated which produced ears with F2 kernels. In order to screen for new mutants, 100 kernels (or all the kernels on the ear if there were less than 100 kernels) were removed from the middle section of each self-pollinated ear and placed in a seed envelope with the pedigree information from the ear tag written on it. The kernel samples were poured onto a plastic tray. Each kernel was inspected under a lamp with a 60-watt bulb and a 2x magnifying lens.

Those ears whose kernels segregated for undeveloped embryos, but normal appearing endosperm had their kernels separated into two groups: those with normal embryos and normal endosperm; and mutant kernels with undeveloped embryos and normal endosperms. The mutant kernels were counted and both the number of mutant and number or normal kernels was written on the seed envelope. The percentage of mutant kernels was calculated and written on the seed envelope. A second small coin envelope was used to put the mutant kernels in and the pedigree information from the seed envelope was written on it as well as the number of mutant kernels and the calculated segregation percentage. The small coin envelope was closed with a paperclip and inserted into the original seed envelope along with the normal kernels. The seed envelope was also secured with a paperclip and then filed.

Morphological Examination of Embryo Specific Mutants

The morphological assessment of development for each mutant was performed by examining 10-15 mature kernels of each mutant. Previously identified mutant kernels were removed from small coin envelopes and were placed on moist filter paper in 120 mm diameter Petri dishes which were covered with a lid and then sealed with Parafilm. The Petri dishes were kept at room temperature for three days before the kernels containing mutant embryos were dissected. A Leica Wild M3Z dissecting microscope with 6.5x-40x magnification range aided by a Chui Technical Corporation Illuminator with two movable light sources was used to dissect and examine the kernels.

The kernels were removed from the Petri dish one at a time and placed under the microscope at 10x magnification and the lights positioned appropriately. A large forceps with teeth was used to hold the kernels embryo side up and oriented with the vertical axis parallel to the forceps. A #11 surgical steel scalpel was used to make two incisions on each side of the midline of the vertical axis. A third incision was made perpendicular to and intersecting the other two incisions near the top of the kernel.   A #3T forceps was used to carefully peel the pericarp back and remove it at the base of the kernel. In some cases, #4 or #5 forceps or the scalpel was used to remove fibrous tissues which remained in contact with the mutant embryo; magnification was adjusted up to 40x to aid in this delicate procedure. The heat from the lights required applying water to the embryo with a dropper and wicking the excess water away with bulbous paper. Photographs were taken of 10 or more embryos of each mutant using a Leica DFC 295 camera attached to the microscope and the Leica Application Suit V4 which accessed the camera and processed the images. Each image was identified by the source ear designation, mutant

designation, an individual embryo designation of that mutant, embryo stage, magnification, and the date. The images were saved in files on the lab computer.

The stages of embryo development were determined using Abbe and Stein's (1954) classification system. The proembryo, transition and coleoptilar stages occur sequentially before the first leaf primordium. The next six stages are designated Stage 1 through 6, in reference to the subsequent development of each leaf primordium.

Germination Test

Germination of the mutant embryos was determined by removing 25 kernels identified as mutant(normal endosperm and mutant embryo) and 25 kernels identified as having normal embryos from an ear segregating for the mutant phenotype. The kernels were planted in a sand bench. The mutant kernels of one ear were planted in a single row, with ~1inch between kernels. In a parallel row the normal kernels from the same ear were planted likewise. Adjacent to the normal kernels, a parallel row of mutant kernels from a different mutant were planted, followed by a parallel row of the normal kernels; each of these rows was separated by about 2-2.5 inches and a total of 45 mutations were evaluated.

Complementation Test

Allelism between mutations was determined using complementation tests in which a cross between two plants of different mutational events are crossed by double pollination as described by Sheridan and Clark (1987). Since the embryo specific mutations are recessive lethal, the tests are performed with the normal appearing kernels (with normal endosperm and normal embryo) of a self-pollinated ear that was identified

as segregating for a given mutant. These kernels will be either homozygous wildtype and not have the mutation present or heterozygous for the mutation; in a 1:2 respective ratio. The first mutant was grown in a colorless yellow kernel stock and the second mutant was grown as in a purple kernel stock caused by anthocyanin production in the aleurone. The purple parent is self-pollinated. The yellow parent has its ear cutback to right above the cob and a knife is used to divide the silks into two halves by cutting into the cob about 0.5-0.75cm. A cardstock paper colored on one side and white on the other is cut into 3-4 cm squares and inserted into the slit in the cob and the shoot bag is replaced. The following day the white side of the ear is self-pollinated, and the shoot bag is replaced. The next day the purple pollen parent is crossed onto the other side of the yellow parent's ear, the colored side of the cardstock. The silks on the white side have stopped growth while the silks on the colored side will have continued growth and it is easy to differentiate. After the ears have been harvested, dried and tagged, the ears from the purple parent are matched with the ears from the yellow parent. Those ears that have matches are then further evaluated. First, all the purple ears had 100 kernels removed and scored for the presence of the mutations. Those that are found to display the mutation are heterozygous for the mutations and the corresponding crossed yellow ear is then evaluated. The kernels on this ear are half yellow and half purple; the self-side and the crossed side, respectively. Kernels from the selfed-side are removed and scored for the presence of the mutant phenotype. Those ears segregating for the mutant phenotype, then have kernels from the crossed side removed and scored. If the kernels from the crossed side are all normal in appearance, then the two mutations complement each other and represent mutations in different genes. Otherwise if the kernels segregate for the mutant

47

phenotype, then they have failed to complement each other, and the two mutations are in the same gene and therefore are allelic.

Confocal Microscope Methods

Fusion Protein Constructs Maintenance

The fusion protein constructs were received from Dr. David Jackson Lab in Cold Spring Harbor and Dr. Anne Sylvester's Lab at the University of Wyoming and now can be obtained from the Maize Cell Genomics Database (http://maize.jcvi.org/cellgenomics/index.php). The constructs were planted in Jiffy pots in the greenhouse. When the seedlings reached the 3 or 4 leaf stage of development the seedlings were sprayed with Bayer Liberty 280 SL herbicide (CAS number 77182-82-2) which contains glufosinate-ammonium as the active ingredient. The plants which have the fluorescent construct also contain a gene for phosphinothricin acetyltransferase from *Streptomyces hygroscopicus* (Thompson *et al., 1987*) and this allows for those plants containing the fluorescent construct to survive the herbicide treatment. The surviving plants were brought to the Maize Research Field in Grand Forks ND and allowed to acclimate to the weather for two or more days before being transplanted into the field. At maturity the plants were self-pollinated and were either crossed by or crossed onto B73 inbreed stock. In subsequent years plants were further crossed onto/by B73 stocks; however, there were occasions when some plants were self-pollinated or in one instance crossed onto W22 inbreed stock.

Fusion Protein Constructs in Embryo Specific Mutant Lines

Ears that had been identified as segregating for the presence of the *emb* phenotype for *emb-16, emb-17, emb-18, emb-19, emb-20, emb-21 emb-22, emb-24, emb-25, emb-38, emb-40,* and *emb-49* were examined. Sixteen kernels with a normal appearing embryo phenotype were removed from those ears and planted into jiffy pots in the greenhouse. On average, two out of every three plants should be heterozygous for the mutant allele. Five days later, an additional planting of 20 normal appearing kernels from the same ears were planted in jiffy pots. Concurrently, 160 kernels for each fluorescent protein construct was planted into jiffy pots from ears whose plants had survived previous herbicide treatment and should contain the construct. Another five days later, a final planting of 16 normal appearing kernels from ears segregating for each *emb* was planted into jiffy pots. At the 3-4 leaf stage the herbicide treatment was applied to the fluorescent protein constructs. The surviving fluorescent protein construct plants and the three sets of *emb* mutant plants were transplanted into the field. All plants grown from kernels of ears segregating for an *emb* phenotype were self-pollinated and crossed onto available fluorescent protein construct ears. Six to eight plants grown from kernels of ears segregating for an *emb* phenotype were crossed onto ears for each of the 12 fluorescent protein constructs.   After harvest, the self-pollinated ears were scored for the presence of the *emb* phenotype and matched to any ears crossed with a construct.

Embryo Tissue Collection for Fresh and Paraformaldehyde Samples

Expression for each of the 12 fluorescent protein constructs in normal developing embryos was evaluated. Each plant was self-pollinated, and the date and time was written on the pollination bag and in a field notebook. Samples of kernels were taken at 7

DAP, 8DAP, 9DAP, 10DAP, 11DAP and 12 DAP in order to find embryos at the proembryo stage, transition stage, coleoptilar stage and stage 1. When the sample were collected, the date and time was again recorded on the pollination bag and in the field notebook. Each sample was taken by peeling back the husk and removing the top portion of the ear; around 6 to 7 kernels down. The sample was put into a shoot bag labeled with the information from the pollination bag and paperclipped closed. The shoot bag was then put into a snack sized Ziploc bag which was labeled with the plant number, collection date and fluorescent protein construct identification. The Ziploc bag was sealed and put into a cooler for transport to the lab in Starcher Hall on the University of North Dakota campus in Grand Forks, ND. All samples were put into the refrigerator until they could be dissected or sectioned for mounting on slides.

When a sample was removed for mounting on slides, the sample was then cut into two equal sections: one section was used for making fresh tissue slides and the other section was treated with paraformaldehyde. The fresh tissue sample was put back in the shoot bag and put on ice in preparation of making slides. A 2.5% solution of paraformaldehyde in 0.14 M potassium phosphate buffer at 6.8 pH was used for fixation. The kernels were left on the cob, but the interior tissue of the cob was removed. . The samples were then put into a 30 ml vial and the 2.5% paraformaldehyde solution was added to fill the vial. The vial was then put into the refrigerator for 1.5 to 2 days. The paraformaldehyde was then poured out and the kernels were subsequently washed with the 0.14M potassium phosphate buffer once before being stored in the 0.14M potassium phosphate buffer for 1 to 2 days. The buffer was then exchanged for new 0.14M potassium phosphate buffer and returned to the refrigerator for storage.

vibratome sectioning

Fresh tissue sample of kernels in the proembryo stage and early transition stage were sectioned with a vibratome. In preparation for sectioning 200 ml of 6% agarose gel was prepared and divided into test tubes of containing 20-30ml of gel each. The tubes were covered with parafilm and refrigerated. At the time of use one of the test tubes was then reheated in the microwave at high power in 15 second intervals until the agarose melted. In between the heating intervals a metal spatula was used to pierce the gel to allow for trapped air to escape and liquid agarose to rise to the top. After all the agarose was melted, air bubbles persisted in the solution due to the high agarose concentration of 6%. To facilitate removal of the air bubbles and to ensure the agarose remained liquid, the test tube was put into a hot water bath at 80 C°.

Five to six kernels were removed from the cob using a scalpel and put into a small vial on ice. A rubber mold with a well 4mm deep by 10mm wide by 40mm long was filled with the 6% agarose gel. The kernels were then inserted into the gel with the embryo side facing down. The mold was transferred to the refrigerator to allow the agarose to solidify for 3 to 5 minutes. The mold was taken from the refrigerator and the agarose gel casting was trimmed using a razorblade to ensure that the top surface was flat. The agarose gel casting was removed from the mold and the edges of the agarose were neatly trimmed. A cyanoacrylate adhesive or superglue (Loctite) was applied to the top of the agarose gel casting and then the agarose gel casting was affixed to the vibratome specimen disc. The kernels are orientated with the embryo's frontal side

facing up and positioned near the top of the agarose surface. The specimen disc was then put into the refrigerator to allow the glue to set.

A VT 1000 S vibrating-blade microtome (vibratome) from Leica Biosystems was used for sectioning. Wilkinson Sword double edge stainless steel razor blades were used as the cutting blade for the sectioning. The blades were cut in half and trimmed to fit into the knife holder of the vibratome. The clearance angle of the knife holder was set halfway between the 5º and 10º indicators on the adjustment bar. The bottom of the cooling bath was filled to about 1.5 cm depth with crushed ice. The buffer tray was then mounted onto the bolt inside the cooling bath. The buffer tray was pushed down into the ice and locked into place; additional ice was added around the buffer tray. The sectioning speed was set to 70 and the sectioning frequencies was set to 7 on the dial (70Hz). The sections thickness mode was set to 150 microns.

The specimen disc was then removed from the refrigerator and attached to the bottom of the buffer tray. The specimen disc was rotated to orient the agarose gel with the smaller (1.0 cm) side parallel to the cutting blade and then secured in place. Potassium phosphate buffer was added to the buffer tray until the agarose gel was completely submerged.

Slides for use with the confocal microscope were labeled with a slide number, the source plants identification number, the days after pollination, date of pollination, date of collection, the construct's protein identification and fluorescent protein identification. Two mats were made from card stock and aluminum foil; the aluminum foil was taped to only one side of the card stock. The mats were each placed on top of an ice pack, aluminum foil side down.   Five or six blank slides were used to temporarily put the

sections on for later inspection. The blank slides were put on one of the mats and the labeled slide was put on the other mat. Each slide had a drop of phosphate buffer solution put on it to maintain moisture of the sections and the ice packs kept the buffer from evaporating and kept the buffer cool.

A #3T forceps was used to delicately grab each section at the endosperm side to avoid damaging the embryo. The first section from the first kernel was placed on the far top left side of the first blank slide. The first section of each subsequent kernel was like wise put on their respective slides. The second section of each kernel was placed to the right of the first section with each subsequent section placed in the same manner; a second row of sections was started below the first section when the top part of the slide was full. After sectioning, the mat and ice pack were brought to the light microscope: A Leica Wild M3Z dissecting microscope with 6.5x-40x magnification range aided by a Chui Technical Corporation Illuminator with two positionable light sources. Each slide was put under the microscope to find which section had the embryo in it. The section containing the embryo was then transferred to the labeled slide. This was repeated for the next 5 slides, ending with the labeled slide having 6 sections with an embryo in each section. A bulbous paper was used to wick away most of the phosphate buffer from the slide. The mounting solution was prepared by mixing 100ml glycerol ultrapure with 100ml of 0.14M 6.8pH potassium phosphate solution to make a 50% glycerol in a 0.07M phosphate buffer mounting solution which was used in making slides. A coverslip was placed over the section and sealed with nail polish. The slide was then put into the refrigerator on some bulbous paper to allow the nail polish to dry for a day, before being put in a slide box.

whole mounts

Kernels in which the embryos could be easily seen were dissected with the aid of the Leica Wild M3Z microscope and the embryos removed. A labeled slide was prepared as described above and put on a mat which was placed on an ice pack. Forceps were used to hold the kernels with the embryo side up. Two incisions were made on each side of the embryo with a #11 surgical steal scalpel. A third incision was made perpendicular to and intersecting the other two incisions near the top of the kernel. A #3T forceps was used to carefully peel the pericarp back revealing the embryo. In some cases, the embryo stuck to the backside of the pericarp. A #4 or #5 forceps was used to gently grab the suspensor of the embryo and remove the embryo from the kernel. The embryo was easily removed and, in some cases, as with those stuck to the pericarp, the embryos were not attached to the kernel. The embryos were moved to the labeled slide with the frontal surface of the embryo proper facing up. In some cases, the embryos would flip over and couldn't be reoriented. After five to six embryos were put on the slide, the phosphate buffer was drawn off with bulbous paper followed by adding a drop of 50% glycerol/0.14M phosphate buffer mounting solution to the slide. The slides had a coverslip put on and were sealed with nail polish, before storing them in the refrigerator.

Confocal Microscope Settings

laser specifications

The confocal analysis was performed with the Zeiss LSM510 Meta confocal microscope provided by the Imaging and Image Analysis Core Facility at UND School of Medicine & Health Sciences. It is equipped with a 10x lens, along with 40x, 63x, and

100x oil emersion lenses.   The light sources include a halogen bulb for bright field view

and a mercury bulb to view fluorescent signals. Three of the available filters were used

with the mercury bulb: filter set 10 for the green fluorescent protein, filter set 40 the

yellow fluorescent protein and filter set 15 for the red fluorescent protein.   Three lasers

were also available for use. An argon-based laser that can emit at four wavelengths: 458

nm, 477nm, 488nm, and 514nm. A Helium-Neon based laser that emits at 543nm

identified as HeNe1. A second Helium-Neon based laser that emits at 633nm identified

as HeNe2. For use with the lasers, multiple dichroic reflectors and emission filters were

available.

zen software program settings

The Zeiss LSM510 confocal microscope was run by the ZEN software package.

The software allows for the user to manipulate the settings for the microscope by

controlling   hardware selection for the lens, filters, light source (halogen or mercury

bulb), lasers dichroitic reflectors and emission filters. In addition, the ZEN software also

controls the setting for image capture, tile scan, z-stack and post image modifications.

The laser set up for each type of the fluorescent proteins is identical except for

which laser and filters are used. The excitation frequency of the fluorescent protein

determined which laser was used: RFP excites at 556nm and uses the HeNe1 set to

543nm; YFP excites at 520nm and uses the argon set to 514nm; and GFP excites at

505nm and uses the argon set to 488nm. The second input is the main dichroic reflector

which only reflect specific wavelengths and must be set to match the wavelength of the

laser: RFP-HeNe1 used HFT 488/543; YFP-argon used HFT 514/633; and GFP-argon

used HFT 488/543. A second dichroic is selected as a mirror to redirect the laser to

channels 2 and 3. The channel selected is dependent on the emission wavelength of the fluorescent protein and a matching filter: RFP emits at 583nm and used channel 3 with filter BP 560-615; YFP emits at 532nm and used channel 2 with filter BP 530-600; and GFP emits at 505nm and used channel 2 with filter LP 505.

The image capture was initially set up to include a base set of options that could be later changed in special situations. The frame size for images was set to 1024 x1024 and never changed. The pin hole size was initially set to 1.00 airy unit which corresponded to a 0.9-micron thick section for most sections. Pin hole size was adjusted up to 3 airy units or 2.7 microns thick. The power of each laser could be adjusted to increase its strength: the argon laser was set between 50-75% power and the HeNe1 was set between 7-20% power. A setting named "speed" determined the time it took to do one pass across the field of view and was set to 4. A setting named "averaging" determined how many passes were done across the field of view and was set to 4. A speed of 4 and averaging of 4 allowed for one frame to capture an image in 2 minutes 5 seconds.

Most of the images were taken while using the 63x oil emersion lens or the 40x oil emersion lens. If the embryo was too large for it to be seen entirely in the field of view of one frame, the ZEN software had an option called Tile scan. This allowed for the microscope to take multiple frames next to each other in order to capture an image of the entire embryo; the input was given as horizontal x vertical frames. If the speed and averaging settings remained the same each frame would still take 2 minutes, meaning one image that was 2x2 frames would take 8 minutes. In the case of large projects, the speed

and averaging would be adjusted to allow one frame to be captured in as little as 30 seconds.

The ZEN software also allowed for a Z-stack to be taken. A Z-stack is accomplished by capturing images that are directly above one another as you pass through the embryo. A range from top to bottom is selected depending on where the signal is limited to inside the embryo. Between 10-15 images were selected for each Z-stack. In some cases, a Z-stack combined with a Tile scan were done.

CHAPTER III

RESULTS

Production and Mutation Frequency of Embryo Specific Mutants

The production of new *emb* mutants by EMS application was generated in both the summer of 2011 and summer of 2012 in the UND maize research field in Grand Forks, ND. In 2011 EMS was used to treat pollen of W22 *r1-scm3* and was applied to W22 *r1-scm3* ears; the 2012 application of EMS involved treating pollen of W22 inbreed stock and crossing it onto B73 ears. The ears produced from these two years were used as the source ears for kernels planted in the subsequent winter planting, winter 2011 and winter 2012, in Molokai, Hawaii. The plants produced from these kernels were selfed pollinated and the subsequent ears had kernels removed and screened for *emb* mutant embryo segregation. A total of 238 ears were screened, 140 in 2011 and 98 in 2012, in which *emb*'s were identified in 30 ears, 17 in 2011 and 13 in 2012. This resulted in a frequency of 12.6 % with both years combined; or 12.1% in 2011 and 13.3% in 2012 for each year. A third EMS treatment in 2013 treatment was performed by treating W22 pollen and crossing the pollen onto B73 ears. The ears produced in this treatment resulted in 27 *emb* mutations although frequency statistics could not be obtained since most of the planting was affected by mold. This information has been presented in the online publication G3 by Brunelle, Clark and Sheridan, 2017.

Segregation Frequency

The segregation frequency in the founder ears of the mutant embryos for the 57 *emb*s identified range from 13.0% in UND-57 to 34.0% for UND-49. The 13 *emb* mutants reported here have a segregation frequency in their founder ears with ranges from 20.3% in UND-19 to 34% seen in both UND-38 and UND-49. However, germination tests were conducted for 45 of the 57 *emb* mutants using a second group of ears which have been crossed with B73. The germination test ears had a segregation range of 12.0% for UND-37 to 40.0% for UND-1. In the 13 *emb* mutants presented here UND-19 and UND-40 had the lowest segregation values of 18.0%; and UND-17 had the highest with 27.0%. In addition, a Chi-squared test was performed on the 45 ears used for the germination test of which only five showed a significant deviation ($P < 0.05$) from the expected 1:3 ratio for single gene Mendelian inheritance. None of the 13 *emb* discussed here showed a significant deviation from the expected value. This information has been presented in the online publication G3 by Brunelle, Clark and Sheridan, 2017.

Germination

The germination test for kernels with normal embryos from ears segregating for kernels exhibiting the *emb* mutant phenotype were done for 45 *emb* mutants which included the 13 *emb* discussed in this dissertation (Brunelle *et al.*¸2017). The kernels with normal embryos taken from ears segregating for the 13 *embs* discussed here resulted in five of the 13 *emb*'s having 24 of 25 kernels germinating with the other eight

producing seedlings for all 25. In addition, four of 13 *emb*'s produced one, two or three

white seedlings: UND-18, UND-22, UND-25 and UND-38. The occurrence of white

seedlings was also observed in normal kernels planted from ears segregating for the *emb*

phenotype in seven other mutants which were planted as part of the 45 *emb* mutants:

UND-3, UND-8, UND-9, UND-29, UND-52, UND-53, and UND-56.

The *emb* kernels used in the germination test for kernels with mutant embryos

were taken from the same ears as the normal kernels discussed above for 45 *emb* mutants

(Brunelle *et al*, 2017). The 13 *emb* mutants discussed in this dissertation showed results

in which eight *emb* mutants showed no germination (UND-16, UND-18, UND-19, UND-

20, UND-21, UND-38, UND-39 and UND-49), three developed three seedlings (UND-

24, UND-25 and UND-40), and two developing one seedling (UND-17 and UND-22). In

addition, the one seedling produced by UND-17 was white. Three other mutants from the

rest of the 45 *emb* mutants tested produced at least one white seedling: UND-28, UND-

52, and UND-56.. None of the seedlings survived past seedling stage except UND-52

which grew a mature plant that appeared normal.   The data for all 57 mutations was

published in the Brunelle, Clark and Sheridan, 2017 G3 mutant screen and the

information specific to the 13 *emb*s discussed in this paper is presented in Table 2.

Complementation Test

Complementation tests were done using 19 of the 57 *emb* mutants in which 35

unique combinations were tested. Only two combinations failed to complement: UND-4

and UND-9; UND-1 and UND-10. As for the 13 *emb* mutants evaluated here, eight of the

mutants were involved in test crosses, along with UND-9, which resulted in in 10 unique

combinations. The pollen parent parents which had colored aleurone kernels included:

UND-9, UND-18, UND-19, UND-20, UND-21, UND-22, UND-25, UND-39, and UND-

49. The ear parents which were in colorless yellow stocks included: UND-9, UND-18,

UND-20, UND-21, UND-22, UND-25, UND-39, and UND-49. Thirty-five crosses were

obtained in which both the pollen parent and ear parent were segregating for their

respective *emb* mutant which is presented in Table 3. The ten unique combination tests

were UND-18/UND-2O, UND-18/UND-21, UND-18/UND-22, UND-18/UND-39,

UND-19/UND-39, UND-20/UND-21, UND-20/UND-39, UND-21/UND-39, UND-

22/UND-25, and UND-49/UND-9. The number of crosses for each unique combination

varied from one cross for UND-19/UND-39 to eight crosses for UND-18/UND-21. Also

seven out of the 10 unique combinations had crosses in which the pollen parent in one

cross was also an ear parent in a cross with the same *emb*. As an example, the eight

crosses for UND-18/UND-21 consisted of three crosses in which UND-21 was the pollen

parent and UND-18 was the ear parent; the other five crosses UND-18 was the pollen

parent and UND-21 was the ear parent. As stated above, all the crosses complement each

other and Table 4 gives a summary of the crosses. The data for all 57 mutations were

published in the Brunelle, Clark and Sheridan, 2017 G3 mutant screen.

Extent of Mutant Embryo Morphogenesis

        The examining of the embryos for the 13 *emb* mutants used mature kernels, which

were harvested and dried for storage. The kernels were rehydrated in petri dishes as

describe in methods, before dissections were performed. Ten kernels for each *emb* were

used and their morphology is described in the following section and summarized in Table 5.

UND-16

Development in the UND-16 mutant embryo was consistently stopped at the late transition to coleoptilar stage. Three embryo mutants were in transition stage with long suspensors and a rounded embryo proper (Figure 4-a,-b,-c) All three showed necrosis of the embryo proper with the most prominent darkening at the top. Five other embryo mutants were stopped where the transition stage progresses into the coleoptilar stage (Figure 4-d,-e,-f,-g,-h) . The embryo has begun to change from the "ice cream cone" appearance of the transition stage and begins to expand more apically and broaden laterally. There is no discernable coleoptilar ring. Necrosis is seen in all five of these embryos with the tip of the developing scutellum being the most prominent necrotic section. In two (Figure 4-f and -g) of the five embryos the necrosis extends down one side of the embryo into an area resembling a triangle reminiscent of polarized cells formed when the axis of development is changing from a vertical to an oblique orientation (Randolph, 1936). The ninth embryo(Figure 4-i) mutant is clearly in the coleoptilar stage with a discernable coleoptilar ring. The entire embryo shows necrosis with the most prominent at the tip of the scutellum and sides of the scutellum. One final embryo (Figure4 -j) mutant had an abnormal embryonic axis. The bottom portion of the embryonic axis appears wider than normal and the top half splits into two smaller portions which appear as a "v" shape. The embryonic axis protrudes from the surrounding scutellum which is oval in appears from the frontal view. The tissue appears healthy except for a small amount of browning near the tip of the scutellum. This embryo appears to have progressed beyond the coleoptilar stage and is similar to stage 3

or stage 4 in development, although the embryonic axis protrudes away from the scutellum, instead of being enclosed by it.

UND-17

Embryo development for UND-17 is blocked at an early transition stage and possibly proembryo stage in eight embryos, at the coleoptilar stage in one embryo and an abnormal stage 2 or later in one embryo. The eight embryos in the transition stage don't have an enlarged embryo proper distinguishing it from the suspensor, which may indicate that the embryos may not have progressed into the transition stage. Five of the embryos (Figure 5 -a,-b,-c,-d,-e) appear as uniformly thick cylinders with round tips and only their bases shows an enlargement of tissue. Most of the tissue in all five embryos is healthy with only some browning at the tip of three (Figure 5 -b, -c, -d) and some browning on the lower three-quarters of a fourth (Figure 5-e); this may indicate the beginning of necrosis. The other three embryos (Figure **5-f, -**g, -h) show a very obvious thickening of the suspensor and in one case (Figure 5-h) the suspensor flattens out. In all three cases the embryos narrow at the top as though a small embryo proper would be protruding from the much thicker suspensor. Necrosis is seen at the base of one (Figure 5-g) and in most of the tissue of another (Figure 5-h). The two groups of embryos may be related in the sense that the second group of three embryos may be the result of continued growth of the suspensor which was seen only in the lowermost portion of the suspensor in the first group. The last two embryos, nine and ten, have passed the transition stage. The ninth embryo has reached the coleoptilar stage (Figure 5-i) and appears to have browning of the tissue throughout the embryo. Additionally, the region of the SAM and coleoptilar ring

appears necrotic. The tenth embryo (Figure 5-j) of UND-17 is an abnormal large

coleoptilar stage or later. Tissue of the embryonic axis appears normal but is enlarged.

The yellow/brown tissue of the scutellum shows signs of more prominent necrosis at the

top.

<p align="center">*UND-18*</p>

Embryo development for UND-18 mutant embryos is stopped in both transition

stage and the coleoptilar stage. Two of the embryos are stopped at a normal appearing

transition stage (Figure 6-a,-b). Necrosis can be seen in both of these embryos with the

necrotic tissue appearing just below the tip of the embryo. A third embryo(Figure 6-3) in

transition stage has an enlarged suspensor which tapers down to the top of the embryo; it

looks similar to some of the UND-17 embryos. Two other embryos have reached a late

transition to early coleoptilar stage, but no visible coleoptilar ring can be seen; necrosis

can be seen throughout one embryo (Figure 6-d) and the second (Figure 6-e) shows

prominent necrosis at the lower part of the embryo proper. The last five embryos reach

the coleoptilar stage with a visible coleoptilar ring. One embryo looks necrotic

throughout the embryo, especially in the coleoptilar ring and apical portion of the

scutellum (Figure 6-f) One embryo looks very healthy with a clear coleoptilar ring

(Figure 6-g). One embryo (Figure 6-h) is very necrotic on the frontal face of the embryo,

but not in the coleoptilar ring region (Figure6-i). Another embryo looks larger than the

others with an enlarged suspensor which may indicate a later coleoptilar stage advancing

into stage 1 (Figure 6-i). The last embryo was in coleoptilar stage but showed abnormal

growth (Figure 6-j).

All ten of the embryos examined from this mutation appear to have developed beyond the coleoptilar stage and are being evaluated based on the scutellum and embryonic axis structure in their frontal view as described by Abbe and Stein (1954). Four embryos appear blocked in stage 1. Two of the four embryos (Figure 7-a,-b) appear normal with abundant yellowing/brown necrotic tissue; The two other embryos are abnormal in growth with one showing the same yellowing/browning of tissue (Figure 7-d), while the second has healthy appearing tissue with only the tip of the scutellum showing necrosis(Figure 7-c). Three additional embryos have appeared to reach an abnormal stage 2 when referenced to the frontal view of development diagramed by Abbe and Stein (1954). One of the three embryos show the same yellow/browning tissue throughout the embryo (Figure 7-f), while the other two embryos have healthy looking tissue with necrosis only visible at the top edge of the scutellum(Figure 7-g). Another embryo (Figure 7-h) appears to have reached Stage 3 with an enlarged embryonic axis, along with the scutellum enlarging and expanding; however, the scutellum never encroached onto the embryonic axis as in stage 4. The final two mutant embryos (Figure 7-i, -g) do show the scutellum encroaching onto the embryonic axis as with stage 4 or stage 5 normal embryos. However, the embryonic axis is stunted in its vertical growth. The scutellum appears to have continued its growth with the cavity that the scutellar groove produces extending further to the top of the scutellum and the edges of the scutellar groove encroaching over the embryonis axis. However, since the embryonic axis is stunted in growth the scutellum covers the top portion of the embryonic axis, but left room for the embryonic axis to grow into. There is also noticeable browning of the

tissue at the apex of the embryonic axis. On the lower part of the embryonic axis the tissue is enlarged and is pushing through the scutellum. It appears that growth continued on the lower portion of the embryonic axis while stopping at the top portion.

UND-20

The majority of the ten mutant embryos for UND-20 are blocked at the coleoptilar stage with only two possibly entering stage 1. Two embryos (Figure 8-a, -b) appear to be at a coleoptilar stage but without an identifiable coleoptilar ring. The next two embryos (Figure 8-c, -d) look almost identical in appearance with a scutellum extending apically and laterally, however there is necrotic tissue at the site where the coleoptilar ring is expected.   Three additional embryos (Figure 8-e, -f, -g) look similar to the previous two except that they are slightly larger, and the necrosis has expanded to cover a larger region. The next two embryos have browning tissue, although no strong necrotic region can be identified. One is in late coleoptilar stage (Figure 8-h) and is further enlarged than the previous three embryos. The second embryo has an enlarged suspensor or RAM and appears to be at stage 1 (Figure 8-i) The last embryo (Figure 8-j) is very large, has an enlarged suspensor and resembles stage 2 of development in size, however there is no coleoptilar ring or embryonic axis present. In seven of the embryos (Figures 8-d to 8-j) the lower suspensor or possibly RAM appears enlarged; it may have continued growth. All embryos given stages beyond the coleoptilar stage have not been verified by sectioning and are only in reference to frontal development as indicated by Abbe and Stein (1954).

UND-21

Most of the ten UND-21 mutant embryos are blocked at the transition to coleoptilar stage and show necrosis throughout the embryo. The two youngest embryos are in an early transition stage (Figure 9-a, -b), and both show necrosis beginning at the apical end of the embryo proper. One embryo (Figure 9-c) is blocked at the transition stage with necrosis in the apical end of the embryo proper which continues toward the suspensor on the external lateral surface. The next four embryos (Figure 9-d, -e, -f, -g) have grown into a mid-transition stage and are no longer "ice-cream cone" shaped, but do not resemble the coleoptilar stage in shape either. All four are also entirely necrotic and appears as a mass of black cells.   The last two mutant embryos show abnormal growth. Both embryos have a coleoptilar ring but don't resemble any normal stage of development. The tissue of both embryos appear as though the scutellum was hindered in growth apically, but the lateral regions on both sides of the embryonic axis appear to have continued with growth. One mutant embryo has two protruding regions on either side of the tip of the scutellum. Necrosis is seen in both embryos.

UND-22

Development of the ten UND-22 mutant embryos is blocked from the early transition stage or possibly proembryo stage to stage 1. Four of the embryos have an elongated suspensor with an increased diameter (Figure 10-a, -b, -c, -d). The apical part of the embryos is rounded and is the same diameter as the region directly below it. The lower part of the suspensor in two of these four embryos shows additional enlargement in diameter (Figure 10-a, -d). The apical part of the four embryos has a small region of necrosis. The embryos appear to be in either in a proembryo stage or early transition

stage. Another embryo (Figure 1-e) displays a similar morphology but has a much-increased thickening of the diameter causing the embryo to appear like a tube; necrosis is also present at the top of the embryo. One embryo in transition stage (Figure 10-f), has a bulbous embryo proper with some necrotic tissue at the top of the embryo and the frontal face, although most of the embryo is healthy in appearance.   Two other mutant embryos (Figure 10-g, -h) are in the transition stage. The suspensor of both embryos appears like healthy tissue, but prominent necrosis can be seen in the embryo proper at the apical region and a small region close to the suspensor in both embryos. The last two embryos had reached coleoptilar stage as evidenced by the presence of the coleoptile (Figure 10-i, -j). However, their development had continued, and they resemble embryos at stage 1with some abnormal growth; verification of leaf primordia was not determined by sectioning and only the morphology of the external face of the embryo in relation to normal embryos as describe in Abbe and Stein (1954).

UND-24

The ten embryos of the UND-24 mutant are blocked in development at the late transition or coleoptilar stage. Two of the embryos (Figure 11-a, -b) have healthy suspensor tissue and the embryo proper has begun to expand apically and laterally. Between the tip of the embryo proper and the suspensor there is prominent necrosis in the region of the coleoptilar ring and meristematic develop. Three other embryos (Figure 11-c, -d, -e) reached the coleoptilar stage with prominent necrosis in the coleoptilar ring and surrounding region. The lower region, where the root meristematic tissue develops, has healthy tissue and is enlarged. An additional two embryos (Figure 11-f, -g) have the same morphological structure, but there is little or no necrosis in the embryos. Figure 11-h

shows an abnormal coleoptilar stage or stage 1 embryo and has an enlarged suspensor or

RAM with a abnormally wide apical scutellum. An abnormal stage 1 embryo (Figure 11-

i) shows growth laterally in the lower scutellum, but the apical growth of the scutellum is

not equally advanced and appears like it is from a younger stage in development; the

coleoptile is necrotic, and the surrounding tissue shows some necrosis. The final embryo

(Figure 11-j) is in an abnormal late coleoptilar stage to stage 1, but the scutellum has

grown irregular and has flattened considerably on the apical portion making it difficult to

distinguish a coleoptilar ring or embryonic axis. All embryo stages beyond the

coleoptilar stage have not been verified and are only in reference to frontal development

as indicated by Abbe and Stein (1954).

UND-25

Development of the embryo of the ten UND-25 mutant embryos was blocked at

possibly the proembryo stage to coleoptilar stage, due to the size of the embryos all

possible proembryos are considered transition stage. Five of the embryos (Figure 12-a to

12-e) have an elongated suspensor with the apical portion rounded, but not forming the

typical bulbous embryo proper indicating that the embryos may still be in the proembryo

stage. The two embryos (Figure 12-a, -b) blocked earliest in development have healthy

appearing tissue and Figure 12-b looks as though the lower half of the embryo contains

purple pigment.   The other three of these first five embryos (Figure 12-c, -d, -e) show

necrosis throughout. The sixth embryo (Figure 12-f) blocked in either the proembryo or

transition stage shows abnormal growth with widening of the suspensor at the base and a

small area of browning of tissue. The seventh embryo is fully in the transition stage

(Figure 12-g) with healthy tissue, although the suspensor is elongated, as with other embryos cause by this mutation. The eighth embryo (Figure 12-h) is blocked at an abnormal transition stage and exhibits necrosis in the embryo proper just below the top of the embryo. The ninth and tenth embryos have reached the coleoptilar stage. The ninth embryo (Figure 12-i) has an elongated suspensor with healthy appearing tissue and the embryo proper region has developed an expanding scutellum with a coleoptilar ring; the scutellum exhibits necrosis above the coleoptilar ring and in the expanding apical region above the coleoptilar ring. The tenth embryo (Figure 12-j) has reached an abnormal stage 1 with prominent irregular growth of the scutellum.

UND-38

Embryo development of the ten UND-38 mutant embryos is blocked from a proembyro stage to stage1 or later. One embryo (Figure 13-a) has developed into an abnormal spherical mass which doesn't resemble any stage of embryo development and is presumably in the proembyro stage. Six other embryos (Figure 13-b, -c, -d, -e, -f, -g) appear to be in a proembryo or transition stage of development although their morphology is variable. Two embryos (Figure 13-b,-c) have a suspensor in which the lower three-quarters is more than double the thickness of the top last quarter. One of the embryos (Figure 13-d) has an elongated suspensor and the apical section is rounded with signs of necrosis. The last three (Figure 13-e, -f, -g) of the six mutant embryos have an excessively long suspensor reaching the length of a fully-grown embryo, but still is in either the proembryo or transition stage; all of the also display necrotic patches throughout the embryo. Both embryos in Figure 13-f and 13-g have curled up at the top. One embryo (Figure 13-h) reached an abnormal transition stage to coleoptilar stage

although no coleoptilar ring is present. The embryo proper sits upon an elongated

suspensor and is rectangular in structure with a small protuberance pushing up from the

center top. The embryo proper is yellow/brown with patches of necrosis; in contrast the

suspensor looks to be healthy tissue. The last two embryos reached the coleoptilar stage

and although no leaf primordia can be verified the two embryos appear as though they

have reached more advance stages in reference to the exterior figures provided by Abbe

and Stein(1954); one seems to be at stage 1(Figure 13-i) and the other at stage 4 or

5(Figure 13-j).

UND-39

The development of the ten UND-39 mutant embryos was blocked between the

transition to coleoptilar stage or later. One embryo (Figure 14-a) had grown an elongated

suspensor with tissue which appears healthy and may be in late proembryo or early

transition stage. A second embryo was blocked at the transition stage (Figure 14-b) with

healthy looking tissue throughout, except for one small spot in the center of the embryo

proper; the embryo appears enlarged in size. Two embryos that had reached the transition

stage (Figure 14-c, -d) and had started to progress to the coleoptilar stage with apical

elongation of the embryo proper; necrosis appeared is in small spots throughout both

embryos. The last embryo in the transition stage (Figure 14-e) has progressed much

farther and appears morphologically closer to the coleoptilar stage although no

coleoptilar ring can be seen; necrosis is concentrated in two areas in the embryo proper

with less sever necrosis throughout the embryo proper and partially into the suspensor.

Six embryos have stopped development in the coleoptilar stage with a variable

morphology. One embryo (Figure 14-f) has a necrotic embryo proper which has caused

the embryo to appear shriveled, however a coleoptilar ring can still be identified. Two

other embryos (Figure 14-g, -h) had reached the coleoptilar stage and have advanced

toward stage 1 in the appearance of their scutellum morphology; necrosis was present in

some tissue on the apical area of the scutellum and in several spots, but not very

extensively. The ninth embryo (Figure 14-i) was blocked in the coleoptilar stage and had

healthy looking tissue, but the embryo appearred enlarged similar to of the transition

stage embryos; some necrosis at the top of the embryo can be seen on the surface. The

last embryo (Figure 14-j) is in an abnormal coleoptilar stage; it also has extensive

necrosis throughout the embryo.

UND-40

The range of development in the ten mutant embryos of UND-40 included a

necrotic transition or coleoptilar stage up to stage 3 or later. The two earliest blocked

embryos (Figure 15-a,-b) are highly necrotic transition stage embryos which appeared to

be progressing to coleoptilar stage, but the necrosis obscures any surface structures and

no coleoptilar ring can be distinguished. The third embryo (Figure 15-c) with a similar

highly necrotic tissue was in the coleoptilar stage with a coleoptilar ring. Three other

embryos that have reached the coleoptilar stage show abnormal growth. One embryo

(Figure 15-d) shows a partial invagination separating the embryo into two sections. The

smaller sections when examined with a frontal view is positioned in what might be the

lower left lobe of the scutellum of a coleoptilar stage or later embryo. The larger section

comprises the rest of the embryo with the coleoptilar ring present. There is some necrosis

in the embryo proper, but the suspensor shows much necrosis. Another (Figure 15-e) of

these three embryos appears more like a normal coleoptilar stage embryo, but with

72

abnormal growth at the junction of the suspensor and embryo proper; there is some

necrosis in the embryo proper, but the suspensor is highly necrotic. The last (Figure 15-f)

of these three embryos has no suspensor and may be further along than coleoptilar stage

although leaf primordia were never identified; necrosis is found at the apical part of the

scutellum, and much of the tissue appeared darkened and unhealthy. The last four

embryos had reached the coleoptilar stage but appear to be in late stages of development.

One was verified to be at Stage 3 or later, by hand dissecting the embryo sagittally and

viewing the tissue under 40x magnification with the Lieca Wild M3Z brightfield

microscope.   Two of these embryos (Figure 15-g, -h) appearred to be in stage 1 although

the internal structures were not viewed for verification. Another embryo (Figure 15-i)

with healthy looking tissue appeared to be at stage 4 or later with some abnormal lateral

growth at the base of the embryo; the presence of leaf primordia wasn't verified but the

external morphology matches that of Abbe and Stein (1954). The last embryo examined

(Figure 15-j) appeared to be at a stage 5 or 6 when compared to the developmental

diagram produced by Abbe and Stein (1954) and showed some necrosis or drying of

tissue on the outer layer of the scutellum; this embryo was cut in half and the internal

structure did show the presence of leaf primordia, however only three leaf primordia

could be clearly identified.

UND-49

Embryo development of the ten UND-49 mutant embryos examined was blocked

from the transition stage to stage 1 or stage 2. One embryo (Figure 16-a) was elongated

with a rounded tip without any expanded growth at the tip and may be a proembryo or

transition stage. Four embryos are very consistent in structure and were in transition stage

(Figure 16-b, -c, -d, -e). All four had a well-developed embryo proper, which had a bulbous embryo proper which has begun to extend apically appearing more ovoid rather than spherical; no lateral growth indicative of the coleoptile stage can be seen. Necrosis in three of the embryos (Figure 16-b,-c,-d) was usually on the apical or lateral edge where it contacts the endosperm, but only in small surface spots; necrosis can be seen in the endosperm which is in contact with the necrotic regions of the embryo. The fifth embryo (Figure 16-e) has prominent necrosis in cells that when examined in the frontal view appear in the peripheral edge of cells extending from the tip of the embryo to the suspensor. The cells in rest of the embryo proper are not necrotic but appear unhealthy. The sixth embryo (Figure 16-f) had abnormal growth of both the suspensor and embryo proper in which the diameter of both had increase substantially. The embryo looks similar to a bulbous transition stage but did not have a coleoptilar ring. Three other embryos (Figure 16-g, -h, -i) in the coleoptilar stage were very consistent in morphology; the scutellum has expanded both apically and laterally and appear to between the coleoptilar stage and stage 1 when evaluating their development against frontal view in the diagram produced by Abbe and Stein (1954). Two of these three embryos (Figure 16-g,-h) have healthy tissue with only a few surface spots of necrosis; the third embryo (Figure 16-i) has prominent necrosis in the suspensor extending to the embryo and also in the coleoptilar ring. The last embryo (Figure 16-j) had healthy looking tissue and had grown to appear fully developed in size but not morphology. The embryonic axis was more prominent in the frontal view, since the scutellum had not moved over it as in normal embryos. The scutellum had a narrow tip with noticeable lateral lobes, in contrast to the ovoid appearance of more mature embryos. When the embryo was cut in half, the

cross sections appeared to resemble stage 2 or later from Abbe and Stein (1954), but only two leaf primordia could be verified.

Confocal Microscope Results

Fusion Protein Constructs in Embryo Specific Mutant Lines

Eleven of the twelve protein constructs have been crossed into the thirteen *emb* lines focused on in this report (except pYABBY). Additionally, UND-25 does not have a cross with the DR5 construct. Plants were grown from the set of 13 *emb's* crossed with DR5, PIN1, pWUS and TCS. These plants were either selfed, crossed by or crossed onto B73 plants; kernels were collected and fixed with 2.5% paraformaldehyde in a 0.14M potassium phosphate buffer and later stored in the 0.14M potassium phosphate buffer. The embryos from some of the fixed kernels were used to verify a signal for PIN1 in UND-16, UND-17, UND-18, UND-19, UND-21, UND-22, and UND-24 as well as one plant with DR5/UND-16. At least one embryo for each mutant and construct combination showed a signal; however, these have not been evaluated to any extent and will not be discussed here but summarized in Table 6.

Summary of Fluorescent Protein Construct Signal in Normal Embryos

Ten of the twelve fluorescent protein constructs were able to be examined; only TCS and ZmPERI were not. Since not all embryos were carrying the fluorescent proteins constructs, these normal embryos were used as controls when identifying signal.   A positive result was determined if two or more embryos gave a similar expression and appeared to come from the subcellular location characteristic for that respective protein

75

or was indicative of that fluorescent protein construct in images provided on the website maize.jcvi.org from which the constructs originated. A negative result was determined by having no expression in a stage of development for a fluorescent protein construct in at least five embryos from kernels which were removed from an ear whose plant showed resistance to herbicide treatment. Seven of the constructs showed expression at the proembryo stage which corresponds to about 6-7 DAP: PIN1, DR5, PRK, MRE11B, ABPHYl1, RAB17, and BES1. Two constructs, pYABBY and pWUS, showed no expression and no material was available for HIS1 at this embryo stage. The transition stage, 8-9 DAP, showed expression in eight of the constructs: PIN1, DR5, HIS1, PRK, MRE11B, ABPHYl1, RAB17, and BES1. Again, pYABBY and pWUS showed no expression in transition stage embryos. The coleoptilar stage embryos, 10-11 DAP, showed positive results with eight of the constructs: PIN1, DR5, HIS1, MRE11B, RAB17, BES1, pYABBY and pWUS. Both ABPHYLL1 and PRK had no material available to examine for the coleoptilar stage. Stage 1, 11-12 DAP, was only examined in three constructs, PIN1, HIS1, and PRK; all three were positive for expression. This information is summarized in Table 7 and one example for each construct is shown in Figure 17. Two of these constructs, DR5 and PIN1, which are involved in auxin movement and response will be examined in more detail below.

DR5 Signal in Normal Embryos

proembryo stage to early transition stage: dr5-e1, dr5-e2, and dr5-e3

Expression of DR5 is very low in all the embryos resulting in using a minimum of 1.8µm per slice to capture signals. The earliest signal observed was in an early proembryo (Figure 18.a, 40x, 3.8µm; and 18.b, 63x, 3.8µm) and it can be seen in

between the embryo and surrounding tissue, along with cells within the embryo (DR5-e1). In Figure 18.a, strong DR5 expression can also be seen in tissue over 50µm away, but not in tissue directly surrounding the embryo. Two Embryos in early transition stage can be seen showing signal (Figure 18.c and d, 40x, 5.0µm; and Figure 18.e and f, 40x, 3.2µm). The first embryo (DR5-e2) shows signal in all of the cells in the slice of the embryo proper (Figure 18.c and d). The second embryo (DR5-e3) shows signal in cells of the suspensor and most of the embryo proper; but approximately the top quarter of the embryo proper lacks any expression (Figure 18.e and f.).

late transition stage: dr5-e4 and dr5-e

In late transition stage an embryo, DR5-e4, has expanded apically and is asymmetric in appearance from a frontal view with the right side of the embryo having a distinctive bulge (Figure 19.a-j and Figure 20.k- n, 2x1 tile, 40x, 2.7µm, 7.09µm, 42.51µm range).   The surface slice (Figure 19.a &b) and the next slice (Figure 19.c &d) into the embryo show strong expression at the apical point of the embryo. Expression can also be seen on the left side of the embryo, although to a lesser extent. In the third slice (Figure 19.e & f), the signal at the tip has increased in area. The signal extends toward the base and through the center of the embryo proper to the suspensor; and around the center of the embryo proper a more intense signal curves to the left side of the embryo resembling a hook. The following slice (Figure 19.g & h) shows a further increase of expression at the tip of the embryo. The expression in the middle of the embryo has faded except for the curved hook, with the basal part of the hook showing stronger expression. In the next slice (Figure 19.i &j) the tip of the embryo maintains roughly the same expression; in contrast the center of the embryo and the base have lost

all the expression, except for a weak signal that is directly below the basal part of the hook. In next two slices (Figure 20.k -n), the embryo only shows signal at the tip of the embryo, but it is reduced in both area and intensity. Another embryo, DR5-e5, in a late transition stage (Figure 20.o -z, 2.7µm, 3.54µm, 21.26µm range), but further along in development is symmetrical and expression has decreased. The first three slices (Figure 20.o -t) show expression starting at the tip and with each successive slice the signal advances toward the center of the embryo along the midline. The fourth slice (Figure20.u & v) shows that the signal splits near the center of the embryo, where the coleoptilar ring forms. The signal goes around the center and closes slightly above the suspensor. In the next two slices (Figure 20.w-z) the signal increases in strength around the center and at the base.

early coleoptilar stage: dr5-e6

In early coleoptilar stage (Figure 21. 1.8µm, 9.67µm, 58.0µm range) the embryo, DR5-e6, is showing the formation of the region of cells that will become the coleoptile and the SAM, although they do not appear differentiated from each other yet. In the surface slice (Figure 21.a), cells bordering the top part of the coleoptile/SAM region show expression and there is expression seen in the center of the coleoptile/SAM region. In the next two slices (Figure 21.b & c), the signal in the cells bordering the coleoptile/SAM region has reduced to only appear in the space between those two regions, but the signal in the center of the coleoptile/SAM region has increased in strength. In the fourth slice (Figure 21.d) the coleoptile/SAM region cannot be distinguished, and this slice may be below that region, however there is a signal coming from the area which corresponds to the coleoptile/SAM region. There is a second signal

at the base of embryo proper, near the suspensor. The fifth slice (Figure 21.e) shows a

similar signal as the fourth slice, although the signal at the center has changed in shape to

look like an arc; the signal at the base is still present but reduced in size. Additionally,

DR5 expression can be seen near the top of the scutellum. The sixth slice (Figure 21.f)

has no basal signal. The signal in the center no longer looks like an arc since only the

most apical region is expressing signal. Extending from the center the signal moves up

the midline of the embryo and fans out as it approaches the tip of the scutellum. The

final slice (Figure 21.g) has signal coming from the same general regions as the sixth

slice, although weaker in the center and a slightly different pattern near the tip of the

scutellum.

late coleoptilar stage: dr5-e7

Late coleoptilar stage, DR5-e7, is larger and the coleoptilar ring is now distinct

from the SAM (Figures 22 and 23, 3x3 Tile, 40x, 1.8µm slice, 6.55µm interval, 72.0µm

range). In figures 22 and 23, the brightfield with DR5 expression is above the same slice

showing only the expression of DR5.   Expression is seen in the center of the SAM and

the coleoptilar ring (Figure 22.a-h) similar to that in the earlier coleoptilar stage of DR5-

e6. The signal in the center of the SAM maintains the same size, but changes relative

location with each successive slice and appears to move to the bottom of the SAM.

Expression can also be seen prominently at the tip of the scutellum along the edges which

fades and moves along the lateral edges of the scutellum toward the base. In the fifth slice

(Figure 22.i & j), the expression in the SAM increases in area and two new areas of

expression appear. At the base of the embryo near the suspensor expression can be seen

and at the midline of the scutellum above the coleoptilar ring. In the subsequent three

slices (Figure 22.k-l; and Figure 23.a-d) the expression at the bottom of the SAM increases in size to resembles the arc, as seen with DR5-e6, and moves upward toward the center of the SAM. The signal at the base near the suspensor is still present but weakens in strength. The expression from the midline of the scutellum gets stronger and broader, while the signal from the lateral edges of the scutellum fade. The next three slices, slice 9 through 11 (Figure 23.e-j), show a loss of expression at the base near the suspensor and a further reduction in expression on the lateral edges of the scutellum. The expression which looked like an arc has moved further upward but is smaller and no longer looks like an arc; The midline expression has extended down and appears to connect to the smaller center expression. With each successive slice from slice 9 to 11, the expression from the center, midline and scutellar edge fades that by the twelfth slice (Figure 23.k-l) only the very tip of the scutellum shows expression.

Pin1 Signal in Normal Embryos

proembryo stage: pin1-e1, pin1-e2, and pin1-e3

The first signal for PIN1(Figure 24.a-f, PIN1-e1, 40x, 2.0µm slice, 15.77µm interval, 78.83µm range) is seen in a few cells in the interior of a proembryo, one or two cell layers below the top of the embryo proper's outer cell layer. The expression in a slightly older proembryo, PIN1-e2, shows the expression widening and expanding up to the outer cell layer, although the strongest signal is still on the interior (Figure 24.g-l, PIN1-e1, 40x, 0.9µm slice, 3.62µm interval, 18.09µm range). The signal from PIN1-e2, along with other embryos not shown, indicate that the expression extends from the frontal surface of the embryo proper to the opposite side of the embryo. An embryo in late proembryo stage or early transition stage, PIN1-e3, (Figure 25.a-f, 40x, 1.5µm slice,

11.15µm interval, 55.76µm range) expression has expanded to cover the top half of the embryo proper with expression being observed 66.91µm from the frontal surface.

transition stage: pin1-e4 and pin1-e5

The next two embryos are in transition stage: PIN1-e4 (Figure 26.a-h, PIN1-e1, 40x, 2.0µm slice, 8.41µm interval, 58.56µm range) and PIN1-e5 (Figure 27.a-i, PIN1-e1, 40x, 2.0µm slice, 9.81µm interval, 78.48µm range). In the PIN1-e4 embryo surface the expression is near the base of the embryo proper, near the suspensor; and expands toward ethe center of the embryo proper (Figure 26.a). As the slices go deeper (Figure 26.b-e) into the tissue the signal increases in area apically and laterally, but not basally; the signal stays in the center of the embryo and doesn't reach the surface cells. In the last three slices (Figure 26.f-h), the signal reduces in area a bit and weakens in strength. The nextmbryo, PIN1-e5, shows a similar pattern of expression as PIN1-e4 with the frontal surface showing weak expression in the center area of the embryo proper (Figure 27.a) with the second slice (Figure 27.b) showing expression at base of the embryo proper near the suspensor. In the next five slices (Figure 27.c-g) the expression increases in area similar to PIN1e4, but the apical expression has extended to the tip of the embryo proper. In Figure 27.f and g, the pattern of expression looks like an "ice cream" cone with the bottom of the cone at the center top of the embryo. In the last to slices (Figure 27.h & i) the signal reduces in strength, but not area or shape.

transition stage: pin1-e6

Another embryo, PIN1-e6 (Figure 28 and 29, 40x, 0.9µm slice, 10.37µm interval, 72.59µm range), in transition stage has a bulbous embryo proper. The frontal surface

(Figure 28.a) shows expression on the apical portion of the embryo and in a prominent

band crossing the center of the embryo which almost reaches the lateral sides of the

embryo proper. The second slice (Figure 28.b) shows a reduction in expression at the

apical portion to the outer layer of cells, but the center band of cells has increased in both

strength and width. The third and fourth slices (Figure 28.c & d) still show some

expression in the apical outer cell layer and the center band has increased in size to a

circular region.   In the fifth slice (Figure 28.e) the circular region has elongated along the

apical-basal axis and shows a very strong oval shaped signal. Additionally, there is a

weaker signal extending from the oval signal area to the top of the embryo. The sixth

(Figure 28.f) and seventh (Figure 29.g) slices show a narrowing of the oval shaped signal

from both lateral sides and maintains the signal extending up to the apical outer layer of

cells. The eighth slice (Figure 29.h) has a weak signal in the same areas as the seventh

slice.

late transition stage: pin1-e7

Further along in development, PIN1-e7 (Figure 30 and 31) is in late transition

stage and the embryo proper has begun to form the lobes seen in the coleoptilar stage.

PIN1-e7 (Figure 30.a-f and Figure 31.g-i, 1x2 tile, 40x, 0.9µm slice, 9.04µm interval,

79.59µm range) is oriented as a rear view of the embryo with the first slice (Figure 30.a)

possibly being above the embryo since the signal is not clear. The second slice (Figure

30.b) is on or near the surface and shows expression on the apical portion of the embryo

proper, which extends down the midline to the center of the embryo proper. There is also

a faint signal coming from the outer edge around the embryo and can be seen in figure

30.b at the base of the embryo proper near the suspensor. In the third slice (Figure 30.c),

the signal remains along the outer edge of the embryo and a weak signal can be seen

extending down to the center of the embryo. The fourth (Figure 30.d) and fifth (Figure

30.e) slices show strong expression extending from the bottom to the top of the embryo

proper in an ovoid shape similar to that of the sixth (Figure 30.f) and seventh (Figure

31.g) slices in PIN1-e6. Expression in the top outer layer of cells can still be seen in both

the fourth and fifth slices of PIN1-e7, but the expression seen in bottom of the embryo

proper has stopped and this may be because these slices are further to the interior. The

sixth slice (Figure 30.f) has maintained the expression from the center of the embryo to

the lower part of the embryo. However, most of the expression in the upper part of the

embryo proper has diminished but still shows enough expression to be contingent with

the top outer layer of cells. The seventh slice (Figure 31.g) shows weak expression in the

outer layer of cells but has lost expression in the other areas of the upper portion of the

embryo proper. Expression in the lower portion of the embryo proper is in the center of

the embryo and tapers as it extends to the bottom of the embryo proper.   The eighth slice

(Figure 31.h) and 2x2 tile images of the same slice (Figure 31.j & k) show a central

"mushroom" shaped pattern. As can clearly be seen in figure 31.k, the outer layer of

cells at the top of the embryo still show expression with the expression fading along the

lateral outer cell layer of the embryo. The ninth slice (Figure 31.i) no longer shows

expression in the lower area near the base of the embryo proper where the stem of the

"mushroom" appeared in the eighth slice. The top portion of the "mushroom" still shows

expression, but it is weaker and may corresponds with the area of expression seen in the

first (Figure 30.a) and second (Figure 30.b) slices of PIN1-e6. As with the other slices,

expression can still be seen in the outer apical cells of the embryo proper.

late transition stage forming shoot apical meristem: pin1-e8 and pin1-e9

The next embryo, PIN1-e8 (Figure 32 and Figure 33.c-d), resembles a coleoptilar

stage embryo in shape, but the coleoptilar ring and SAM have not fully formed. PIN1-e8

is shown with six slices in figure 32 (Figure 32.a-f, 2x2 tile,40x, 0.9μm slice, 9.76μm

interval, 48.80μm range) and a close up of the surface slice figure 32.a in figure 39.c and

d. The surface of the embryo shows a morphologically distinct set of cells corresponding

with the PIN1 signal which can clearly be seen when comparing figure 33.c, a brightfield

image with the PIN1 signal, to an image of the brightfield only figure 33.d. A second

embryo, Pin1-e9 (Figure 33.a-b, 0.9μm slice, 40x), shows the same type of relationship

between the PIN1 signal and the morphological differences between the cells. The

surface slice (Figure 32.a) also shows very weak expression in cells slightly above the

prominent PIN1 signal in the center and there is a weak signal coming from the outer

layer of cells at the apical region of the scutellum. The second slice (Figure 32.b) shows

expression coming from the same general area, but the signal has expanded slightly to the

right of the embryo and has expanded to the bottom of the embryo proper. In the second

slice (Figure 32.b) the apical region of the scutellum and the region slightly above the

more prominent signal area still have cells with weak signals.   In the third slice (Figure

32.c) the signal broadens to form an oval shape similar to younger embryos; the signal

reaches from slightly above the morphologically differentiating cells to the bottom of the

embryo proper.   A signal can also be seen from a thin band of cells extending up the

midline from the top of the oval shaped signal to the top of the embryo and then on the

outer layer of cells on the top of the embryo. The fourth slice, (Figure 32.d), shows a

slight broadening of the central oval shaped signal. The midline signal has also

broadened and increased in strength, although the outer layer of cells has maintained the same intensity of signal as in the other slices. The signal is reduced in the fifth slice (Figure 32.e) and has receded slightly from the base. The sixth slice (Figure 32.f), shows signal in the outer layer of cells at the top of the embryo similar to intensity as other slices and an even fainter signal extending partially toward the interior of the embryo. In both PIN1-e8 and PIN1-e9, the signal is stronger in all slices from the side of the embryo that is showing morphologically different cells.

late transition stage, SAM formed, no coleoptile ring: pin1-e10

In the next two embryos, PIN1-10 and PIN1-11(Figure 34), the group of morphologically distinct cells in PIN1-8 & 9 have reached to the other half of the embryo and a distinct division between these cells with surrounding cells which appear as a half-oval of cells in the center of the embryo; these cells are probably the beginnings of the SAM. The younger embryo PIN1-10 (Figure 34.a-f, 2x2 tile, 40x, 0.9μm slice, 12.1μm interval, 60.49μm range), shows clear expression in the apical region of the scutellum (Figure 34.a). The pre-SAM show expression which extends to the cells below the pre-SAM region. Expression from the more basal cells then circle up and are expressed in cells that are where the coleoptilar ring forms. The second slice (Figure 34.b) shows increased intensity in expression for cell in the outer cell layer of the apical region of the scutellum and has lost expression in cells further interior, except for those in the midline of the embryo. The pre-coleoptilar ring cells and pre-SAM cells still show expression although weaker in strength. The cells directly below the pre-SAM region increased in signal and have broadened in area along as well as extending down the midline to the base of the embryo proper. The next three slices (Figure 34.c, d, &e) have very similar

expression patterns that look similar to younger embryos already discussed. There is a large oval shaped signal in the center of the embryo, with a band of cells in the midline extending up to the top of scutellum. The expression from the midline band of cells widens out as it reaches the top of the scutellum and the expression continues in the outer layer of cells along the lateral edges to half-way down the embryo. The sixth slice (Figure 34.f) still shows expression in the other layer of cells at the top of the scutellum along with a weak signal coming from the midline band of cells and a faint signal from some central cells.

late transition stage, SAM formed, no coleoptile ring: pin1-e11

The second embryo showing the pre-SAM cell morphology but lacking the coleoptilar ring is PIN1-e11 (Figure 34.g-l, 2x2 tile, 40x, 1.8µm slice, 9.67µm interval, 48.3µm range). In the first slice (Figure 34.g), the pre-SAM region no longer appears a half-oval, but a three-quarters oval. Unlike younger embryos, there is no signal coming from the apical region of the scutellum or the outer layer of cells. The signal is localized around the pre-SAM region and the pre-coleoptile cells. Within the pre-SAM region the expression is restricted to a smaller region that resembles an oval with an apical-basal orientation. The lower portion of the pre-SAM signal has stronger expression than the apical portion. The cells surrounding the pre-SAM region show expression stronger at the base and weaker in the more apical pre-coleoptile region. The second slice (Figure 34.h) shows an increase of expression in the lower area surrounding the pre-SAM region, but no longer shows any expression in the upper most portion of the pre-coleoptile region. The oval shaped expression in the pre-SAM region had reduced in size to a smaller circular area with stronger expression and is positioned at the bottom of the pre-

SAM region. The third slice (Figure 34.i) still shows expression coming from the same area as the second slice, although the signal coming from the cells in the pre-coleoptile region doesn't extend as far apically. The pre-coleoptile signal is stronger on the lower lateral edges of the signal and the circular region in the pre-SAM region still shows strong signal. In addition, a faint signal extending basally and contiguous with the rest of the signal reaches to the base of the embryo proper. The fourth slice (Figure 34.j) has a reduced expression in the pre-coleoptile region, although clear expression can still be seen from the two lateral sections that had strong expression in slice three. The strong circular signal at the base of the pre-SAM region is now indistinguishable from the signal extending to the base of the embryo proper and forms an oblong signal. Between the center of the embryo and the top of the scutellum a weak signal is coming from some cells stretching from the left to the right side of the embryo. This signal may be at the edge of the embryo, but the tissue closer to the confocal microscope lens may be obstructing the view. The fifth slice (Figure 34.k) shows an expanding of the oblong signal laterally and apically. The basal end of the signal shows a weakening of the signal in the center which appears like a ring of strong signal around a center of weaker signal. The strongest portion of the signal is in the center to apical section although not at the utmost apical end of the signal. The apical portion of the signal is in the center of the embryo proper and from there a weak signal extends further upward along the midline of the embryo into the scutellum. The signal widens to form an arc and increases in expression; the arc may be at the apical edge of the embryo. The sixth slice (Figure 34.l) has signal coming from the same region as the fifth slice, however the lower oblong section has weakened in intensity. Also, the signal from the oblong signal to the apical

end of the scutellum has widened and increased in intensity. A seventh slice, not shown, had expression in the same area but much weaker. *Notably, this is the first embryo to not display a large oval signal indicative of all embryos from PIN1-e5 to PIN1-e10.*

coleoptilar stage: pin1-e12

The first embryo observed to have a coleoptilar ring is PIN1-e12. A Z-stack of the entire embryo shows the expression of PIN1 in figure 35 (Figure 35, 40x, 3x3 tile, 0.9µm slice, 7.11µm interval, 64.00µm range) and the signal around the SAM/coleoptilar ring is shown enlarged in figure 36 (Figure 36, 40x, 3x3 tile, 0.9µm slice, 7.11µm interval, 35.55µm range) for the first six slices of the Z-stack from figure 35. The expression is localized to the SAM and coleoptilar ring in the first two slices (Figure 35.a & b). The first slice is of the frontal surface and figure 36.a shows the brightfield view, while figure 36.b shows the signal only. In figure 36.a, the SAM and coleoptilar ring have shrunk to a smaller circular structure than in younger embryos. In figure 36.b, the entire coleoptilar ring shows strong expression with the strongest expression coming from the upper lateral portion of the ring. The SAM shows a strong expression at the middle base of the structure with weaker expression extending up and around in the outer layer of perimeter cells of the SAM. At the top of the SAM, expression has widened and is in all cells with a stronger expression in a few cells in the center top. Finally, there is weak expression connecting the expression in the top cells to the basal cells leaving two small sections with no expression in the center region between the perimeter and midline of the SAM. The second slice (Figure 36.c) has a reduction in expression in the top portion of the coleoptilar ring until the two upper lateral edges are reached which still show strong expression; the width of the coleoptilar ring's expression has also narrowed. The SAM

shows increased expression in the basal portion but has lost expression in the lower cells

of the perimeter. The entire upper half of the SAM shows signal and expression is

coming from the upper portion of the two regions previously not showing expression.

The third slice (Figure 35.c) maintains expression in the coleoptilar ring and the SAM but

has been reduces in both. Figure 36.d shows that all expression in the upper part of the

coleoptilar ring is gone, but the two upper lateral regions still shows strong expression.

There is still strong expression coming from the lower region of the SAM. Expression

from the upper most region of the SAM is gone, but the center of the SAM shows

expression which extends to the base of the SAM.   Also, weak expression appears in the

basal portion of the embryo directly below the coleoptilar ring and in the midline of the

upper scutellum, which can be seen in both figure 35.c and 36.d. The fourth slice (Figure

35.d), shows increase strength of expression in the midline of the upper scutellum which

reaches to tip of the scutellum and widens to a few cells on either side of the midline;

however, there is a gap in signal from the coleoptilar ring signal and the bottom of the

midline signal in the scutellum. The basal signal has also increased in strength and

resembles a "lightbulb" in shape with the wider portion at the base of the embryo near the

suspensor. The signal around the coleoptilar ring is further reduced and in figure 36.e it

shows that the coleoptilar ring expression has reduced in area to the lateral edges and a

weak expression in cells in the lower region. The expression in the SAM has moved

more basal and is contiguous with the "lightbulb" signal; the area at the base of the SAM

with the most intense signal is now part of a larger intense signal which extends further

toward the base of the embryo. The third or fourth slice may be below the SAM and the

expression may not reflect expression in the SAM.   In the fifth slice (Figure 35.d) the

signal from the midline of the scutellum has increased in strength but is in the same area. The bulb shaped signal at the base of the embryo has a weaker signal in the center of the bulb with a perimeter of stronger signal. The coleoptilar ring (Figure 36.e) only has signal at the very lower lateral edges and the signal from the "lightbulb" has widened although it has not moved further up. The midline expression appears to have reached where the top of the coleoptilar ring is present in more shallow slices. The sixth slice (Figure 35.f and Figure 36.g)) has lost all the coleoptilar ring signal and may be in tissue beneath the coleoptilar ring. The "lightbulb" shaped signal at the base of the embryo looks the same as in slice five, and the midline expression in the scutellum has further increased in strength as well as moved slightly closer to the "lightbulb" signal. The seventh slice (Figure 35.g) shows that the midline expression has reached from the tip of the scutellum to the "lightbulb" shaped signal. The eight slice (Figure 35.h) maintains much of the same signal as the seventh, but the lowest portion of the "lightbulb" no longer is showing signal. The ninth slice (Figure 35.i) is further reduced in expression, although the midline expression still reaches from the tip of the scutellum to the middle of the embryo where the strongest expression remains. The tenth slice (Figure 35.j) shows the faintest of signal from the same general area as that of the ninth slice.

stage 1: pin1-e13

In the embryo PIN1-e13, 12 DAP , the development of the embryo has reached Stage 1: the SAM, first leaf primordia and coleoptilar ring are shown in figure 37 (Figure 37, 40x, 3x3 tile, 0.9µm slice, 10.04µm interval, 110.45µm range). The first slice (Figure 37.a) only indicates expression at the very tip of the first leaf primordium. The second slice (Figure 37.b) still shows expression at the tip of the first leaf primordium, but also at

the base of the first leaf primordium and along its edge where it contacts the coleoptilar ring. The SAM, which is situated above the leaf primordium and below the coleoptilar ring shows expression. A faint signal can be seen in the center of the upper portion of the coleoptilar ring. The third slice (Figure 37.c) shows expression in the first leaf primordium in the same area, but slightly further to the base; also the structure of the leaf primordium can be seen as two small bumps on both sides of the SAM of which show some expression. The SAM shows expression. The coleoptilar ring has strong expression at the base of the first leaf primordium, but also expression can be seen around the entire ring. In the fourth slice (Figure 37.d), the first leaf primordium no longer appears to be over the SAM, but resembles a "U" in which the SAM is place inside and the "bumps" from slice three are the top of the "U". There is expression in the coleoptilar ring as before with a stronger signal at the upper lateral edges and the where the base of the first leaf primordium and coleoptilar ring meet. A small strong circular signal is coming from the first leaf primordium directly below the SAM, but still above the coleoptilar ring. Additional weak signals can be seen at the top of the SAM and out of each "bump" on either side of the SAM. The fifth (Figure 37.e) and sixth (Figure 37.f) slices show the same pattern of expression as the fourth slice, but the signal in the coleoptilar ring at the base of the first leaf primordium gets progressively weaker. Also, the coleoptilar ring's signal in the upper lateral sections moves progressively to the base along the arc of the coleoptilar ring and weaken at the top of the coleoptilar ring; as does expression in the two "bumps" of the first leaf primordium. The strong expression at the base of the leaf primordium maintains its strength, but it also moves basally. Expression in the SAM weakens in the fifth slice and further weakens in the sixth slice but covers the

whole SAM in the sixth slice. The seventh slice (Figure 37.g) has lost all expression in the lower coleoptilar ring below the SAM and first leaf primordium and has lost expression in the upper portions of the lateral signals. The expression in the first leaf primordium has moved further to the base and is contiguous with the SAM signal, which extends up to near the top of the SAM. The strong signal at the base of the first leaf primordium is still present, and a weak signal is appearing even further toward the bottom of the embryo.   In the eight slice (Figure 37.h) the lateral coleoptilar ring signal appears to move further to the base of the coleoptilar ring and the signal at the bottom of the first leaf primordium is still prominently strong. The signal in the area of the SAM and first leaf primordium look more like an extension of the more basal "bulb"-like signal, although noticeably there is a lack of signal where the coleoptilar ring would be located. In the ninth slice (Figure 37.i), the "bulb" shaped signal is stronger and still extends into the SAM, but only on the inner edge or the first leaf primordium. The lateral signals of the coleoptilar ring have moved further to the base and flank the larger signal; notably there is an increase in signal in the region where the basal coleoptilar ring would be located. In the tenth through the twelfth slice (Figure 37.j, k & l) the "bulb" shaped signal remains roughly the same in strength and area but is no longer showing signal in the SAM region. However, the lower coleoptilar ring area now shows signal which is contiguous with the lateral signals in the tenth slice (Figure 37.j). The signal along the coleoptilar ring is further reduced in area by losing expression in the most lateral regions in the eleventh slice (Figure 37.k) and more so in the twelfth slice (Figure 37.l). A weak signal in the midline, similar to embryo PIN1-e12, was first seen in a slice (not shown) between the tenth and eleventh slice. The embryo was quite large, and no signal was

92

obtained which was deeper into the embryo but may be due to the amount of tissue obscuring the signals.

DR5 and PIN1 Expression in Late Transition Stage wtih SAM Present

An embryo with both PIN1 and DR5 present (which are involved with auxin) was produced with both signals shown in figure 38. (Figure 38, 2x2 tile, 40x, 1.8µm slice, 9.67µm interval, 48.3µm range). The distribution of DR5 and PIN1 in this embryo has already been discussed separately as DR5-e5 (Figure 21) and six of the seven slices were discussed as PIN1-e10 (Figure 34.g-l), therefore this section will only address their expression in relation to each other. In the first slice (Figure 38.a) PIN1 expression is in both the pre-SAM region and the pre-coleoptilar ring region. The DR5 expression is seen only faintly in the middle of the pre-SAM region and only in the upper lateral regions of the pre-coleoptilar ring. The DR5 expression in the upper lateral regions is wider than that of the PIN1. In the second slice (Figure 38.b) PIN1 and DR5 both are still expressed in the center of the pre-SAM region. PIN1 is still seen in the pre-coleoptilar ring, but DR5 can now only seen in the border that separates the pre-SAM region from the upper pre-coleoptilar ring area. In the third slice (Figure 38.c) PIN1 expression has expanded to

the base of the embryo proper and DR5 is also seen at the base, but only a small region at the most basal area. DR5 and PIN1 both are showing the strongest expression of each in the lower center of the pre-SAM region. PIN1 still shows expression in the lower part of the coleoptilar ring. In the fourth slice (Figure 38.d), PIN1 was expressed in the upper scutellum with a reduction in expression in the pre-coleoptilar ring. PIN1 and DR5 have increased in expression in the area reaching from the lower edge of the pre-SAM region to the base of the embryo proper. However, DR5 shows a gap in expression where PIN1

expression weakens and appears at the utmost basal portion of the PIN1's range of expression; the DR5 expression here is notably stronger than the PIN1. The fifth slice (Figure 38.e) shows that the apical portion of the scutellum has strong PIN1 expression and DR5 has begun to be expressed in the upper midline area with weaker expression extending toward the top edge of the embryo. Expression for PIN1 in the lower region of the embryo resembles a "bulb" with a reduction of expression in the middle of the lower portion. DR5 shows the strongest expression in the upper portion of this "bulb" and, as before; has a gap in expression, before showing strong expression at the base of the PIN1 expression region; the expression of DR5 then extends further basally toward the region between the embryo and suspensor, although expression in the suspensor could not be determined. The sixth slice (Figure 38.f), shows that the PIN1 expression has reached from the "bulb" region up the midline of the scutellum to just below the top of the embryo. DR5 expression is lost in the most basal region of the embryo with the strongest expression at the top of the "bulb" which is in the center of the pre-SAM region. DR5 expression then follows the midline and coincides with PIN1 expression, except that two portions of the signal extend up to the outer layer of the embryo. In the seventh slice (Figure 38.g) PIN1 maintains expression the same area as in the sixth slice, but the has decreased in strength. In Addition, the upper portion which has formed an arc and is parallel with the top edge of the embryo has expanded laterally. DR5 has also maintained expression in the same area but has expanded expression at the top of the embryo and is coming from more cells in the outer layer of cells, although only mainly in two main areas.

CHAPTER IV

DISCUSSION

Comparison with Previous Screening of Embryo Specific Mutants

The generation of *emb* mutants in this report was accomplished by chemical mutagenesis using EMS and has produced different results from the Clark and Sheridan (1991) results using Robertson's *Mutator* maize stocks. Clark and Sheridan reported that out of 1000 self-pollinated ears, 51 *emb* mutations were identified in which at least 45 were independent mutation events resulting in a frequency of 4.5%. In contrast, the EMS mutagenesis generated 30 selfed ears with an *emb* segregating out of 238 ears resulting in a 12.6% mutation frequency. In comparing these two results, it is apparent that the EMS treatment can generate almost three times the amount of *emb* mutants as is generated using *Mutator* transposons. The use of transposons may limit the gene loci that can be interrupted by transposition events, since the transposon must both move and have a basis for the target gene. Genes in which a transposon is not close by may have a decreased probability of transposon insertion. In contrast, EMS mutagenesis requires that the gene only contain a G-C nucleotide pairing in the gene which when changed to an A-T nucleotide pair will result in a mutation. In addition, EMS acts on the entire genome which allows for the mutation of virtually all genes. As shown in the results reported here, EMS is effective at generating a large number of *emb* mutations.

The segregation frequency for the *emb* phenotype on self-pollinated ears for the 57 *emb* mutants ranged from 11% to 38.9% with an average of 22.3% for all ears, which indicates single-gene Mendelian inheritance. This is similar to the Clark and Sheridan (1991) *Mutator* transposon results which ranged from a 10% to 29% segregation frequency; only four *emb's* from the EMS treatment were above 29%. Clark and Sheridan reported that 12 of the mutants had a low segregation frequency which they stated were those between 10% and 18% *emb* segregation. Likewise, the EMS treatment also resulted in 12 of the *emb* mutants segregating between 10-18%.

Germination

The low germination of the frequency of most mutants indicate that many of the genes that result in the *emb* mutant phenotype may be required for normal development from the proembryo stage oneward, In addition, some mutants have been identified to form embryos that are further along in development, as with UND-19 or UND-40, and may have problems with establishing the conditions for late SAM development, or germination.

Mutation Frequency and Complementation Tests

The complementation test resulted in only two of the 24 unique combinations failing to complement each other and therefor are allelic: UND-1 and UND-10; UND-4 and UND-9. Since the crosses were selected based on similar phenotype the results are not entirely unbiased. However, the majority of the combinations tested failed to complement and with the high frequency of mutation rate observed this may indicate hundreds of loci which may produce the *emb* phenotype when mutated.

Most Embryos are Blocked in Phase 2

Normal embryo development has been described in nine stages by Abbe and Stein (1954) and in three developmental phases as described by Clark and Sheridan (Clark and Sheridan, 1991; Sheridan and Clark, 1993). Thirty-four *emb* mutants have been evaluated of which the 13 *emb* mutants described in this report are represented by 130 embryos, these were categorized according to Abbe and Stein (1954) and are presented in Table 5. Since Table 5 is a reprinted from Clark and Sheridan (1991), the three developmental phases are presented in reference to the nine stages of development by Abbe and Stein (1954).Although the delineation between the first and second phase of Clark and Sheridan categorization divides the transition stage embryos into early transition stage which is in the first phase and late transition stage which is in the second phase. The second phase ends with the differentiation of the first leaf primordium and coincides with stage 1 of Abbe and Stein (1954), while the third phase includes stages 2 through stage 6.

In the two Clark and Sheridan reports, they categorized the 51 *emb* mutants into the three phases which resulted in a distribution of 12 in the first phase, 29 in the second phase and 10 in the third phase. Using their guidelines, the 13 *emb*s described in detail here and the additional 21 *emb*, include in the Brunelle, Clark and Sheridan (2017) report, would divide the embryos as: 6 in the first phase, 25 in the second phase and 3 in the third phase. The categorization for the Brunelle, Clark and Sheridan material was based on which phase was best represented by each *emb*, and was determined by 5 or more embryos in that phase. In comparing these results, it is obvious that the majority of embryos are blocked in the second phase; 56.8% in Clark and Sheridan, and 73.5% in

Brunelle, Clark and Sheridan. The high proportion of embryos blocked in the second phase may indicate that there is an abundance of processes involved with SAM, coleoptile, and primordial leaf formation, as well as morphogenesis of the scutellum.

Many Different Phenotypes

A more detailed look at the 13 *emb* embryos presented here than described in Brunelle, Clark, and Sheridan 2017 show that 36 embryos were blocked in the first phase, 82 embryos were blocked in the second phase, and 12 were blocked in the third phase. The majority of those embryos blocked in the first phase, 30 embryos, appear to be at the late proembryo to early transition stage with an elongated suspensor. This mutant phenotype occurred in UND-17, UND-22, UND-25, and UND-38. The genes that these mutations are in may be involved with the establishment of the protoderm or in the shift from radial to bilateral symmetry which marks the change from a proembryo to a transition stage (Randolph, 1936).

Two other *embro specific* mutants, UND-20 and UND-24, both show a uniform block at a late coleoptilar stage, where the scutellum has grown apically, but doesn't appear to have grown as much laterally. They also both have either an enlarged suspensor or the RAM was established and wasn't hindered in development and reached maturity. Additional examination of the two *emb* mutants is needed such as sectioning. This may indicate that a gene or subset of genes may be involved in the apical expansion of the scutellum apart from the lateral expansion.

Embryo UND-49 shows an interesting divide; six of its embryos stopped in a transition stage with a bulbous embryo proper and the other four embryos are at a late

coleoptilar stage or near stage 1 with one a verified stage 2 embryo. The gene that the mutation is in could be involved in the establishment of the oblique meristematic axis (Randolph, 1936). However, since there are four embryos that appear to be blocked in latter stages, which have established oblique meristematic axis, then there may be other developmental processes occurring that allow for the further development of the embryo. The gene which the UND-49 mutation is in may also be required for scutellar development. The first six embryos are blocked at the point in development prior to the scutellum expanding apically and also forming the lateral lobes. In addition, the four embryos in the later stages all appear with a scutellum resembling a coleoptile shape instead of becoming ovoid. This morphology is even present in the largest embryo which has been confirmed to be in at least stage two.

Three embryos, UND-16, UND-18, and UND-39, all show a majority of their embryos in a later transition stage or early coleoptilar stage, where the scutellum has formed. In UND-16 the embryo is mainly in the transition stage and only forms a SAM/coleoptilar ring. UND-18 and UND-39 do attain coleoptilar rings, but never develop their scutellum much past the younger structure and still have a thin suspensor.

UND-40 had three very necrotic embryos in the transition or coleoptilar stage, three similar looking embryos in the later coleoptilar stage that appear to have some necrosis, and four embryos that appear to be in stage1 to stage 4 with less necrosis or none. The UND-40 embryo mutants may be needed in at different points in development which correspond with each of the stages for which it is blocked.

UND-21 has seven of its mutant transition stage embryos with strong necrosis throughout the embryos. Three addition embryos are not highly necrotic but are similar

in structure. They have not progressed as far in necrosis but were still blocked in development. Since the mutation results in a highly necrotic phenotype the lack of a functional product not only stops the development of the embryo, but triggers cell death. The UND-21 mutation may therefore be in a gene which is very important in advancing into the coleoptilar stage. Additionally, UND-40 has two mutant embryo (Figure 15-a nd-b) that show very similar phenotype to the seven highly necrotic transition stage embryos of UND-21 and may be both involved in the same processes.

The last emb mutant UND-19 is the only one of the 13 emb mutants in which all of the mutant embryos appear to have advance past the coleoptilar stage and into the later stages, however, this is based only on frontal view morphology and hasn't been internally verified by identification of primordial leaves. The UND-19 mutation may be in a gene that doesn't activate until after the establishment of the first leaf primordia, which allows for the additional growth and development. However, it may also be needed for growth or development. UND-19's germination test resulted in zero germination and the two embryos that appear furthest along in development have a stunted embryonic axis; these two instances may allude to a problem in the SAM's ability produce a viable plant.

Normal Embryo Development and Fluorescent Proteins

In order to understand how development is affected in *emb* mutant embryos it is not only useful to look at the morphology of the embryos, but also their physiological processes. The thirteen protein constructs which were crossed into the *emb* lines allow us to observe processes which cannot be seen by morphological analysis alone. When comparing the expression patterns of the eleven fluorescent protein constructs, which were examined for normal embryos, a few observations are worth noting. First, the

100

expression patterns for some of the fluorescent proteins are similar at younger stages as shown in the Figure 17 of images e, g, and h, but diverge as the embryo matures (not pictured). Second, expression in tissues, like the SAM, can display similar patterns of expression as with MRE11B in Figure 17.j and PIN1 in figure 36.b, but expression patterns in other tissue don't overlap. Third, expression in tissue like the SAM can show differences in expression, Abphyl1 (not pictured) shows expression in the entire SAM and not just the specific patter seen for MRE11b and PIN1. These differences in expression patterns for these eleven proteins indicate that there are multiple processes directing tissue formation and differentiation in which the genes that result in the *emb* phenotype may be involved.

Current and New DR5 Expression

DR5 is an auxin induced promoter that reports the presence of auxin in cells and tissues and which has not been well studied in maize embryos. It has been found to be expressed in the apical portion of the normal proembryo and in the same relative location in the normal late transition stage embryo (Chen *et al.*, 2014). The research here confirms that expression occurs at these locations, but that there is additional expression not previously reported. The first expression detected in this report is at the early proembryo stage but may not have originated from the embryo. It could be residual expression from the pre-fertilization embryonic sac, antipodal cells and "sporophytic tissues of the nucellus" as reported by Chettoor and Evans (2015). The next stage where expression was detected was in the transition stage, but due to low expression the image was originally identified as having no expression. After verifying that low DR5 expression which was detected in other stages of development could be seen more clearly

101

if laser strength, slice thickness and contrast settings were increased, these embryos were reevaluated with post image capture contrast/brightness settings. Therefore, the images of the transition stage embryo are only of the frontal surface. Chen *et al.* (2014), reported detecting signal in the endosperm on the adaxial side of the embryo and believed the embryo may be the receiving auxin from the endosperm. They didn't see any signal in the embryo, but the low expression may have been overshadowed by the bright endosperm expression. Further analysis of this stage is needed to determine if expression of DR5 is seen within the embryo at this stage. The next two embryos in Figure 19 and Figure 20 are a frontal view of embryos in late transition stage. The Chen *et al.* report detected apical expression in a late transition stage embryo, however their embryo was from a sagittal view which make comparisons difficult. Also, when viewing expression for DR5-e4 the endosperm tissue in the background and the tip of the embryo are excessively bright because the contrast was increased to see the DR5 expression in the embryo.   In Figure 1 of Chen *et al.* (2014), the surrounding tissue shows strong expression, but the intensity looks much weaker than that seen in Figure 19 and Figure 20 of this report. The additional expression of DR5 in the early coleoptilar stage and late coleoptilar embryos has not been previously reported.

Current and New PIN1 Expression

PIN1 is localized to the plasma membrane and is involved in auxin efflux transport. PIN1 expression in embryo development has been reported by both Forestan *et al*. (2010) and Chen *et al.* (2014). Forestan's Figure 4 "A" and "B" examples of expression starting at the proembryo stage with cells in the interior and appear similar to Figure 24 images "a" through "f", however Figure 24 maybe earlier in development since

fewer cells exhibit expression, or it could be that Figure 24 is a frontal view and not sagittal views. Also, expression seen in early transition stage embryos in Figure 24 "g" through "l" and Figure 25 looks like Chen *et al.*'s Figure 1 "O, P, Q, and R". The next stage of development described by Forestan *et al.* is in the transition stage at the initiation of the SAM and internally scutellum presented in Figure 4 "D". The saggital view makes it difficult to match it to one of the embryos in this report, but it would most likely be similar to Figure 30. The embryo PIN1-e7 shows the accumulation of PIN1 on the frontal face in a manner similar to Figure 4 "D" in Forestan *et al.*(2014), along with signal in the interior of the embryo which may be developing the scutellum. In Chen *et al.* (2014) Figure 1 "U" through "W" show a sagittal view of a late transition stage and may be close in development to PIN1-e8 in Figure 32 of this report. You can discern a separation of signal toward the front of the signal before it is more solid and stretches the along the apical-basal axis of the embryo. Of interest in this embryo (PIN1-e8) and another like it (PIN1-e9) presented in Figure 33, the SAM region has started to differentiate from the surrounding tissue beginning on the left side of the embryo and advancing toward the right side. Forestan *et al. (2014)* also has a sagittal view of an embryo in both the coleoptilar stage and Stage 1. The frontal views presented in Figures 35, 36 and 37 of this report verify the same general expression.

In both the Forestan *et al.* (2010) and Chen *et al.* (2014) PIN1 expression during embryo development has a gap in information which begins after each of their images of PIN1 at the early transition stage which both coincide with the PIN1-e3 embryo (Figure 25) of this dissertation. The next embryos they report on much further along in development. Forestan *et al.* reports on a transition stage embryo that likely corresponds

with the PIN1-e7 embryo (Figure 30 and 31) and Chen *et al.* reports on a late transition

stage embryo which may be an embryo between PIN1-e7 and PIN1-e8 (Figure 32).

This would indicate that the embryos which are shown in Figures 26 through 29 of this

report present information which has not been reported. PIN1 appears at the frontal

surface of embryo PIN1-e4 in transition stage (Figure 26) and widens as you advance into

the embryo. Could the embryo be already setting up the location for the SAM and

scutellum differentiation? This signal is maintained in PIN1-e5(Figure 27), but the

interior signal now extends to the top of the embryo. The next embryo, PIN1-e6, shows a

long band across the frontal surface of the embryo (Figure 28 and 29) which could be

delineating the lower boundary of the SAM across the face of the embryo.

Another gap in information is between the late transition stage and the coleoptilar

stage; this corresponds to the time after the SAM develops, but before the coleoptilar ring

develops.   Embryos at this time in development appear to be in the coleoptilar stage, but

if you stay strictly to Abbe and Stein's (1954) categories they are in the transition stage.

In Figure 34 two embryos are shown PIN1-e7 (images a-f) and PIN1-e8(images g-l).

Both show that PIN1 is being expressed in the region above the SAM and appears as

though this is for coleoptilar ring formation. The interior expression which appears wide

and globular in PIN1-e7 has reduced in area to focus in the basal portion of the embryo;

most likely establishing the RAM.

CHAPTER V

CONCLUSION

Normal maize embryo development is a complex process that needs to be better understood. The *embryo specific* mutants discussed here may provide insight into how many genes are involved in the processes when evaluating the variety of morphology displayed by the 13 *emb* described. In light of previous research with both *dek* and *emb* mutants this research supports the idea that there are likely hundreds of genes involved in maize embryo development and even in the *emb* mutant class alone.

This research has shown that the use of EMS increases the occurence of *emb* mutations by nearly three-fold and allows for blanket coverage of the genome. However, unlike *Mutator*, there is no transposon to aid in gene identification and further research will be needed to identify the genes of interest. Further complementation test between current *emb* mutants need to be done and the generation of more *embryo-specific* mutants by additional EMS treatment or planting of current materials will aid in finding more mutant alleles.

In evaluating the 130 embryos from the 13 *emb's* , along with the expression patterns of the 10 fluorescent protein constructs, it is clear that the process involved in the development of the embryo from the transition stage to the coleoptilar stage is very complex. Evaluation of the PIN1 expression, it shows that there are multiple changes in expression for PIN1 as the embryo develops from a proembryo stage to a coleoptile

stage. Each new region that begins expressing PIN1 may require new signals to begin

expression; as well as signals which direct tissues to stop expression of PIN1.

Additionally, the nine other fluorescent protein constructs display many changes in

expression during development and expression pattern which are mostly different from

each other; again suggesting many genes involved in embryogenesis that need to be

identified.   In order to evaluate the *emb* mutants, a more complete set of expression

patterns from the 12 florescent proteins are needed to distinguish the multiple changes

during embryo development from transition to coleoptilar stage.

The *embryo specific* mutants produced in this project are a part of an overall goal

to identify the genes involved specifically in embryo development. Producing the

mutations in the W22 inbreed line and crossing them repeatedly into the B73 inbreed line

has prepared materials for bioinformatics analysis. Both the W22 genome (Spring *et al.,*

2018) and B73 genome (Schable *et al.*, 2009) are available as references sequences and

will be used in the bioinformatics analysis to located genes of interest for each *emb*

mutant. The production of additional *emb* mutants and the use of complementation test

will be valuable in finding alleles for each *emb* mutant which will allow for better

identification of the mutated genes.

The discovery of genes that are specific to embryo development is the

foundational step to understanding the pathways and systems involved in embryo

development. As more genes are discovered and their functions determined, the

development of a Systems Biology for maize embryogenesis becomes possible. Kernel

viability, germination, and plant growth are dependent on the genes involved with

embryogenesis which may be essential in future application of genetic modifications of

106

maize when climate change or overpopulation will demand more food grown in more

diverse conditions.

Protein	Description of Activity	Subcellular location
DR5	Promoter used to report auxin inducible tissue specific expression	Rough and smooth ER
PIN1	Auxin efflux transport gene involved in plant architecture	Plasma membrane
TCS	Synthetic cytokinin reporter	Nucleus
pWUS	Transcription factor involved in meristem maintenance, most notably as part of the CLAVATA3-WUS feedback loop.	Nucleus
Abphyll1	A-type cytokinin-induced response regulator involved with phyllotactic patterning.	Nucleus and cytoplasm
BES1	Induced by Brassinoid steroids and is found in growing stems and elongating cells.	Nucleus
HIS1	Repressor or control element for gene expression Chromatin linker protein	Nucleus
RAB17 (dehydrin 1)	A GTPase/GTP binding protein associated with exocytic and endocytic organelles and transport vesicles between compartments.	Transport between recycling endosomes
pYabby14	Transcription factor restricted to the three adaxial tiers of cells of the maize embryo and may be involved in adaxial/abaxial patterning.	Nucleus
PRK FEA4	Chloroplast localized kinase involved in the Calvin Cycle.	Chloroplasts or amyloplasts
MREIIB	DNA repair enzyme located in the nuclei of growing tissue	Nucleus
ZmPeri	bZip transcription factor	Nucleus

Table 1. The twelve fluorescent protein constructs with a description of their activity and subcellular location.

Mutation	Founder Ear	Percent mutant kernels	Source Ears for germination test	Percent mutant kernels (χ^2)	Normal kernels		*emb* kernels	
					Number of kernels planted	Number of seedlings	Number of kernels planted	Number of seedlings
UND-16	FF609-1	24.4%	KK121-11	23.0% (0.644)	25	24	25	0
UND-17	FF609-3	23.0%	KK122-15	27.0% (0.644)	25	24	25	1
UND-18	HH110-1	22.1%	KK124-5	19.0% (0.166)	25	25(1w)	25	0
UND-19	FF610-6	20.3%	JJ252-2	18.0% (0.106)	25	24	25	0
UND-20	FF611-8	23.4%	KK105-8	24.0% (0.817)	25	25	25	0
UND-21	FF614-1	26.3%	KK131-4	24.0% (0.817)	25	25	25	0
UND-22	FF613-5	24.2%	JJ266-12	20.0% (0.248)	25	25(1w)	25	1(w)
UND-24	FF625.1	24.1%	KK134-3	25.0% (1.000)	25	24	25	3
UND-25	FF625-3	23.1%	KK135-9	23.0% (0.644)	25	25(2w)	25	3
UND-38	GG293-9	34.0%	HH494-2	24.0% (0.817)	25	25(3w)	25	0
UND-39	GG294-11	28.8%	KK113-4	26.0% (0.644)	25	25	25	0
UND-40	GG295-3	21.0%	KK139-2	18.0% (0.106)	25	24	25	3
UND-49	GG301-1	34.0%	KK143-5	19.0% (0.106)	25	25	25	0

Table 2. Germination test results. The thirteen *emb* constructs founding ears with their segregation frequency are in the second and third column. The ears used for the germination test and their segregation frequency are in the fourth and fifth column. In parentheses below the segregation frequency is the p-value of a chi-squared test for single gene Mendelian inheritance. The sixth and seventh columns are the results for germination tests of normal kernels. The eighth and ninth columns are the results for germination tests for *emb* kernels. A "w" preceded by a number and in parenthesis indicates the number of seedlings which were colored white.

Ear No.	Pollen Parent Selfed-colored		Ear Parent Selfed side-colorless		Crossed side-colored	Complement	
1	UND-9	Seg 27.0%	UND-49	Seg 24.6%	UND-49xUND-9 (LL931-13x929-2)	No Seg	Yes
2	UND-9	Seg 18.0%	UND-49	Seg 19.5%	UND-49xUND-9 LL931-10x929-8	No Seg	Yes
3	UND-18	Seg 25.0%	UND-20	Seg 24.5%	UND-20XUND-18 MM536-2X525-5	No seg	Yes
4	UND-18	Seg 17.1%	UND-20	Seg 25.9%	UND-20XUND-18 MM537-1X523-2	No seg	Yes
5	UND-18	Seg 23.1%	UND-21	Seg 35.1%	UND-21XUND-18 MM538-1X523-4	No seg	Yes
6	UND-18	Seg 23.1%	UND-21	Seg 31.4%	UND-21XUND-18 MM538-2X523-4	No seg	Yes
7	UND-18	Seg 25.1%	UND-21	Seg 26.2%	UND-21XUND-18 MM538-3X523-5	No seg	Yes
8	UND-18	Seg 25.4%	UND-21	Seg 30.6%	UND-21XUND-18 MM540-1X522-5	No seg	Yes
9	UND-18	Seg 25.4%	UND-21	Seg 29.3%	UND-21XUND-18 MM540-11X522-5	No seg	Yes
10	UND-18	Seg 16.0%	UND-22	Seg 26.3%	UND-22xUND-18 KK687-8x680-1	No Seg	Yes
11	UND-18	Seg 16.0%	UND-22	Seg 20.0%	UND-22xUND-18 KK688-1x680-1	No Seg	Yes
12	UND-18	Seg 17.9%	UND-39	Seg 20.0%	UND-39XUND-18 MM543-7X523-7	No seg	Yes
13	UND-18	Seg 17.1%	UND-39	Seg 25.5%	UND-39XUND-18 MM545-4X523-2	No seg	Yes
14	UND-19	Seg 18.7%	UND-22	Seg 16.8%	UND-22xUND-19 MM688-11x681-6	No Seg	Yes
15	UND-20	Seg 20.7%	UND-18	Seg 23.1%	UND-18xUND-20 MM530-4x525-1	No seg	Yes
16	UND-20	Seg 28.0%	UND-21	Seg 17.8%	UND-20XUND-21 MM539-4X524-3	No seg	Yes
17	UND-20	Seg 22.4%	UND-21	Seg 27.0%	UND-21XUND-20 MM540-2X525-7	No seg	Yes
18	UND-20	Seg 32.7%	UND-21	Seg 28.2%	UND-21XUND-20 MM540-6X525-2	No seg	Yes

19	UND-20	Seg 22.4%	UND-21	Seg 23.3%	UND-21XUND-20 MM540-9X525-7	No seg	Yes
20	UND-20	Seg 32.7%	UND-39	Seg 19.8%	UND-39XUND-20 MM545-6X525-2	No seg	Yes
21	UND-21	Seg 18.8%	UND-18	Seg 25.0%	UND-18XUND-21 MM530-1x526-8	No seg	Yes
22	UND-21	Seg 18.9%	UND-18	Seg 22.7%	UND-18XUND-21 MM530-3X526-3	No seg	Yes
23	UND-21	Seg 14.0%	UND-18	Seg 25.0%	UND-18-UND-21 MM530-9X527-12	No seg	Yes
24	UND-21	Seg 27.0%	UND-20	Seg 16.9%	UND-20XUND-21 MM537-6X527-14	No seg	Yes
25	UND-21	Seg 27.8%	UND-20	Seg 32.8%	UND-20XUND-21 MM537-9X527-3	No seg	Yes
26	UND-21	Seg 15.0%	UND-39	Seg 22.2%	UND-39XUND-21 MM543-8X526-5	No seg	Yes
27	UND-21	Seg 14.0%	UND-39	Seg 25.3%	UND-39XUND-21 MM543-11X524-12	No seg	Yes
28	UND-21	Seg 27.0%	UND-39	Seg 32.0%	UND-39XUND-21 MM543-12X527-14	No seg	Yes
29	UND-22	Seg 19.0%	UND-25	Seg 20.0%	UND-25xUND-22 KK690-1x682-5	No Seg	Yes
30	UND-25	Seg 19.3%	UND-22	Seg 14.8%	UND-22xUND-25 KK687-10x683-9	No Seg	Yes
31	UND-39	Seg 22.5%	UND-20	Seg 30.6%	UND-20XUND-39 MM536-3X528-3	No seg	Yes
32	UND-39	Seg 20.0%	UND-20	Seg 25.0%	UND-20XUND-39 MM536-10X528-6	No seg	Yes
33	UND-39	Seg 23.0%	UND-21	Seg 39.0%	UND-21XUND-39 MM541-4X529-6	No seg	Yes
34	UND-49	Seg 24.0%	UND-9	Seg 21.6%	UND-9xUND-49 LL932-7x930-1	No Seg	Yes
35	UND-49	Seg 29.0%	UND-9	Seg 22.0%	UND-9xUND-49 LL932-3x930-6	No Seg	Yes

Table 3. Detailed results of the complementation tests involved with the thirteen *emb*s. The first column is number 1 -35 and correspond to the same number in Table 4. The second column is the *emb* identification of the pollen parent followed by the segregation values for that plant's selfed ear in the third column. The fourth column is the *emb* identification of the ear parent followed by the segregation values for the selfed half of its ear in the fifth column. The sixth column shows the cross side of the ear parent and the sources wplants are listed in the seventh column. The eighth column gives the segregation frequency of the crossed side. The ninth column indicated if the two *emb*s complement each other.

Pollen parent	UND-9	UND-18	UND-19	UND-20	UND-21	UND-22	UND-25	UND-39	UND-49
Ear parent									
UND-9									C(34), C(35)
UND-18				C(15)	C(21), C(22), C(23)				
UND-20		C(3), C(4)			C(24), C(25)			C(31), C(32)	
UND-21		C(5), C(6), C(7), C(8), C(9)		C(16), C(17), C(18), C(19)				Cw(33)	
UND-22		C(10), C(11)					C(30)		
UND-25						C(29)			
UND-39		C(12), C(13)	C(14)	C(20)	C(26), C(27), C(28)				
UND-49	C(1), C(2)								

Table 4. Complementation tests involving eight of the thirteen *emb's* focused on in this report. The pollen parents are listed across the top and the ear parents are listed down the side. The "C" indicates that the *emb*'s complimented each other. The number in parenthesis corresponds to the detailed information provided in Table 3.

Days after pollination	0-10	10-12	12-14	14-18	18-22	22-28	28-37	37-50	50+
Embryo Stage:	pro	trans	col	1	2	3	4	5	6

	Pro	T	C	1	2	3	4	5	6
UND-17		8	1		(1)				
UND-25		8	1	(1)					
UND-38		7		(1)			(1)		
UND-22		8		(2)					
UND-16		8	2						
UND-18		5	5						
UND-21		8	0						
UND-39		5	5						
UND-49		5	2	(2)	1				
UND-24		2	5	(3)					
UND-20			8	(1)	(1)				
UND-40		2	4	(2)					
UND-19				(4)	(3)	(1)	(2)		
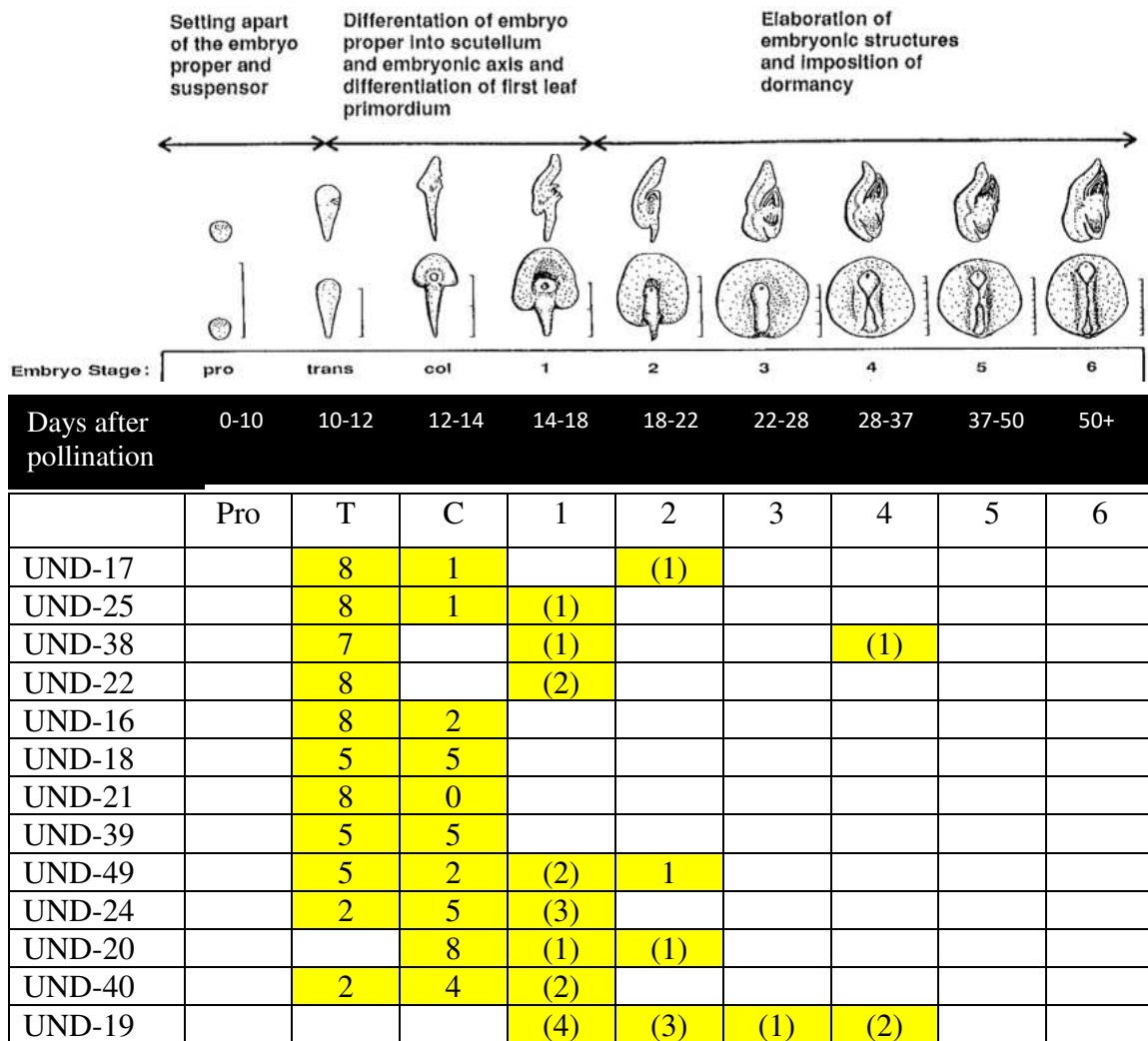
Table 5. The frequency of embryos blocked at each stage is shown for each of the 13 *emb* mutants under the embryo stage heading. For stages 1–6, values in "()" indicate the number of embryos that appear morphologically farther along in development beyond the coleoptilar stage; however, we have not confirmed the development of leaf primordia. col, coleoptilar stage; pro, proembryo stage; trans, transition stage; Stages 1-6 are indicated by their number only.

	DR5	PIN1	pWUS	TCS	HIS1	PRK	MRE 11B	AB1	RAB17	BES1	Zm PERI
UND-16	+ S	+ S	+	+	+	+	+	+	+	+	+
UND-17	+	+ S	+	+	+	+	+	+	+	+	+
UND-18	+	+ S	+	+	+	+	+	+	+	+	+
UND-19	+	+ S	+	+	+	+	+	+	+	+	+
UND-20	+	+	+	+	+	+	+	+	+	+	+
UND-21	+	+ S	+	+	+	+	+	+	+	+	+
UND-22	+	+ S	+	+	+	+	+	+	+	+	+
UND-24	+	+ S	+	+	+	+	+	+	+	+	+
UND-25	-	+	+	+	+	+	+	+	+	+	+
UND-38	+	+	+	+	+	+	+	+	+	+	+
UND-39	+	+	+	+	+	+	+	+	+	+	+
UND-40	+	+	+	+	+	+	+	+	+	+	+
UND-49	+	+	+	+	+	+	+	+	+	+	+

Table 6. Thirteen *emb* crossed with eleven fluorescent protein constructs. "+" indicates an ear segregating for the *emb* from a plant which was positive for herbicide resistance for one of the fluorescent protein constructs. "-" indicates no such ear is available. "S" indicates that a signal for that fluorescent protein construct was identified in the corresponding *emb* mutant.

Protien	Proembryo 6-7 DAP	Transition 8-9 DAP	Coleoptile 10-11 DAP	Stage1 11-12DAP
PIN1	+	+	+	+
DR5	+	+	+	na
TCS	na	na	na	na
HIS1	na	+	+	+
PRK	+	+	na	+
MREIIB	+	+	+	na
ABPHYl1	+	+	na	na
RAB17	+	+	+	na
BES1	+	+	+	na
ZmPERI	na	na	na	na
pYABBY	-	-	+	na
pWUS	-	-	+	na

Table 7. Florescent protein construct signals for normal embryos. The top row indicates the stage of development as determined by Abbe and Stein (1954) with the days after pollination (DAP) that the stages were likely collected. The protein-fluorescent constructs are listed in the leftmost column. A "+" indicates that an embryo of the corresponding stage was identified for that protein-fluorescent construct in the left column. A "-" indicates that no embryo was identified for that construct and stage for at least five-six embryos. The "na" indicates that there is no data for these materials.
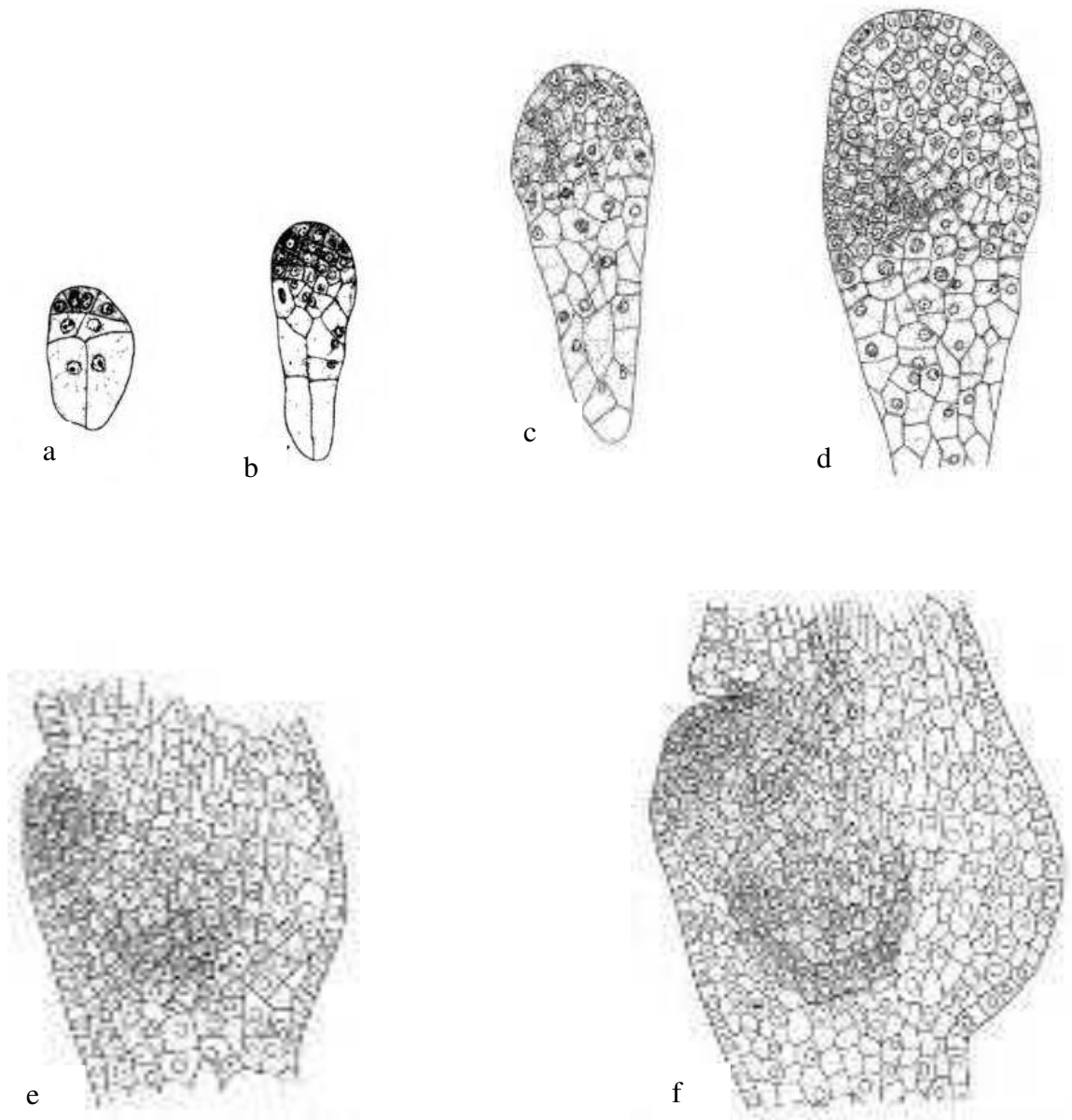
Figure 1. Normal development of a maize embryo from proembryo stage to coleoptilar stage. (a) early proembryo; (b) proembryo; (c) Late proembryo; (d) transition stage; (e) late transition stage; (f) coleoptilar stage.
Note. Figure. Modified from "Developmental morphology of the caryopsis in maize" by L.F. Randoloph, 1936, *Journal of Agricultural research,* Figure 5, 892; and Figure 6 893.
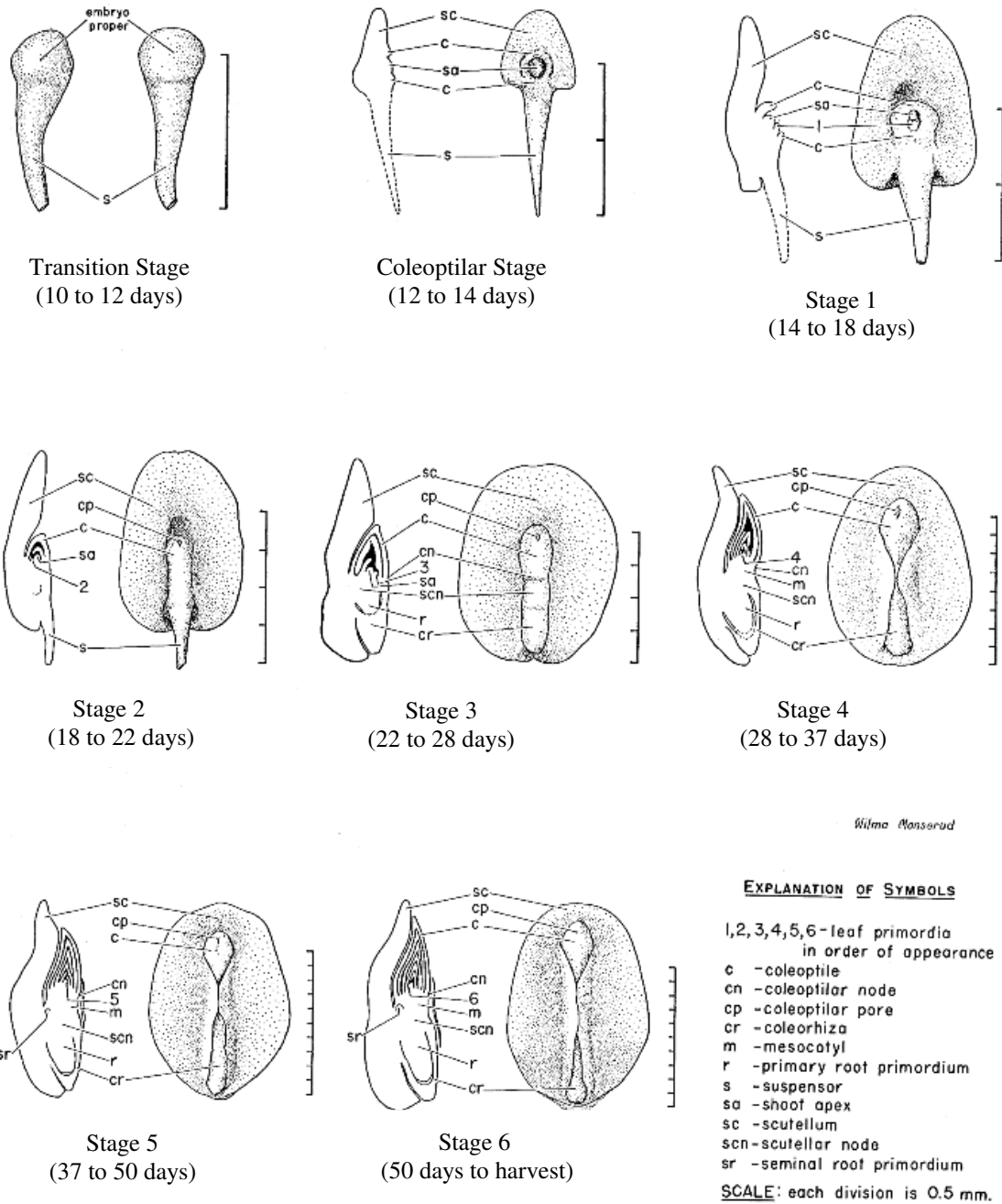
Figure 2. Eight of the nine stages of development as proposed by Abbe and Stein. Each stage of development has the sagittal view on the left and the frontal view on the right. Beneath the pictures are the stages of development proembryo (pro), transition (trans), coleoptile (col) and Stage 1 through Stage 6. The days after pollination is presented below the stage of development. In between the sagittal view and frontal view are symbols that are referenced in the legend which identify important structures for each stage of development.

Note. Figure. Modified from "The growth of the shoot apex in maize:embryogeny" by Abbe and Stien 1954, *American Journal of Botonay 41,,* Figures 2-9 pg287.
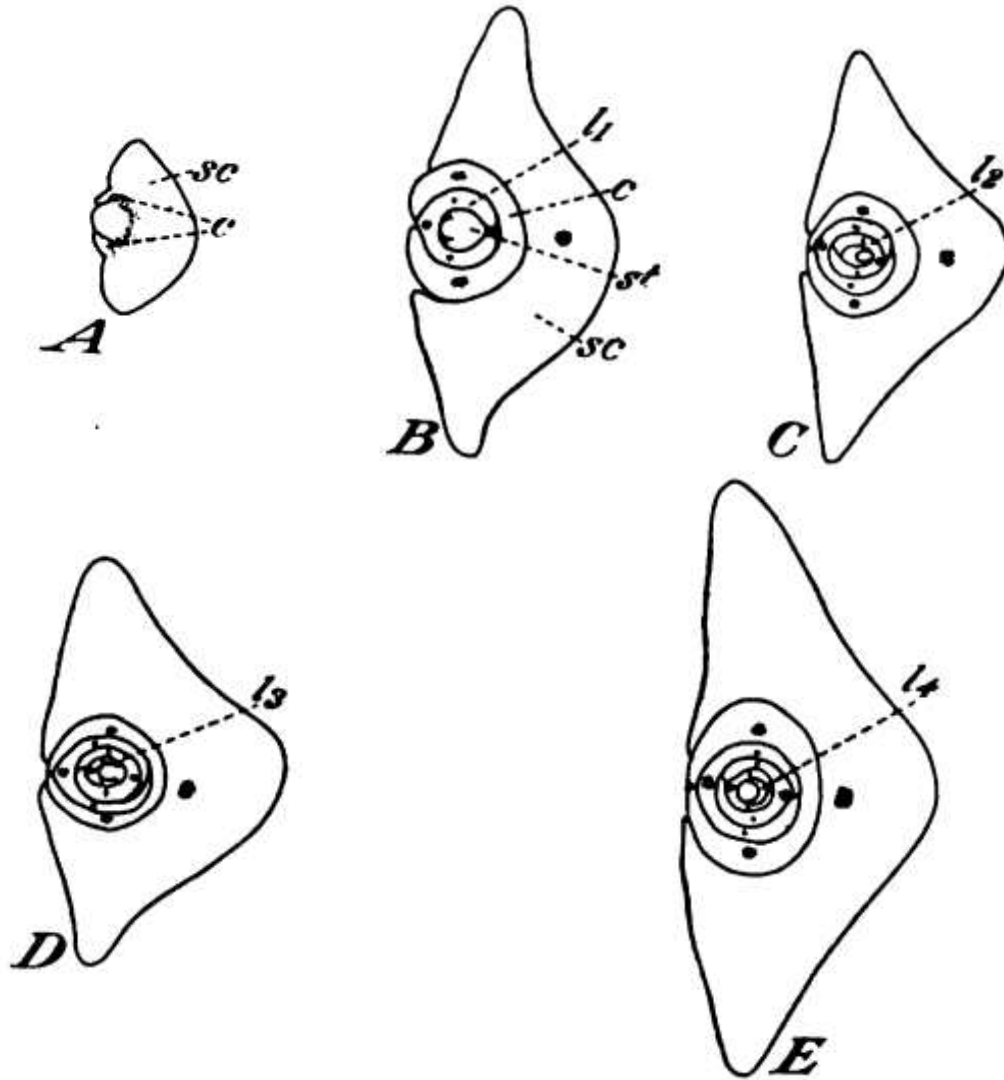
Figure 3. A cross-section of embryos for five stages of development (a) coleoptilar stage (b) stage 1 (c) stage 2 (d) stage 3 € stage 4. Sc= scutellum, c=coleoptile, st= shoot apical meristem, l_1= first leaf primordium, l_2=second leaf primordium, l_3 = third leaf primordium, l_4 = fourth leaf primordium. *Note*. Figure. Modified from "Developmental morphology of the caryopsis in maize" by L.F. Randoloph, 1936, *Journal of Agricultural research,* Figure 8, р. 896.
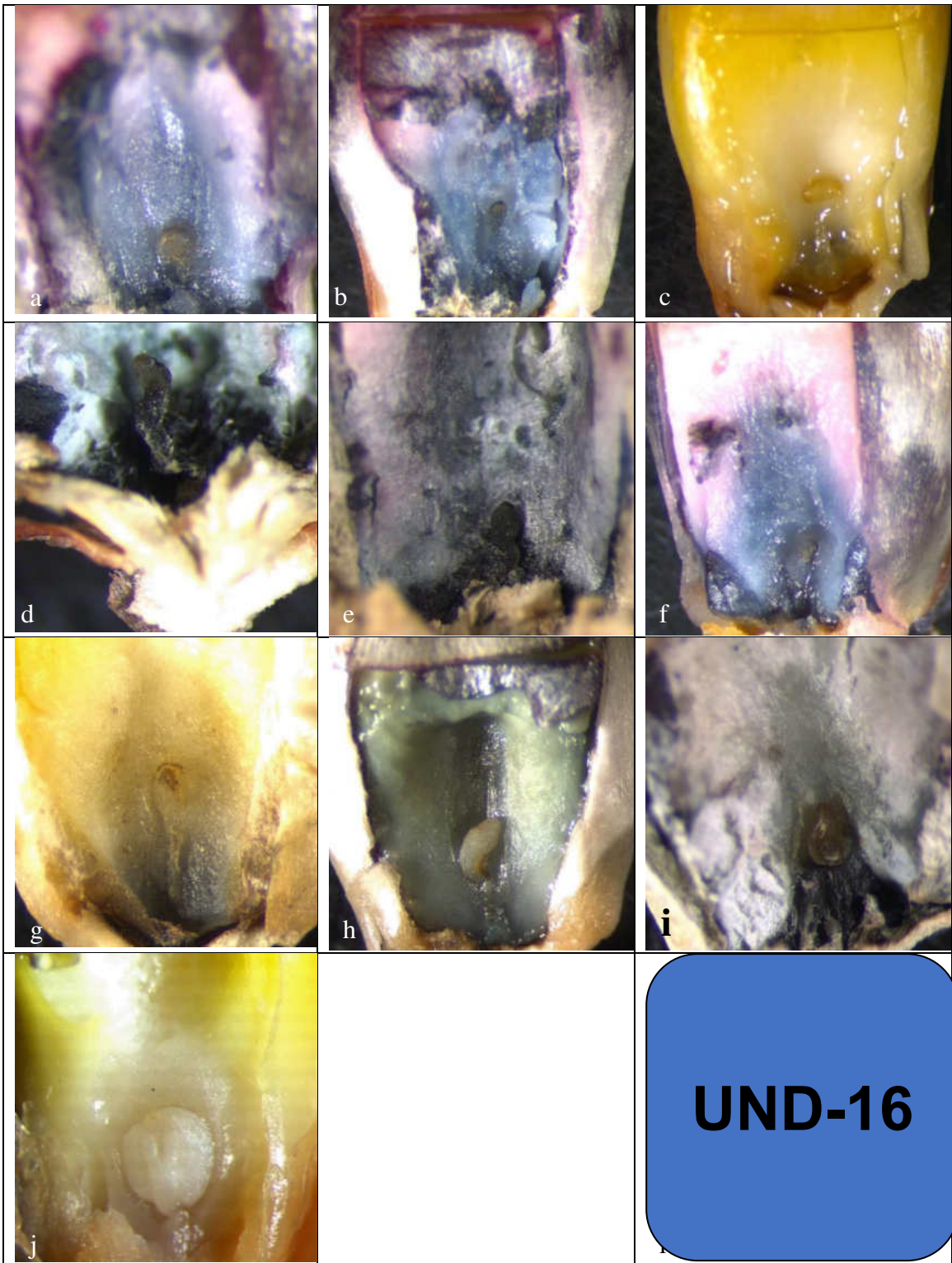
Figure 4. UND-16 embryos blocked in development (a) transition stage; (b) transition stage; (c) transition stage; (d) late transition stage; (e) late transition stage; (f) late transition stage; (g) late transition stage; (h) late transition stage; (i) coleoptilar stage; (j) abnormal coleoptilar stage.
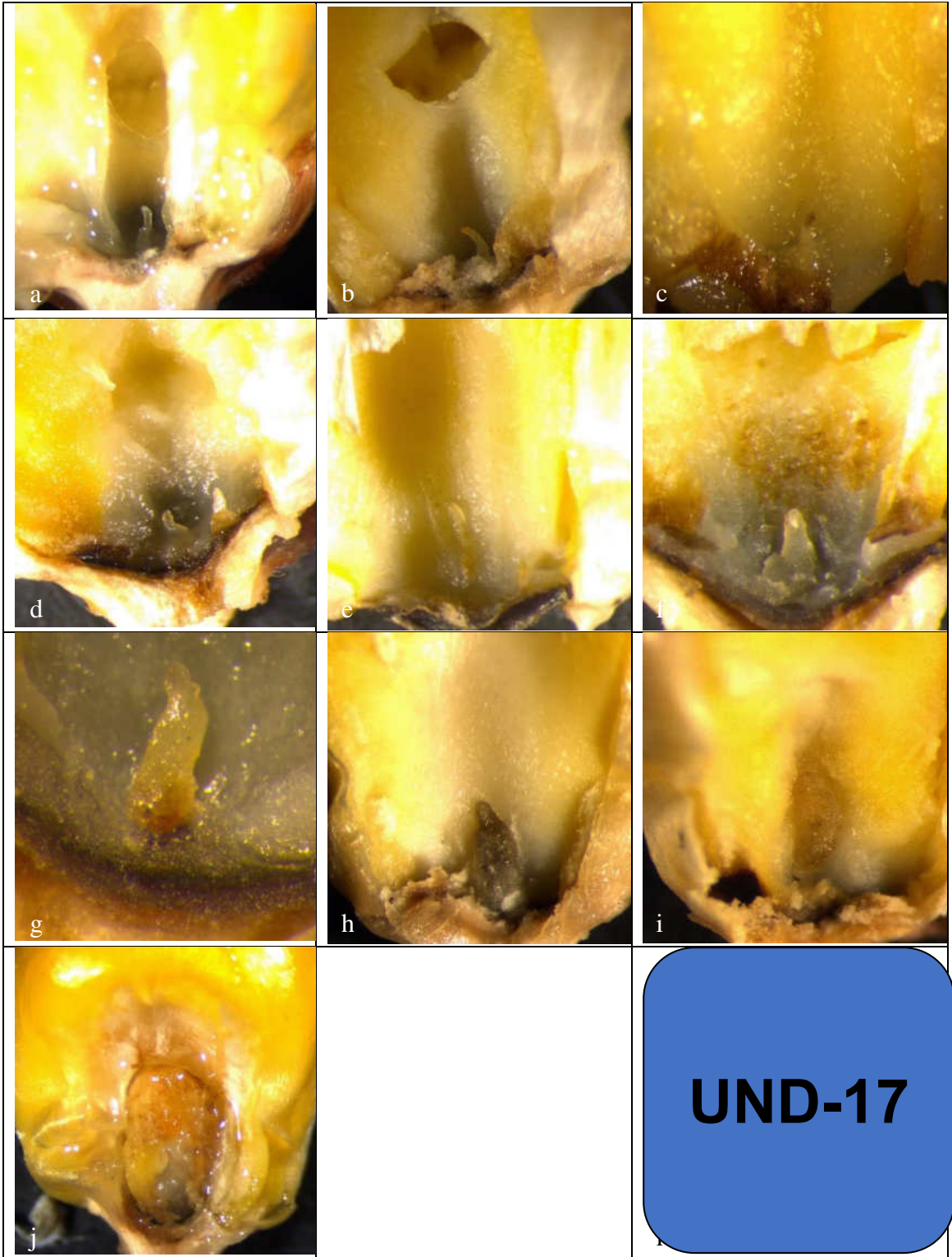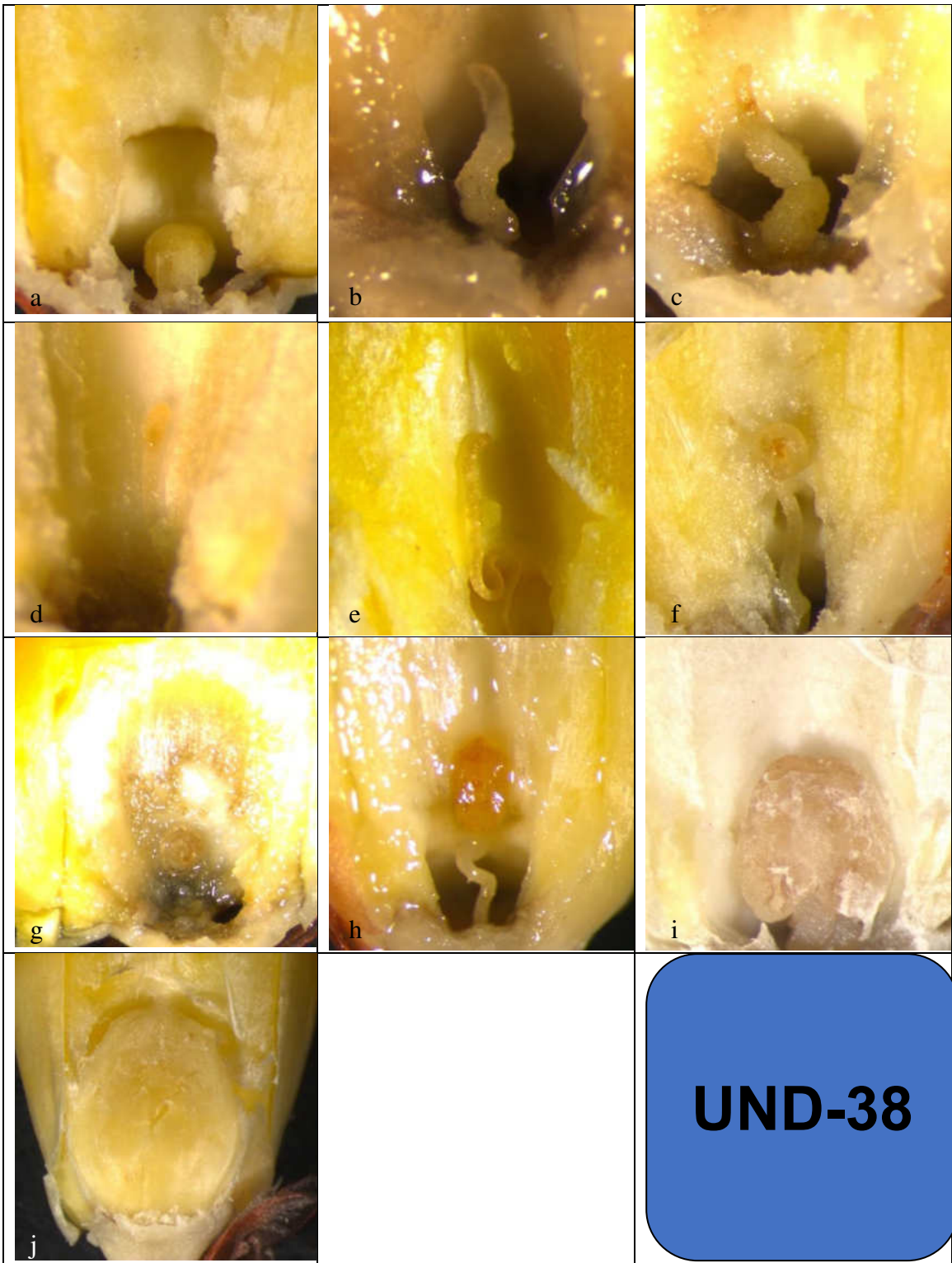
Figure 5. UND-17 embryos blocked in development (a) early transition stage; (b) early transition stage; (c) early transition stage; (d) early transition stage; (e) early transition stage; (f) early transition stage; (g) early transition stage; (h) early transition stage; (i) coleoptilar stage; (j) abnormal coleoptilar stage possible Stage 2.
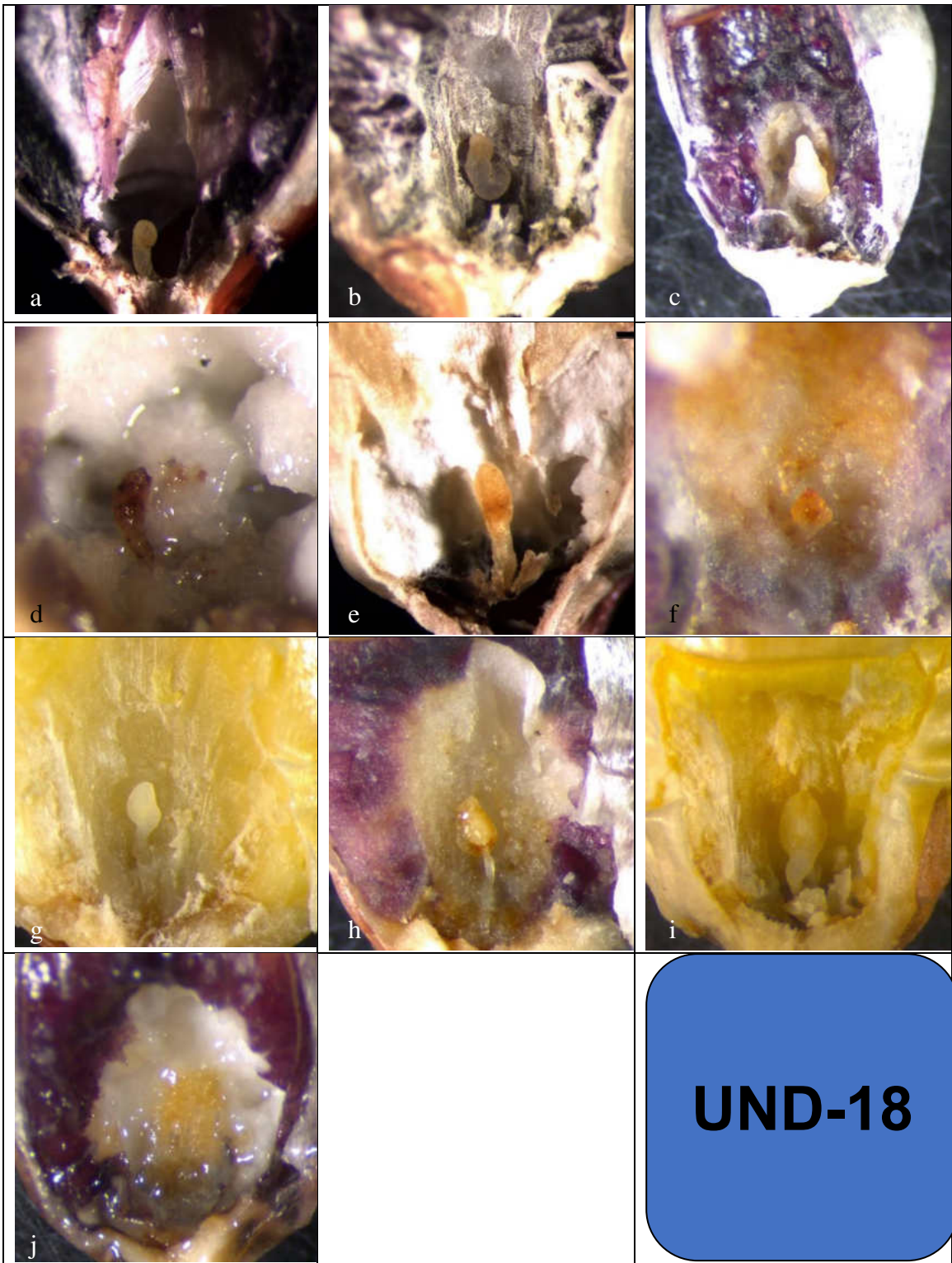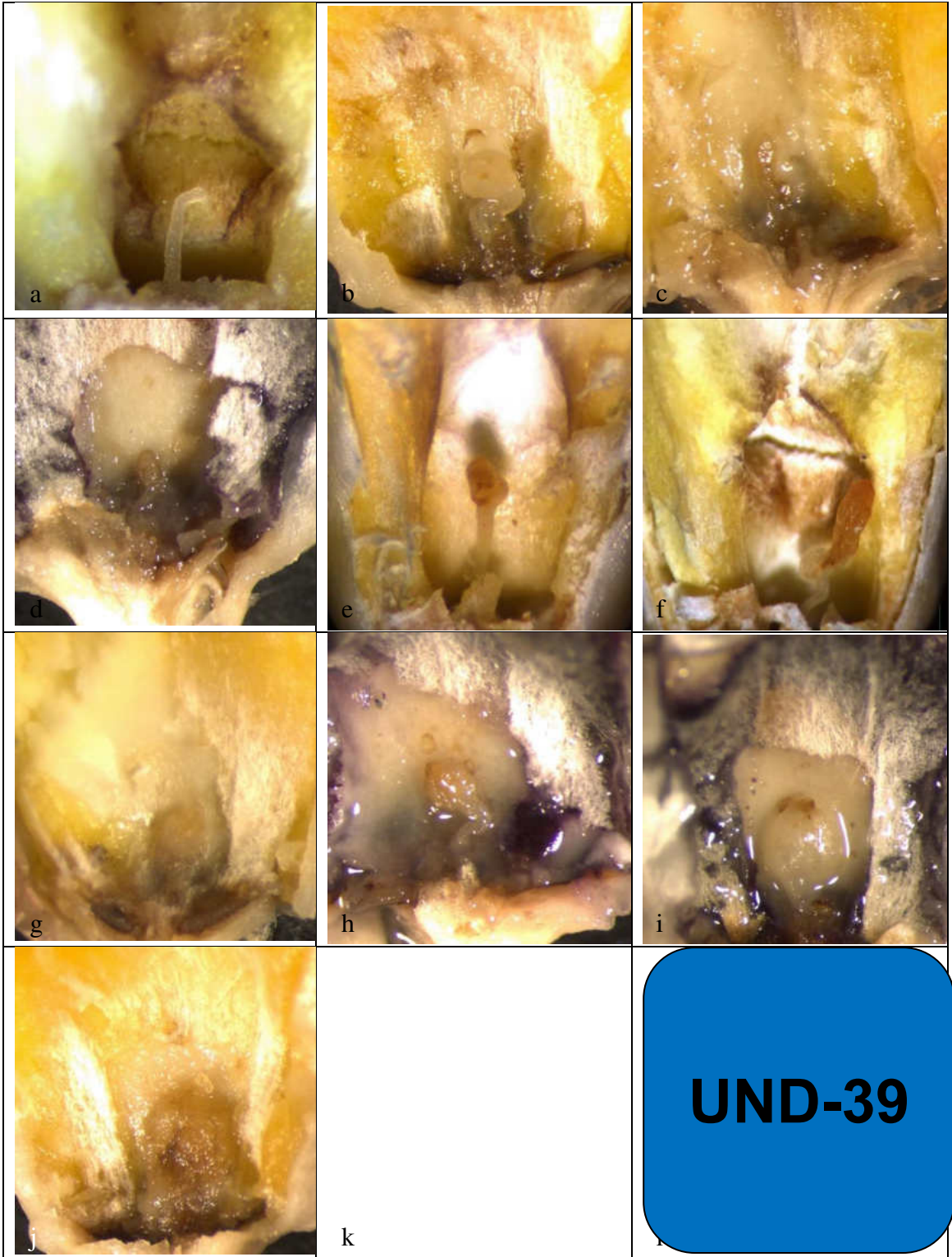
Figure 6. UND-18 embryos blocked in development (a) transition stage; (b) transition stage; (c) transition stage; (d) late transition stage; (e) late transition stage; (f) coleoptilar stage; (g) coleoptilar stage; (h) coleoptilar stage; (i) late coleoptilar stage; (j) abnormal coleoptilar stage.
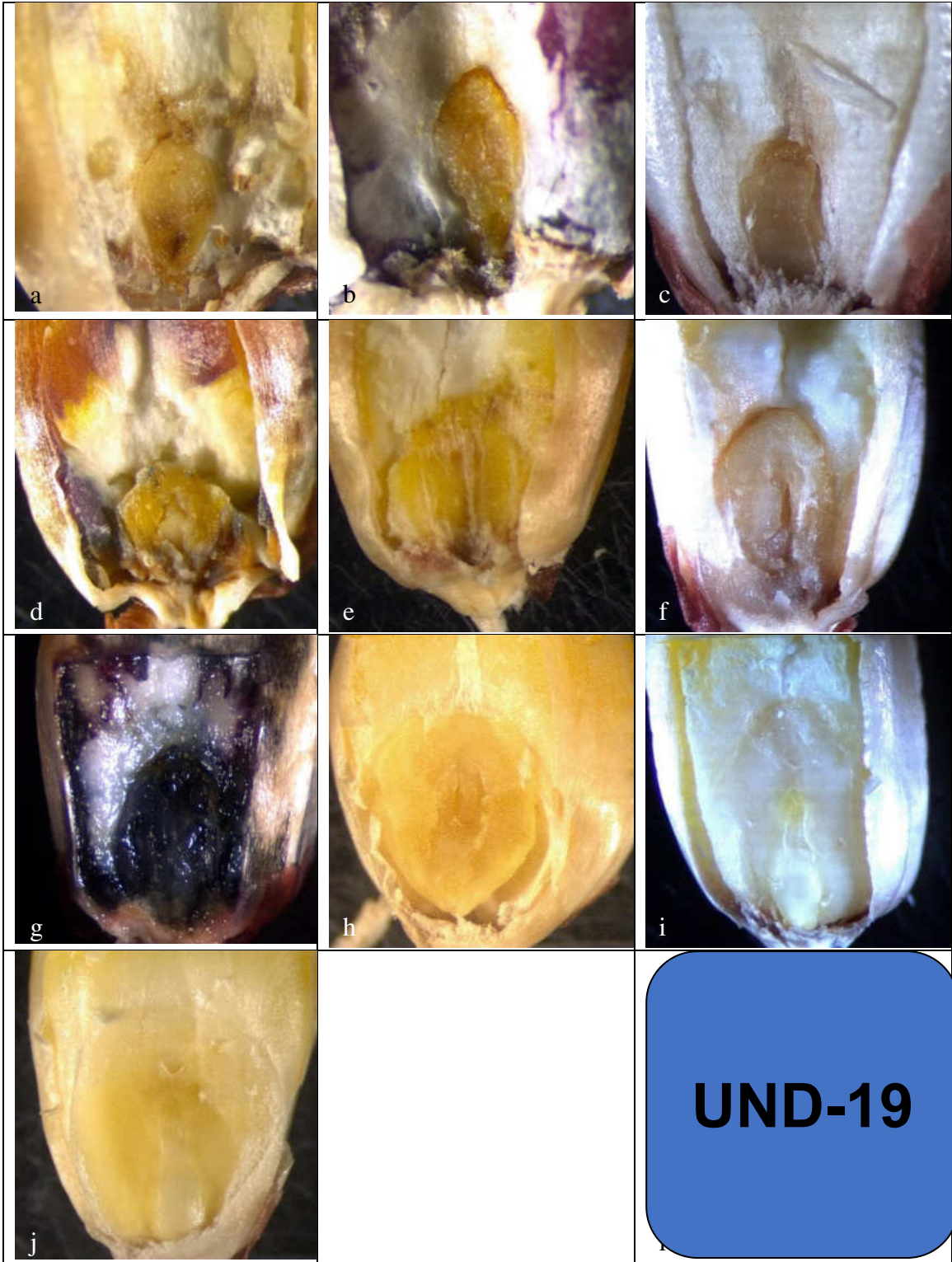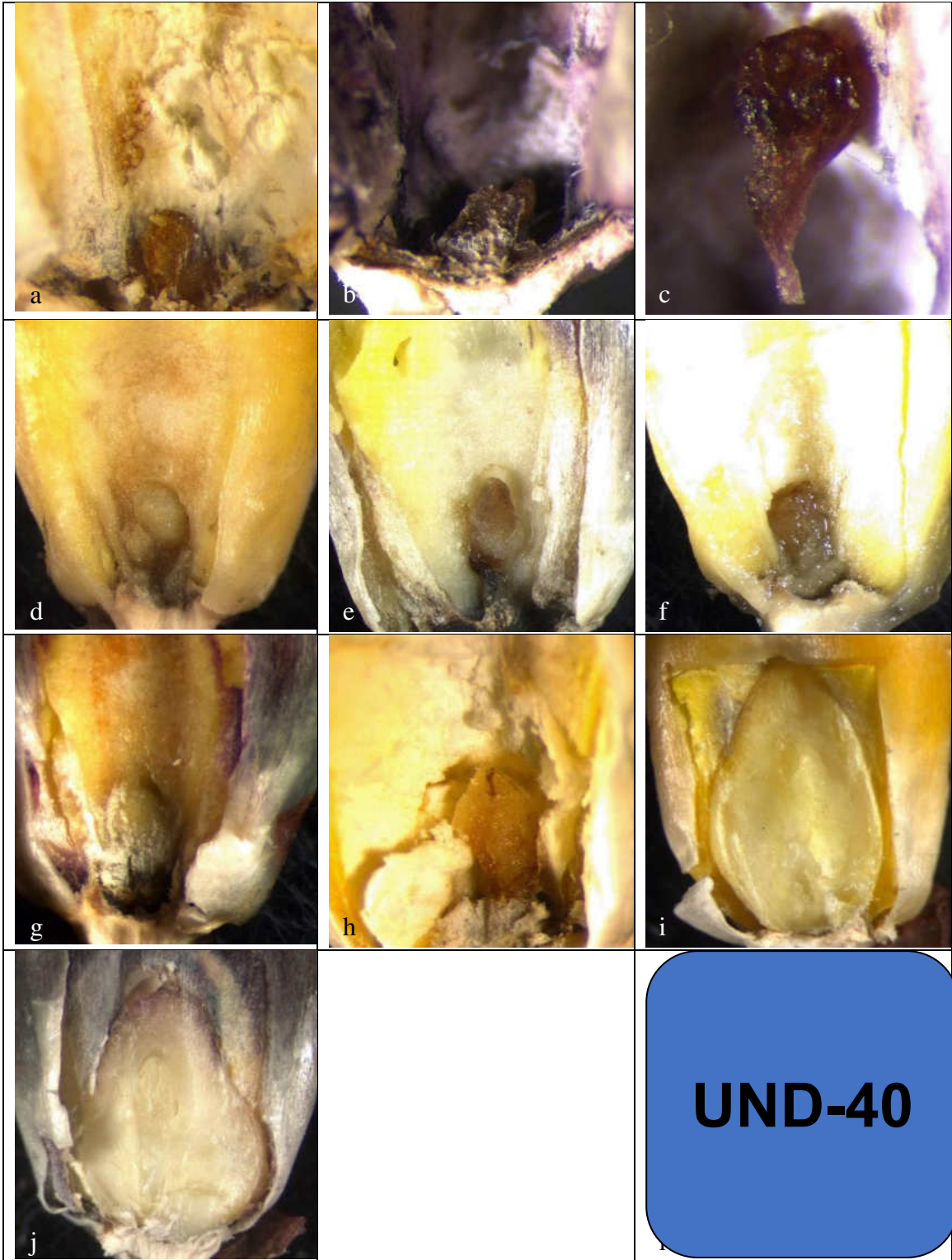
Figure 7. UND-19 embryos blocked in development. All of the embryos appear to have developed beyond the coleoptilar stage and are being evaluated based on the scutellum and embryonic axis structure in their frontal view as referenced to Abbe and Stein (1954). (a) stage1; (b) stage 1; (c) stage 1; (d) stage 1; (e) stage 2; (f) stage 2; (g) stage 2; (h) stage 3; (i) stage 4; (j) stage 4.
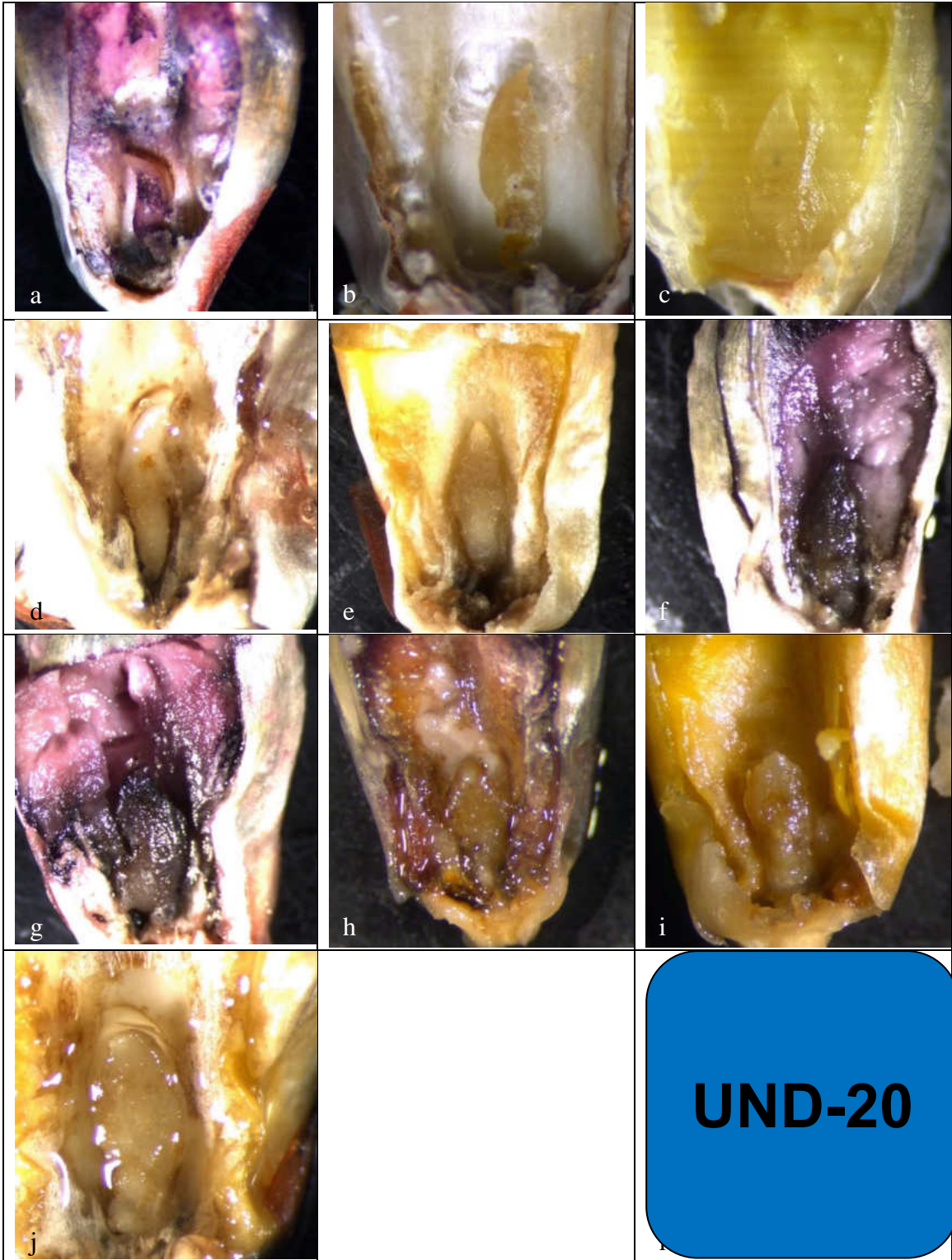
Figure 8. UND-20 embryos blocked in development (a) early coleoptilar stage; (b) early coleoptilar stage; (c) coleoptilar stage; (d) coleoptilar stage; (e) coleoptilar stage; (f) coleoptilar stage; (g) coleoptilar stage; (h) late coleoptilar stage; (i) stage 1; (j) stage 2. Those embryos beyond the coleoptilar stage have not been verified and are only in reference to frontal development as indicated by Abbe and Stein (1954).
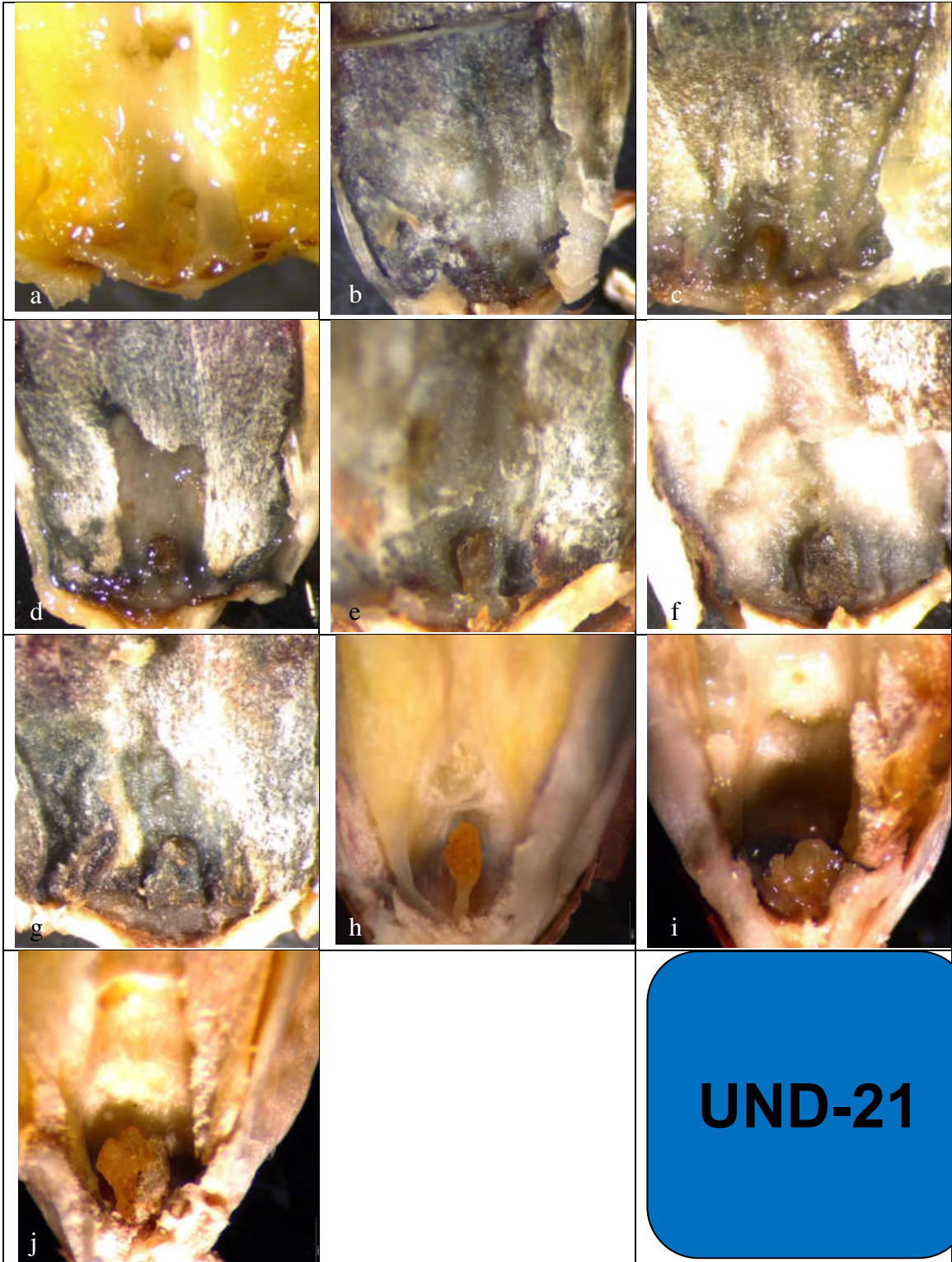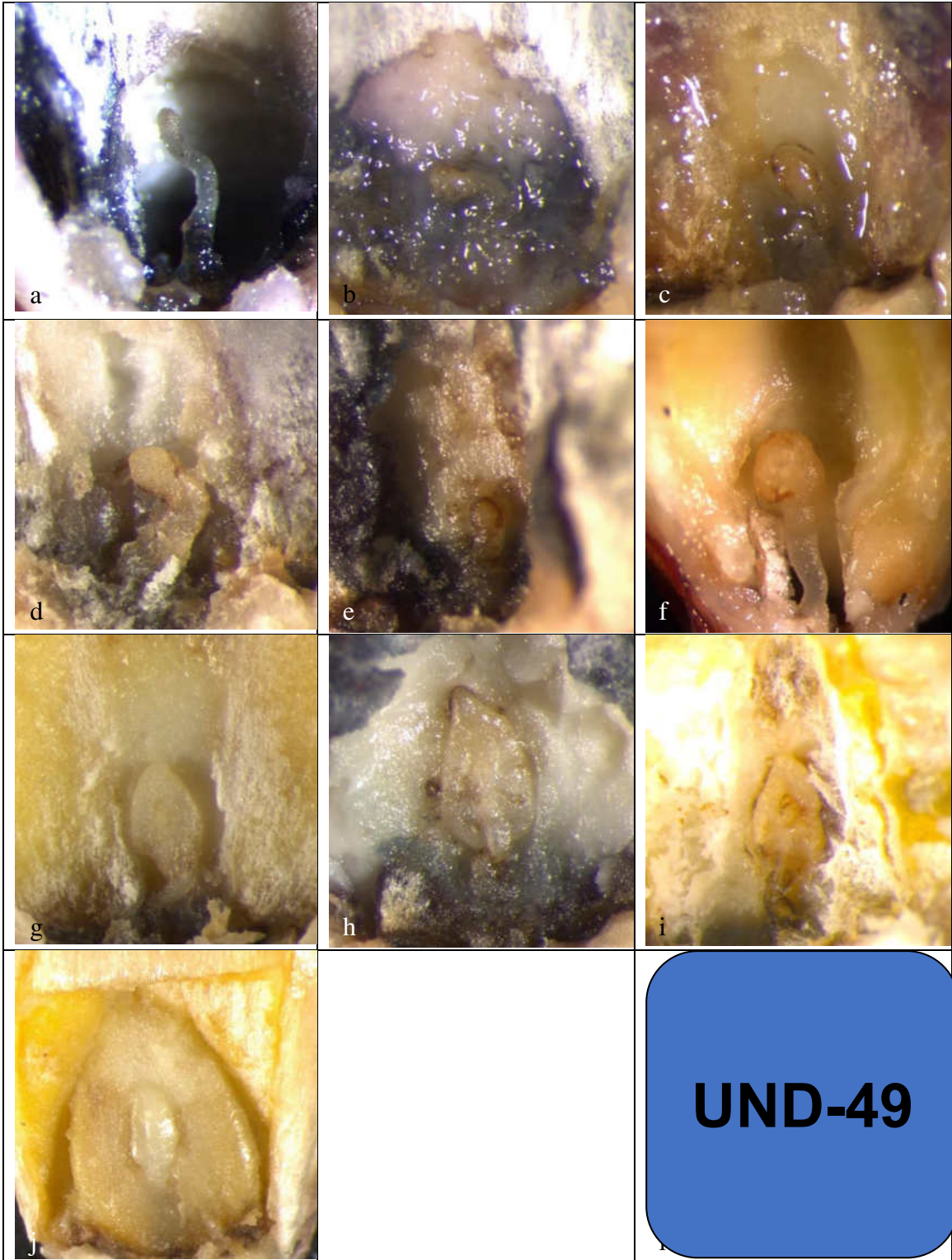
Figure 9. UND-21 embryos blocked in development (a) early transition stage; (b) early transition stage; (c) transition stage; (d) transition stage; (e) transition stage; (f) transition stage; (g) transition stage; (h) late transition stage; (i) abnormal coleoptilar stage; (j) abnormal coleoptilar stage.
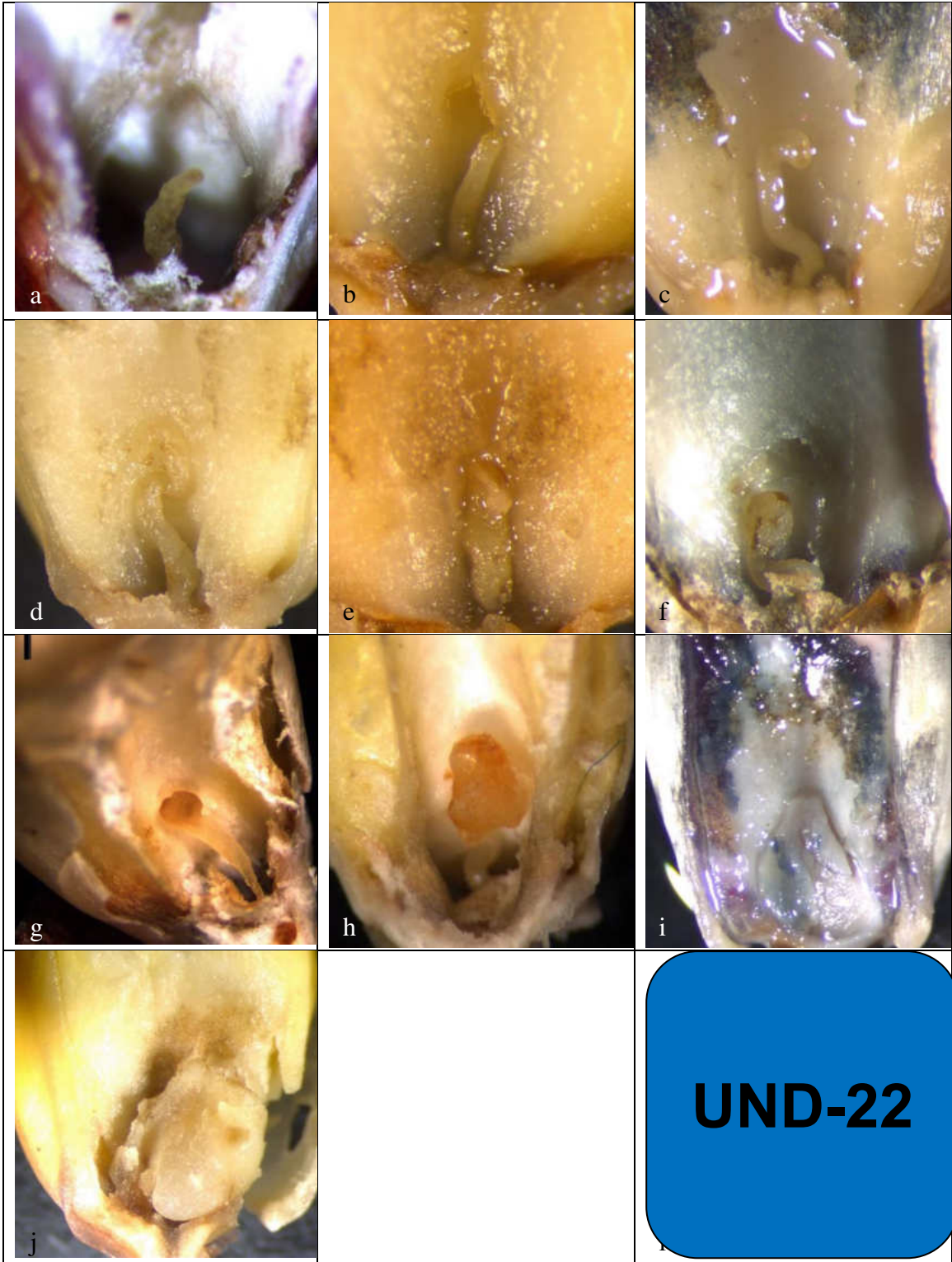
Figure 10. UND-22 embryos blocked in development (a) early transition stage; (b) early transition stage; (c) early transition stage; (d) early transition stage; (e) abnormal transition stage; (f) transition stage; (g) transition stage; (h) late transition stage; (i) stage 1; (j) Abnormal stage 1.

Those embryos beyond the coleoptilar stage have not been verified and are only in reference to frontal development as indicated by Abbe and Stein (1954).

126
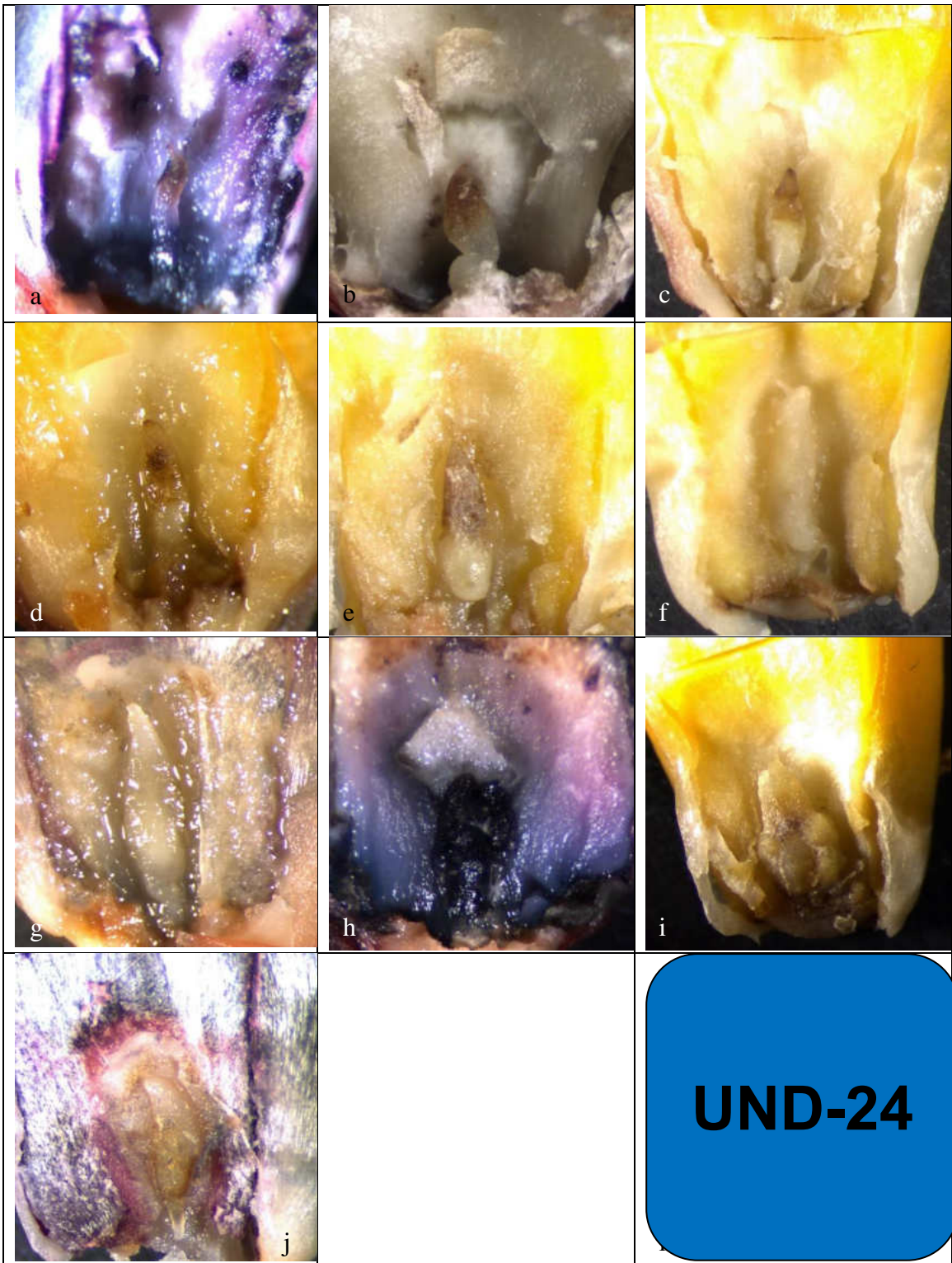
Figure 11. UND-24 embryos blocked in development (a) late transition stage; (b) late transition stage; (c) coleoptilar stage; (d) coleoptilar stage; (e) coleoptilar stage; (f) coleoptilar stage; (g) coleoptilar stage; (h) abnormal stage 1; (i) abnormal stage 1; (j) abnormal stage 1.

Those embryos beyond the coleoptilar stage have not been verified and are only in reference to frontal development as indicated by Abbe and Stein (1954).
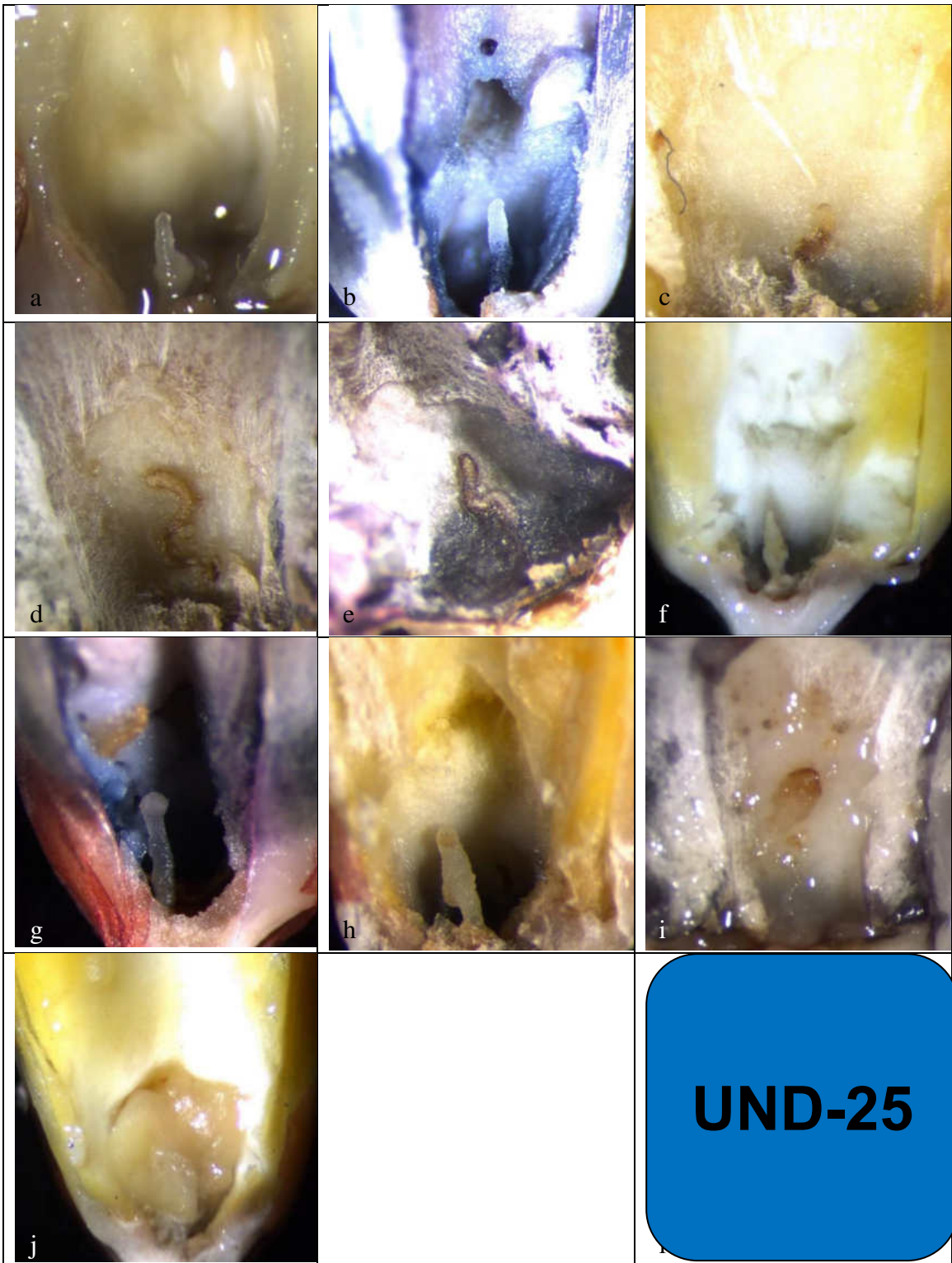
Figure 12. UND-25 embryos blocked in development (a) early transition stage; (b) early transition stage; (c) early transition stage; (d) early transition stage; (e) early transition stage; (f) early transition stage; (g) transition stage; (h) transition stage; (i) coleoptilar stage; (j) abnormal stage 1.
Those embryos beyond the coleoptilar stage have not been verified and are only in reference to frontal development as indicated by Abbe and Stein (1954).

Figure 13. UND-38 embryos blocked in development (a) proembryo; (b) early transition stage; (c) early transition stage; (d) early transition stage; (e) early transition stage; (f) early transition stage; (g) early transition stage; (h) late transition stage; (i) stage 1; (j) stage 4
Those embryos beyond the coleoptilar stage have not been verified and are only in reference to frontal development as indicated by Abbe and Stein (1954).

Figure 14. UND-39 embryos blocked in development (a) transition stage; (b) transition stage; (c) transition stage; (d) transition stage; (e) late transition stage; (f) coleoptilar stage; (g) coleoptilar stage; (h) coleoptilar stage; (i) coleoptilar stage; (j) abnormal coleoptilar stage.

Figure 15. UND-40 embryos blocked in development (a) transition stage; (b) transition stage; (c) coleoptilar stage; (d) coleoptilar stage; (e) coleoptilar stage; (f) coleoptilar stage; (g) stage 1; (h) stage 1; (i) stage 4; (j) Stage 4 or 5

Those embryos beyond the coleoptilar stage have not been verified and are only in reference to frontal development as indicated by Abbe and Stein (1954).

Figure 16. UND-49 embryos blocked in development (a) transition stage; (b) transition stage; (c) transition stage; (d) transition stage; (e) transition stage; (f) abnormal coleoptilar stage; (g) coleoptilar stage; (h) coleoptilar stage; (i) coleoptilar stage; (j) Stage 2 verified by cross section.

Those embryos beyond the coleoptilar stage have not been verified and are only in reference to frontal development as indicated by Abbe and Stein (1954).
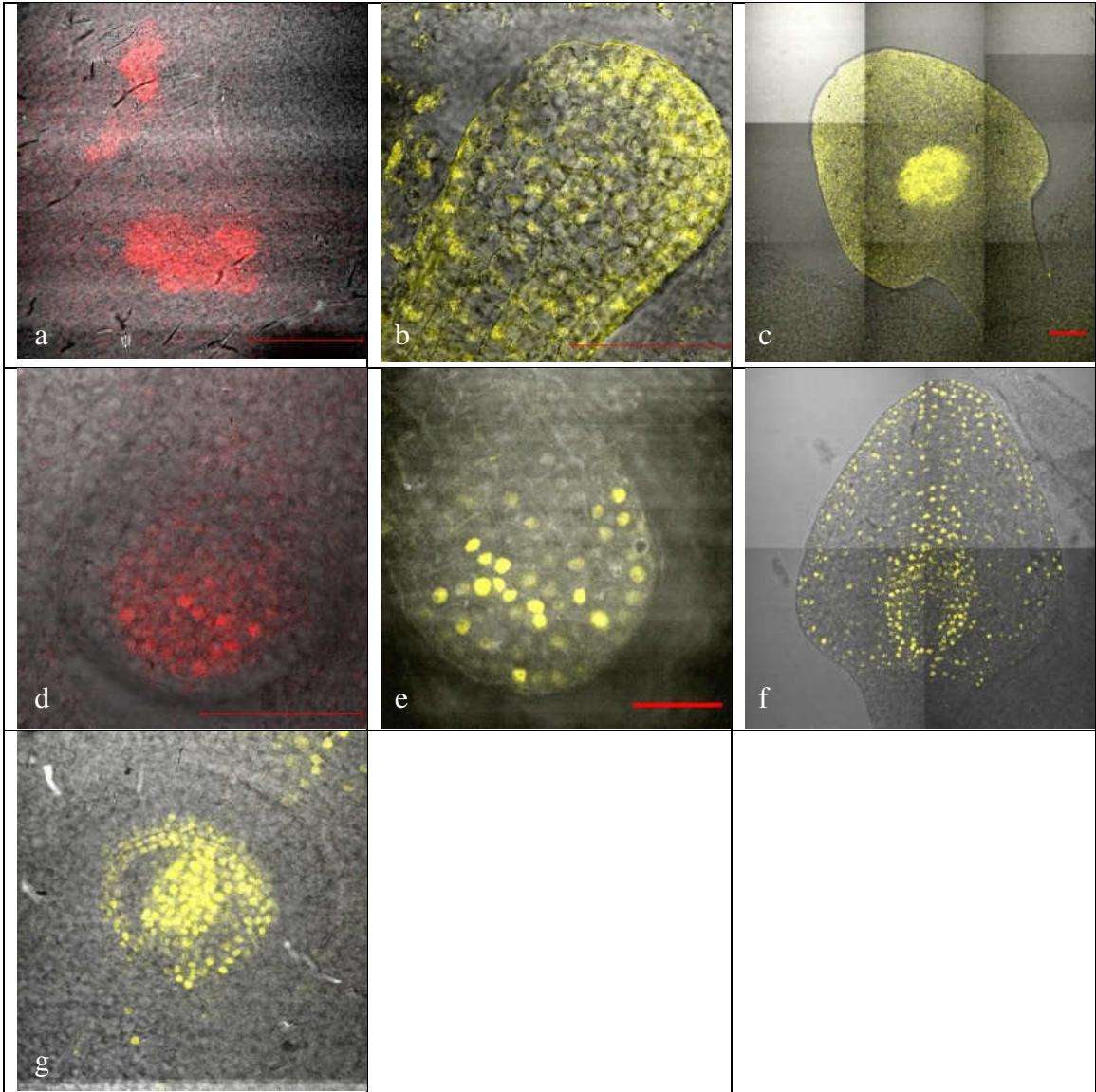
Figure 17. Examples of expression for seven fluorescent protein constructs in normal developing embryos (a) pWus coleopotilar stage; (b) RAB17 transition stage; (c) PRK coleoptilar stage; (d) Abphyll1 transition stage; (e) BES1 transition stage; (f) HIS1 coleoptilar stage; (g) MRE11B coleoptilar ring.
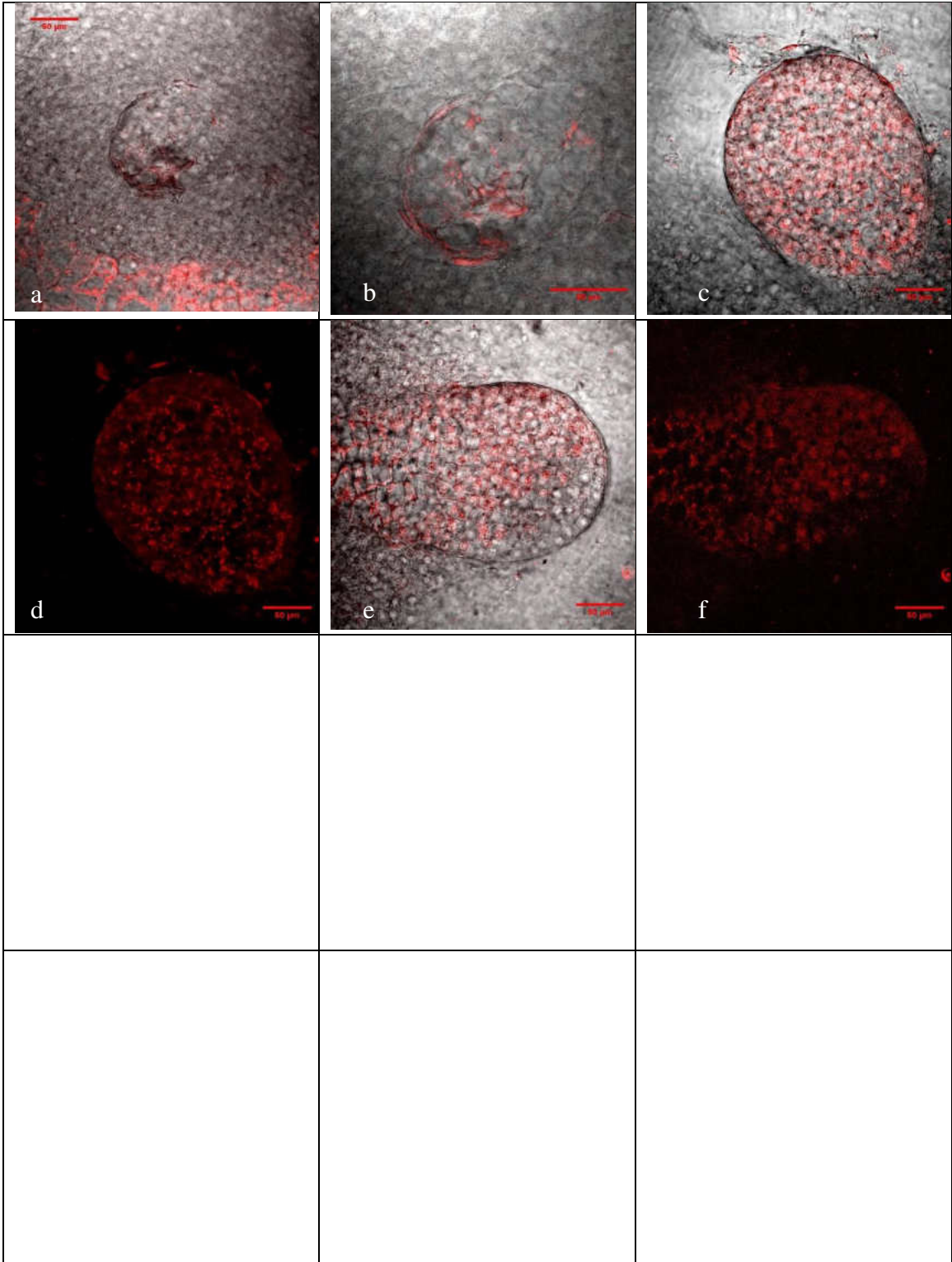
Figure 18. DR5-RFP expression in normal embryos: DR5-e1, DR5-e2, DR5-e3. (a) DR5-e1, proembryo, 40x, 3.8µm; (b) DR5-e1, proembryo, 63x, 3.8µm; (c) DR5-e2, 40x, 5.0µm, signal/brightfield; (d) DR5-e2, 40x, 5.0µm, signal only; (e) DR5-e3, 40 x, 3.2µm; (f) DR5-e3, 40x, 3.2µm, signal only. All bars are 50µm.
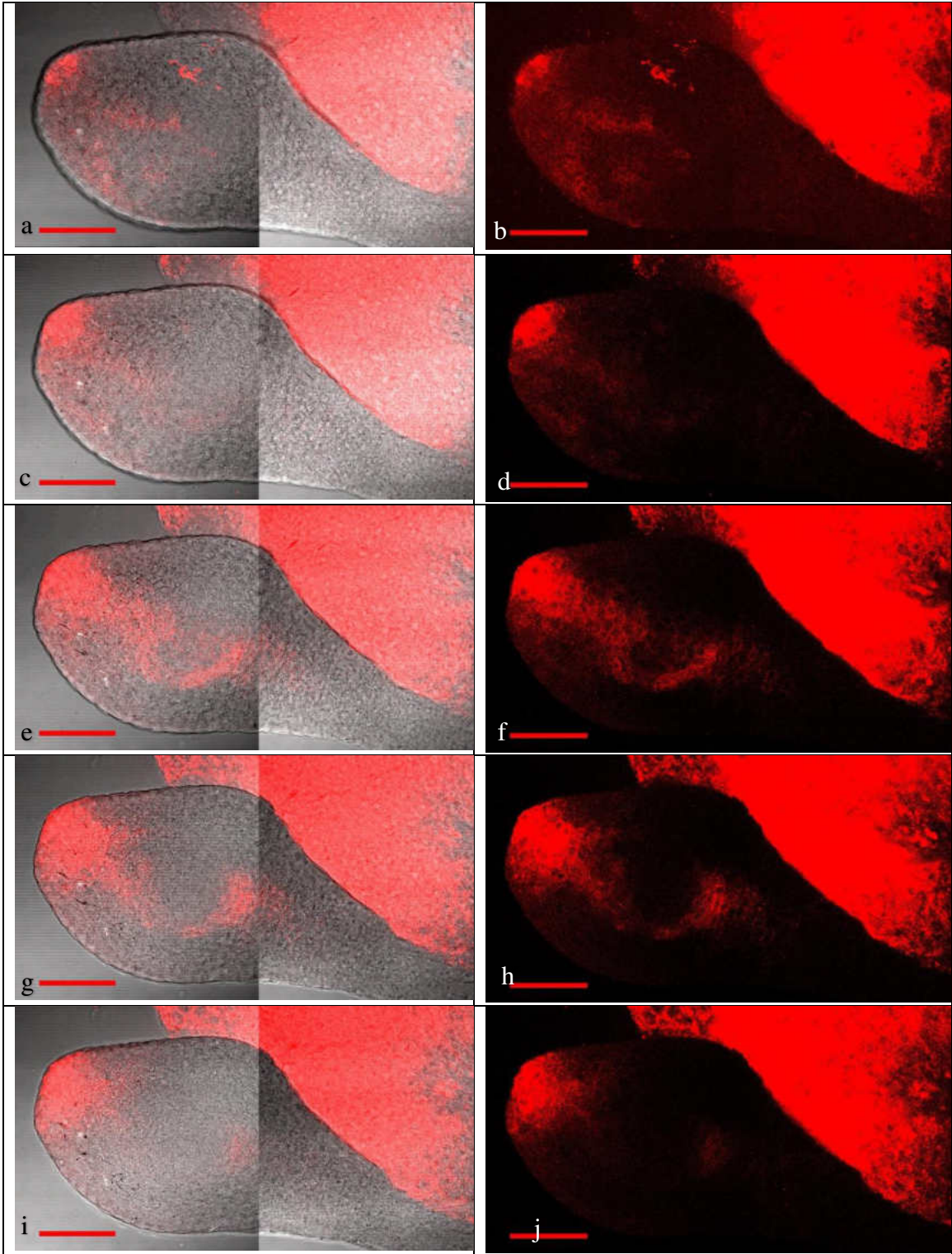
Figure 19. DR5-RFP expression in normal embryo: DR5-e4. Late transition stage, 2x1 Tile, 40x, 2.7µm slice, 7.09µm interval, 42.51µm range. Each slice is paired with the signal/brightfield image preceding the signal only of the same image. (a-j) slices 1 through 5 of 7. All images 100µm bar.
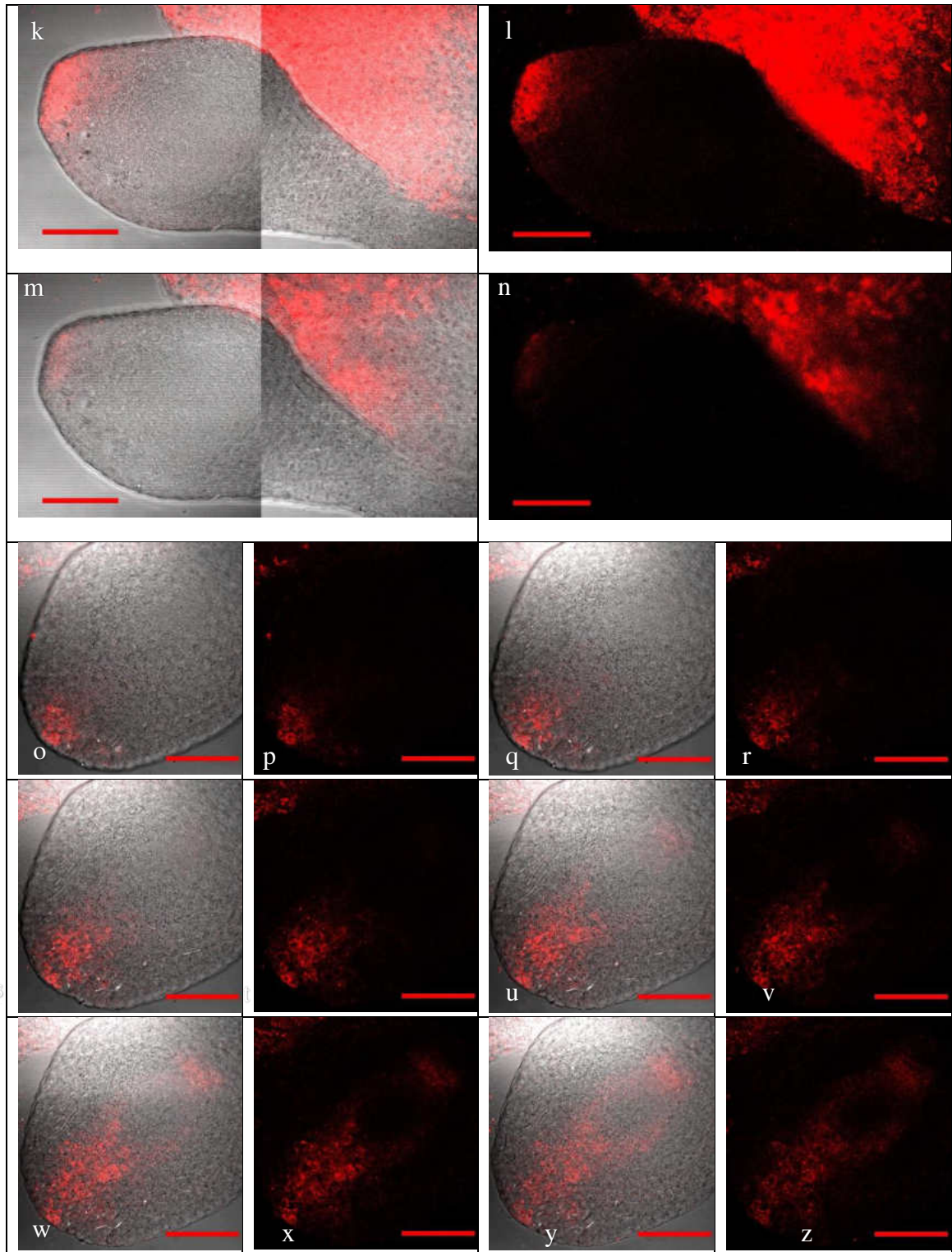
Figure 20. DR5-RFP expression in normal embryos: DR5-e5, DR5-e6. Late transition stage. Each slice is paired with the signal/brightfield image preceding the signal only of the same image (k-n) DR5-e5, 2x1 tile, 40x, 2.7µm slice, 7.09µm interval, 42.51µm range. Slices 6 and 7 of 7; (o-z) DR5-e6, 40x, 2.7µm slice, 3.54µm interval, 21.26µm range. All images 100µm bar.
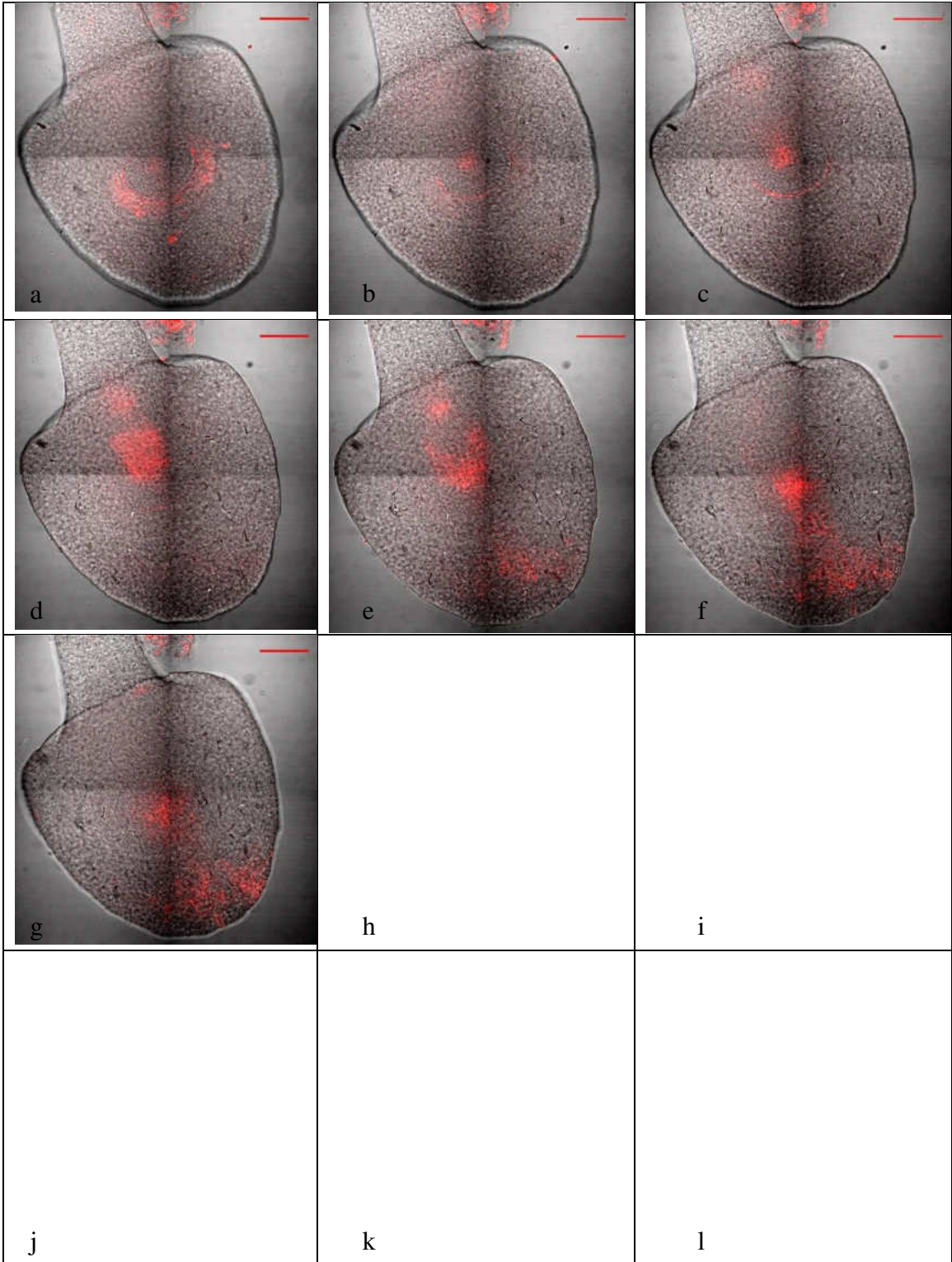
Figure 21. DR5-RFP expression in normal embryo: DR5-e6. Early coleoptilar stage, 2x2 Tile, 40x, 1.8µm slice, 9.67µm interval, 58.0µm range. Images taken with PIN1 (see Figures 34 and 38) All images 100µm bar.
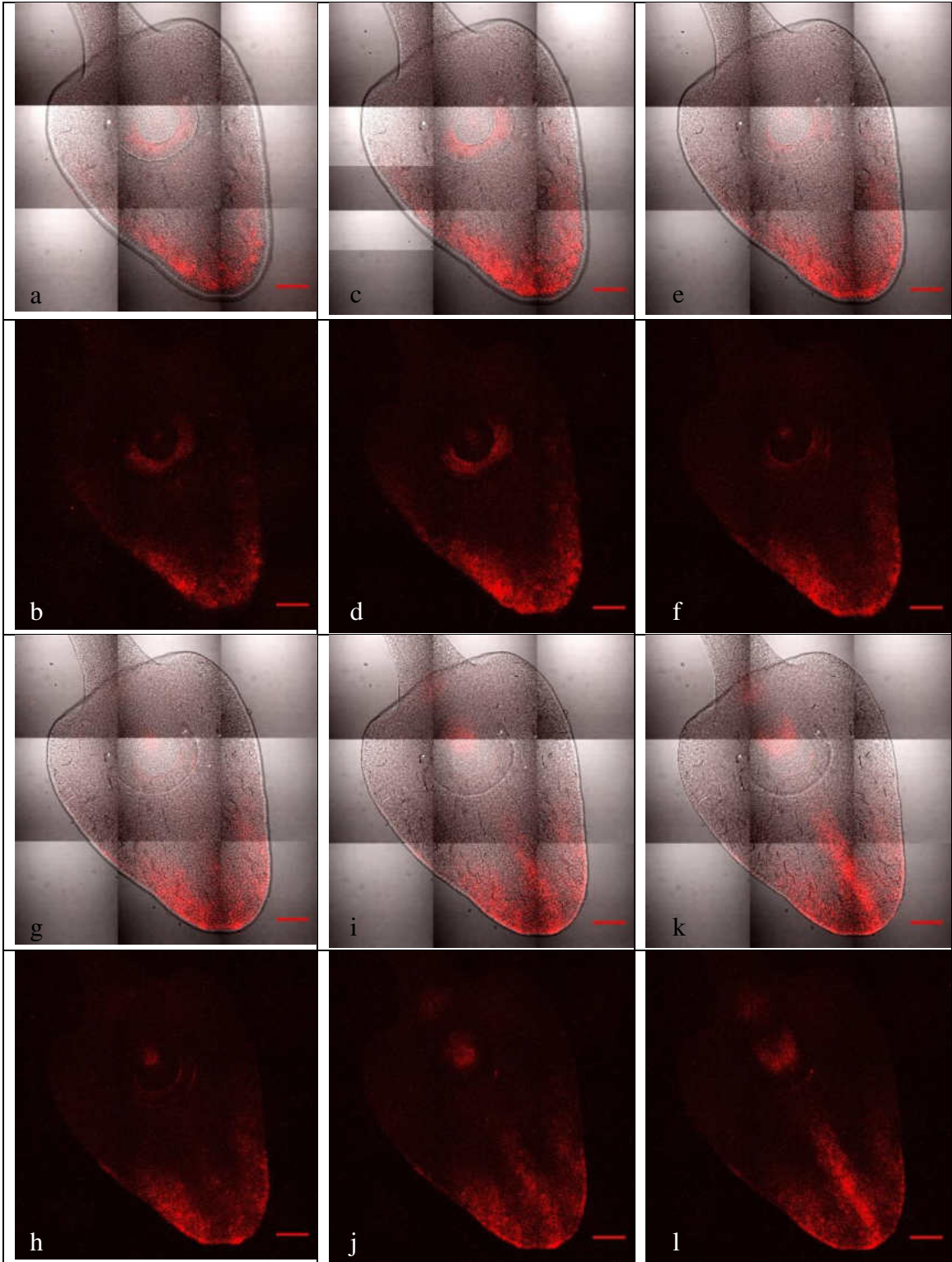
Figure 22. DR5-RFP expression in normal embryo: DR5-e7. Late coleoptilar stage, 3x3
tile, 40x, 1.8µm slice, 6.55µm interval, 72.0µm range. The first 6 of 12 slices. Each slice is paired with the
signal/brightfield image above the signal only of the same image. All images 100µm bar.

138
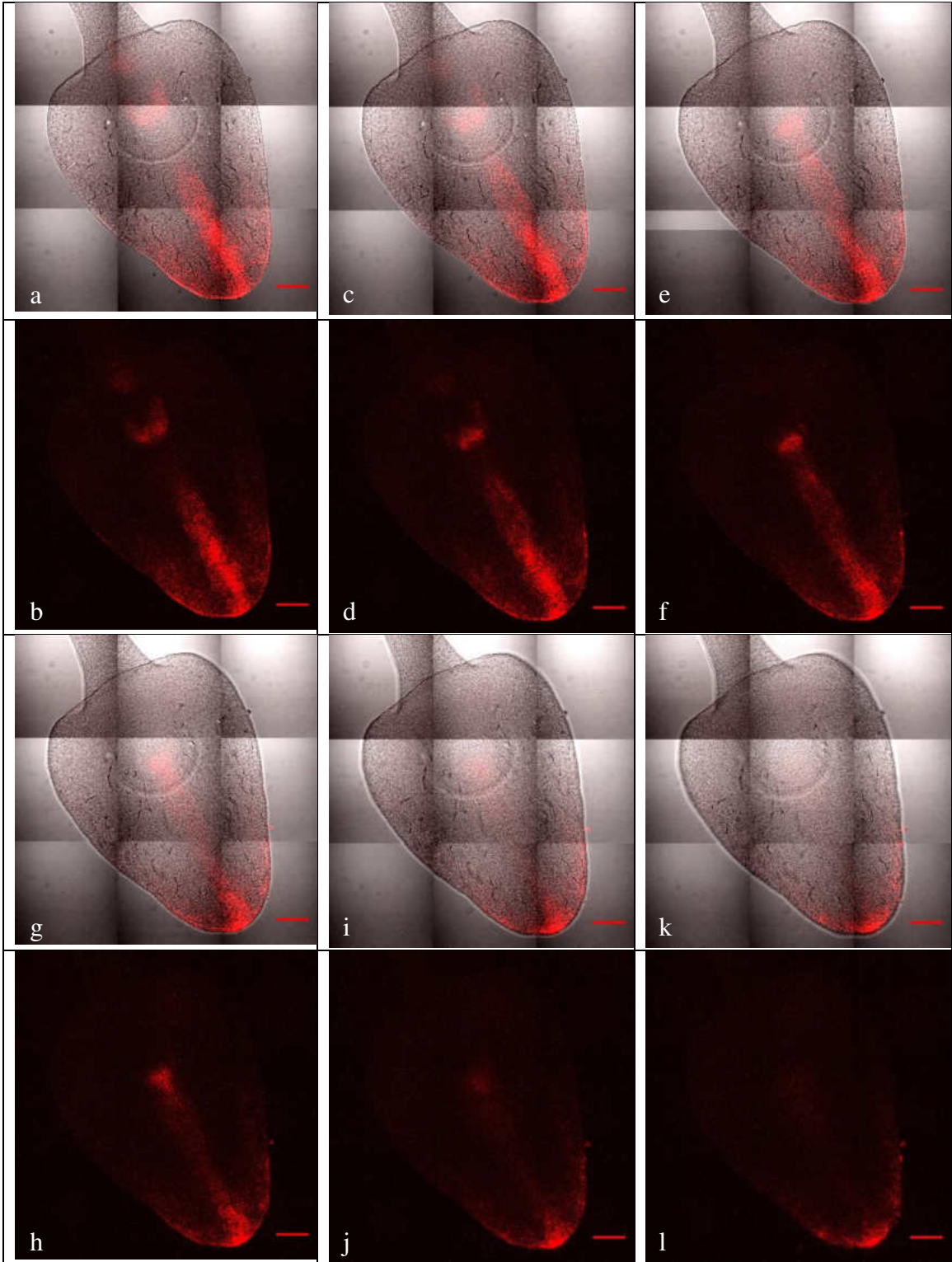
Figure 23. DR5-RFP expression in normal embryo: DR5-e7 continued. Late coleoptilar stage, 3x3 tile, 40x, 1.8µm slice, 6.55µm interval, 72.0µm range. The 7 through 12 of 12 slices. Each slice is paired with the signal/brightfield image above the signal only of the same image. All images 100µm bar.
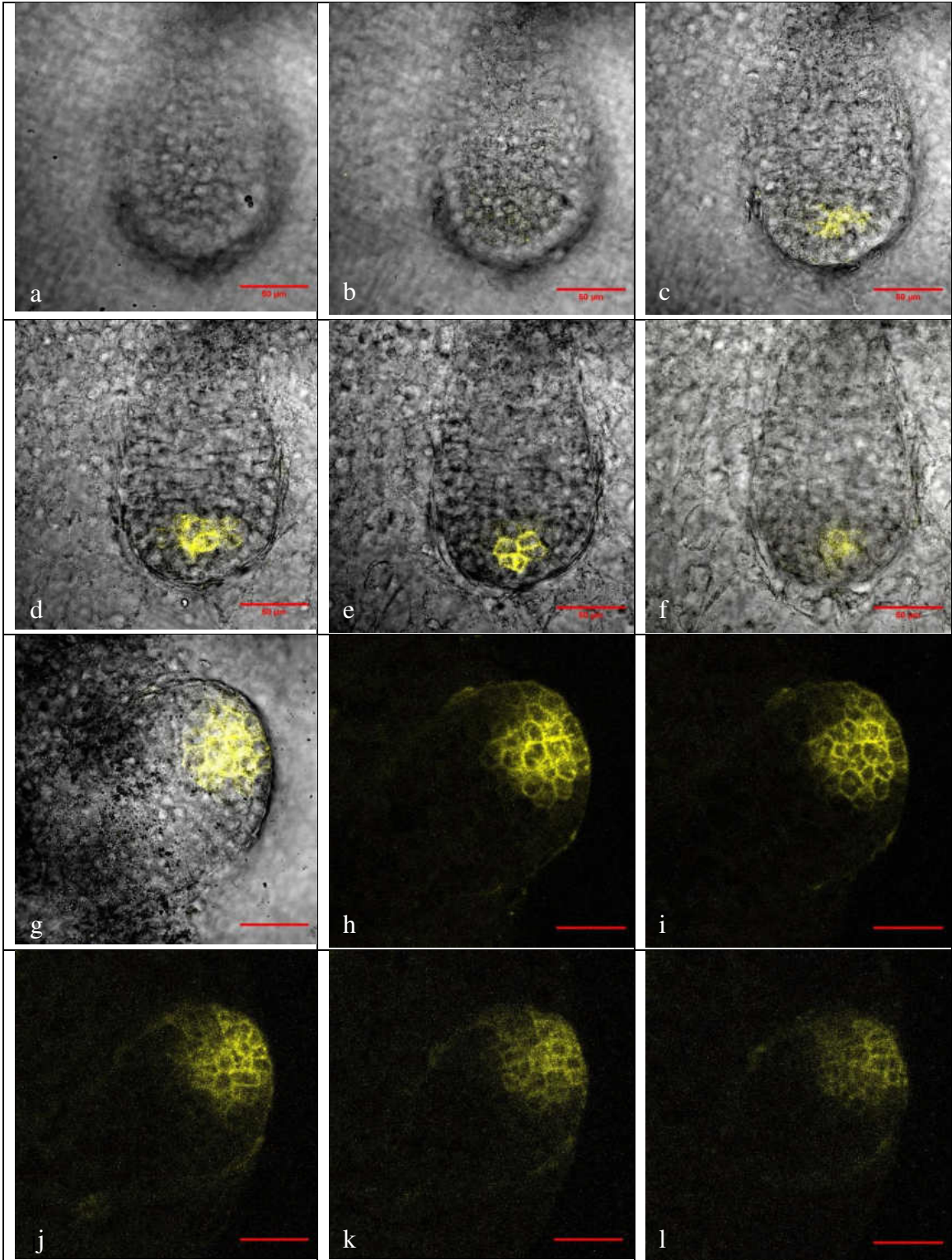
Figure 24. PIN1-YFP expression in normal embryos: PIN1-e1, PIN1-e2. Proembryo stage (a-f) PIN1-e1, 40x, 2.0µm slice, 15.77µm interval, 78.83µm range; (g-l) PIN1-e2, 40x, 0.9µm, 3.62µm interval, 28.94µm range. Image "g" is a brightfield with signal and "h"- "l" are subsequent images with signal only. All Images have 50µm bar.
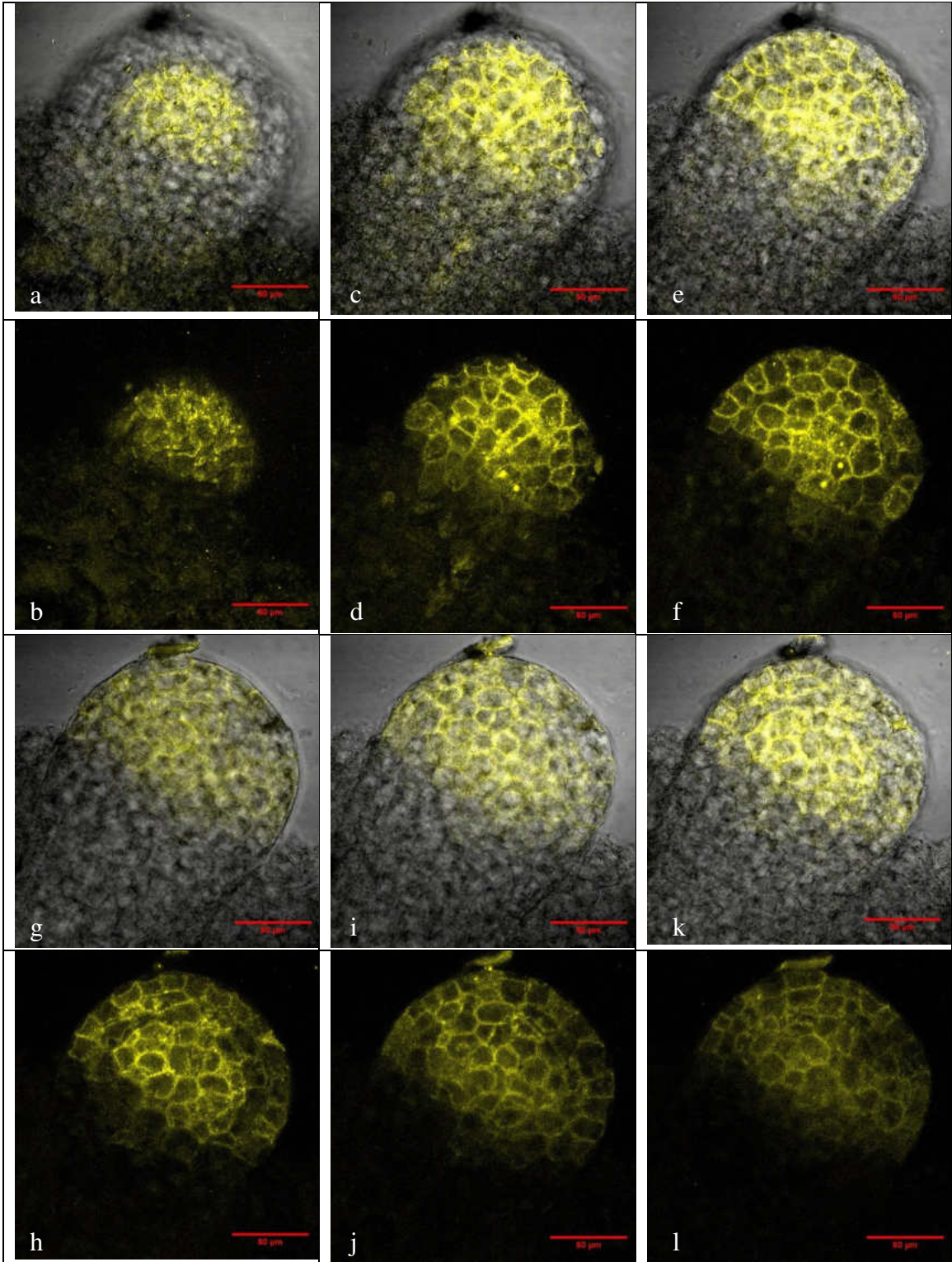
Figure 25. PIN1-YFP expression in normal embryo: PIN1-e3. Early transition stage, each slice is paired with the signal/brightfield image above the signal only of the same image. PIN1-e3, 40x, 1.5µm slice, 11.15µm interval, 55.76µm range. All images have 50µm bars.

141
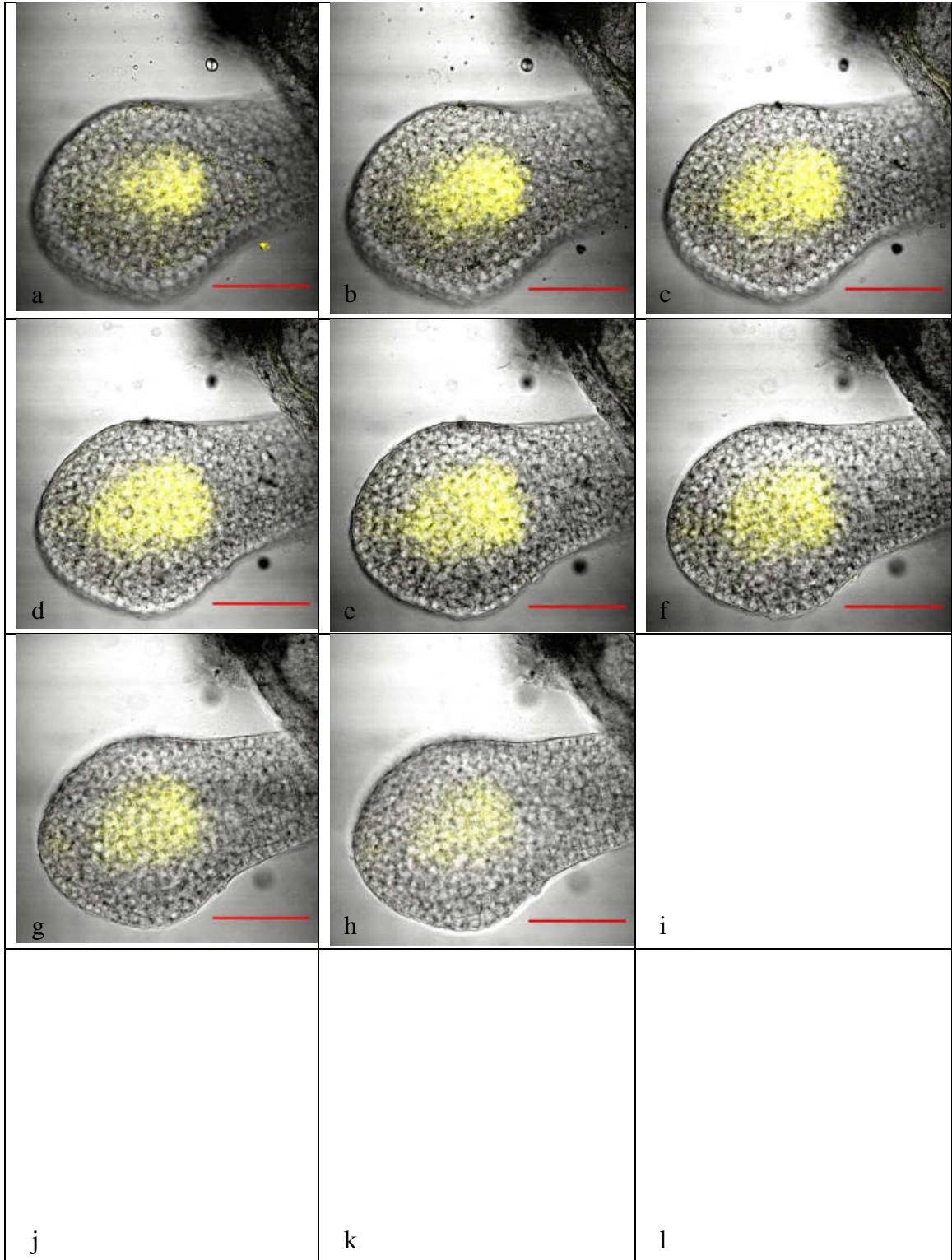
Figure 26. PIN1-YFP expression in normal embryo: PIN1-e4. Transition stage, 40x, 2.0µm slice, 8.41µm interval, 58.56µm range. All Images have 100 µm bar.
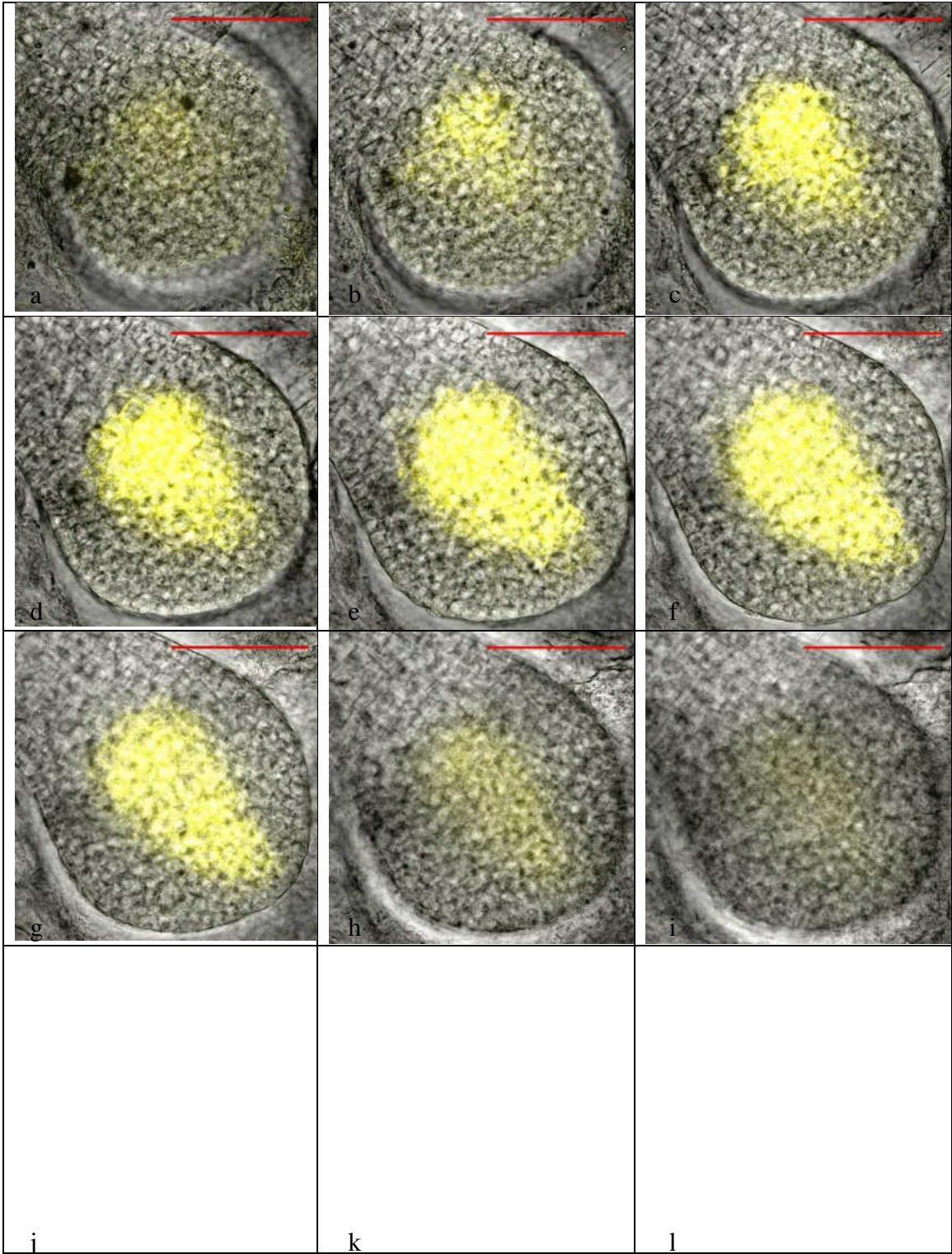
Figure 27. PIN1-YFP expression in normal embryo: PIN1-e5. Transition stage, 40x, 2.0µm slice, 9.81µm interval, 88.29µm range. All Images have 100 µm bar.
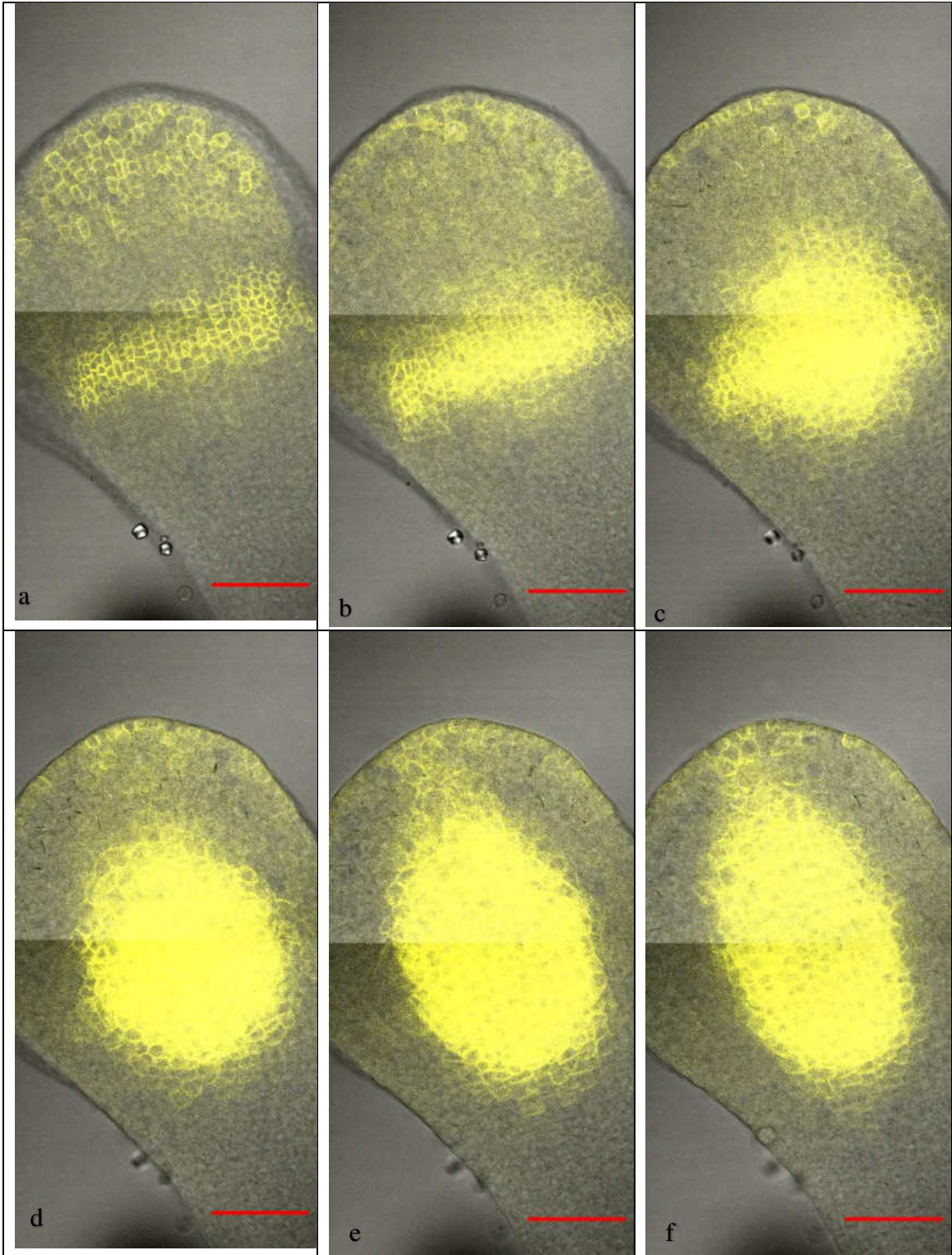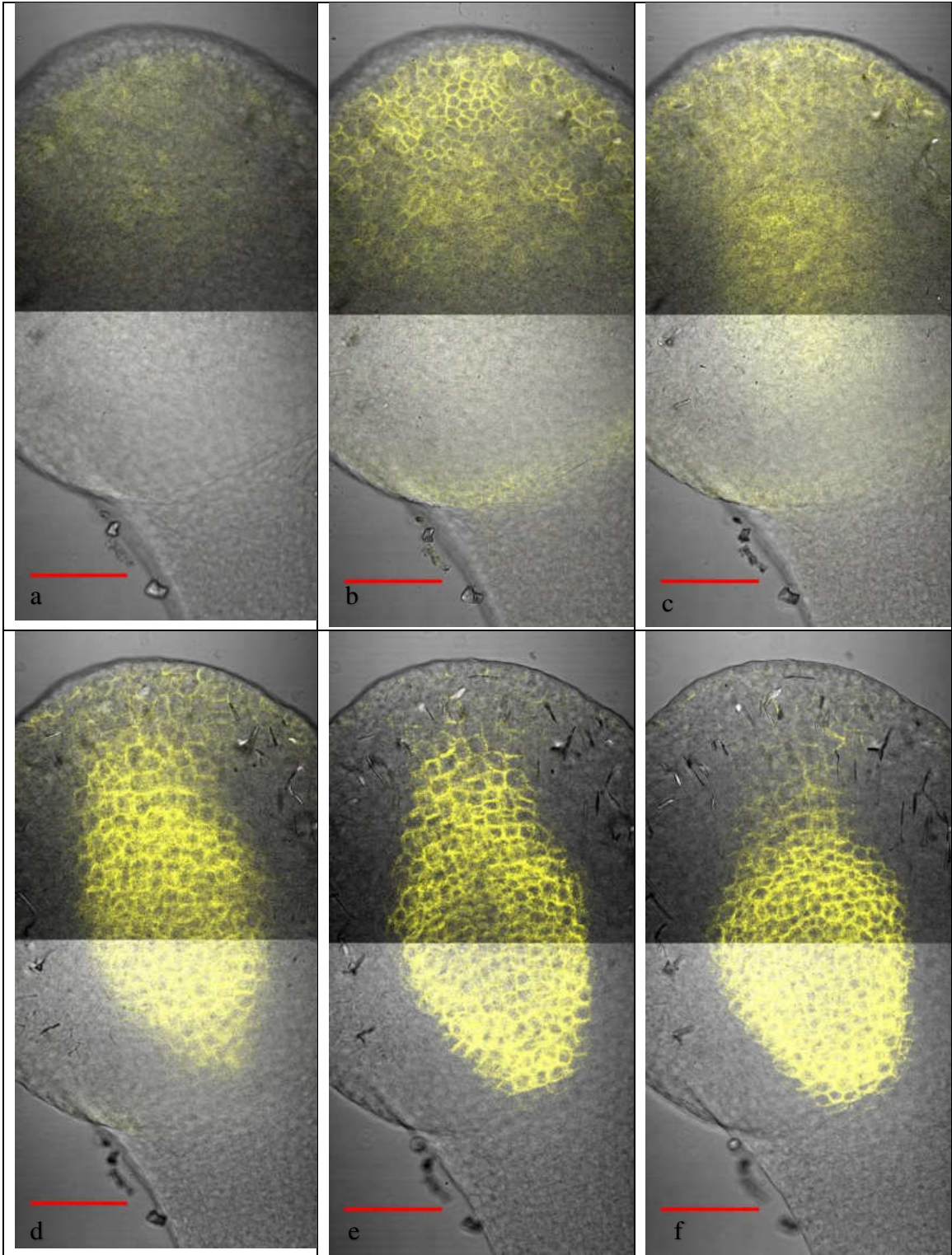
Figure 28. PIN1-YFP expression in normal embryo: PIN1-e6. Transition stage, 40x, 1x2 tile, 0.9µm slice, 10.37µm interval, 72.59µm range. (a-f) Images of the surface (image "a") to 51.85µm (image "f") into the embryo. All Images have 100 µm bar.
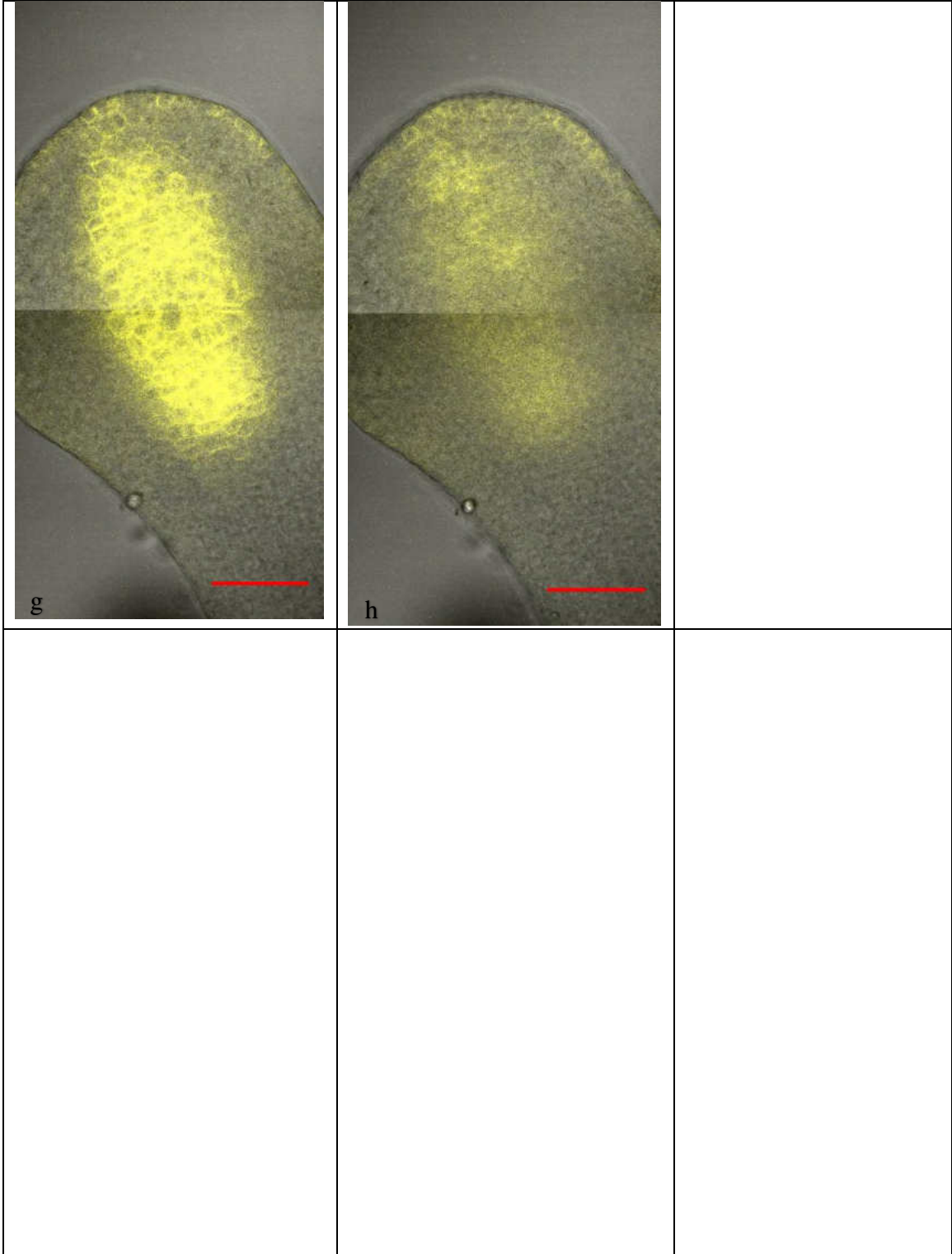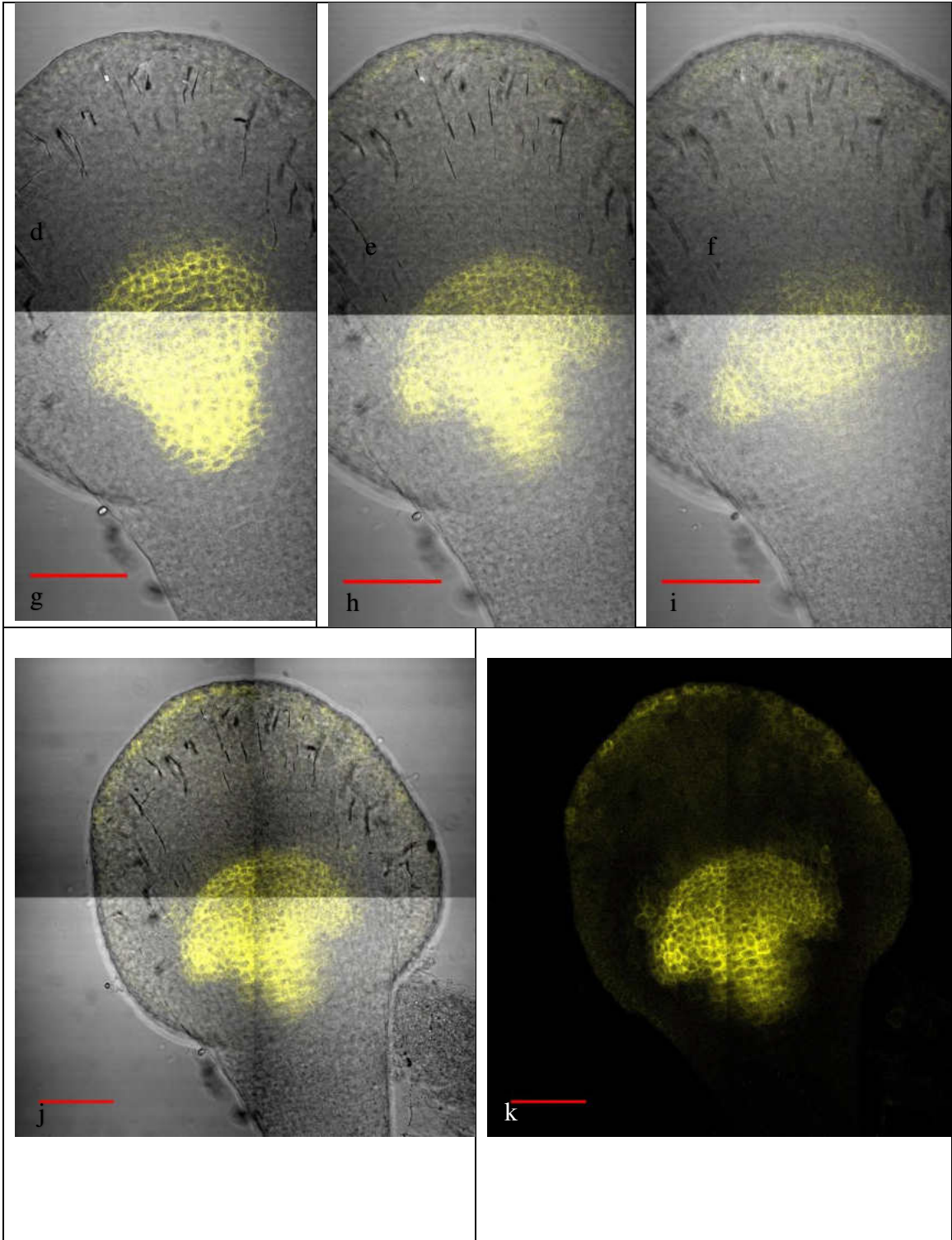
Figure 29. PIN1-YFP expression in normal embryo: PIN1-e6 continued. Transition stage, 40x, 1x2 tile, 0.9µm slice, 10.37µm interval, 72.59µm range; (g) 62.22µm deep slice; (h) 72.59µm deep slice and last slice. All images have 100 µm bar.

Figure 30. PIN1-YFP expression in normal embryo: PIN1-e7. Rear view, late transition stage, 40x, 1x2 tile, 0.9µm slice, 9.07µm interval, 72.59µm range; (a-f) Images of the surface (image "a") to 45.37µm (image "f") into the embryo. All Images have 100 µm bar.

Figure 31. PIN1-YFP expression in normal embryo: PIN1-e7 continued. Late transition stage, 40x; (g-i) Embryo, 1x2 tile, 0.9μm slice, 9.07μm interval, 72.59μm range; (j) 2x2 tile of image "h'; (k) 2x2 tile of image "h', signal only. All images have 100 μm bar.
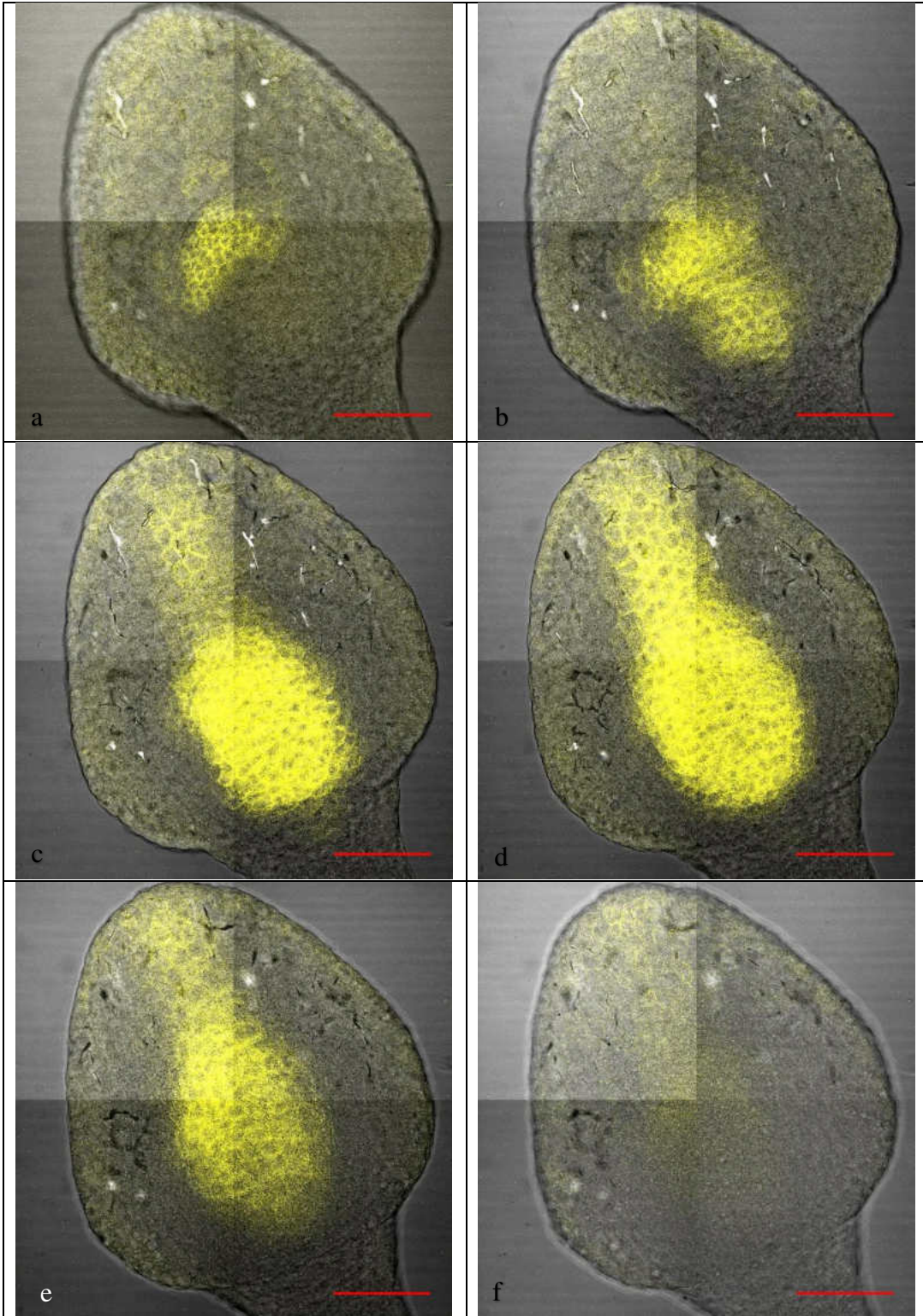
Figure 32. PIN1-YFP expression in normal embryo: PIN1-e8. (a-f) PIN1-e8, transition stage to coleoptilar stage, 40x, 2x2 tile, 0.9µm slice, 9.76µm interval, 48.80µm range; All images have 100 µm bar.
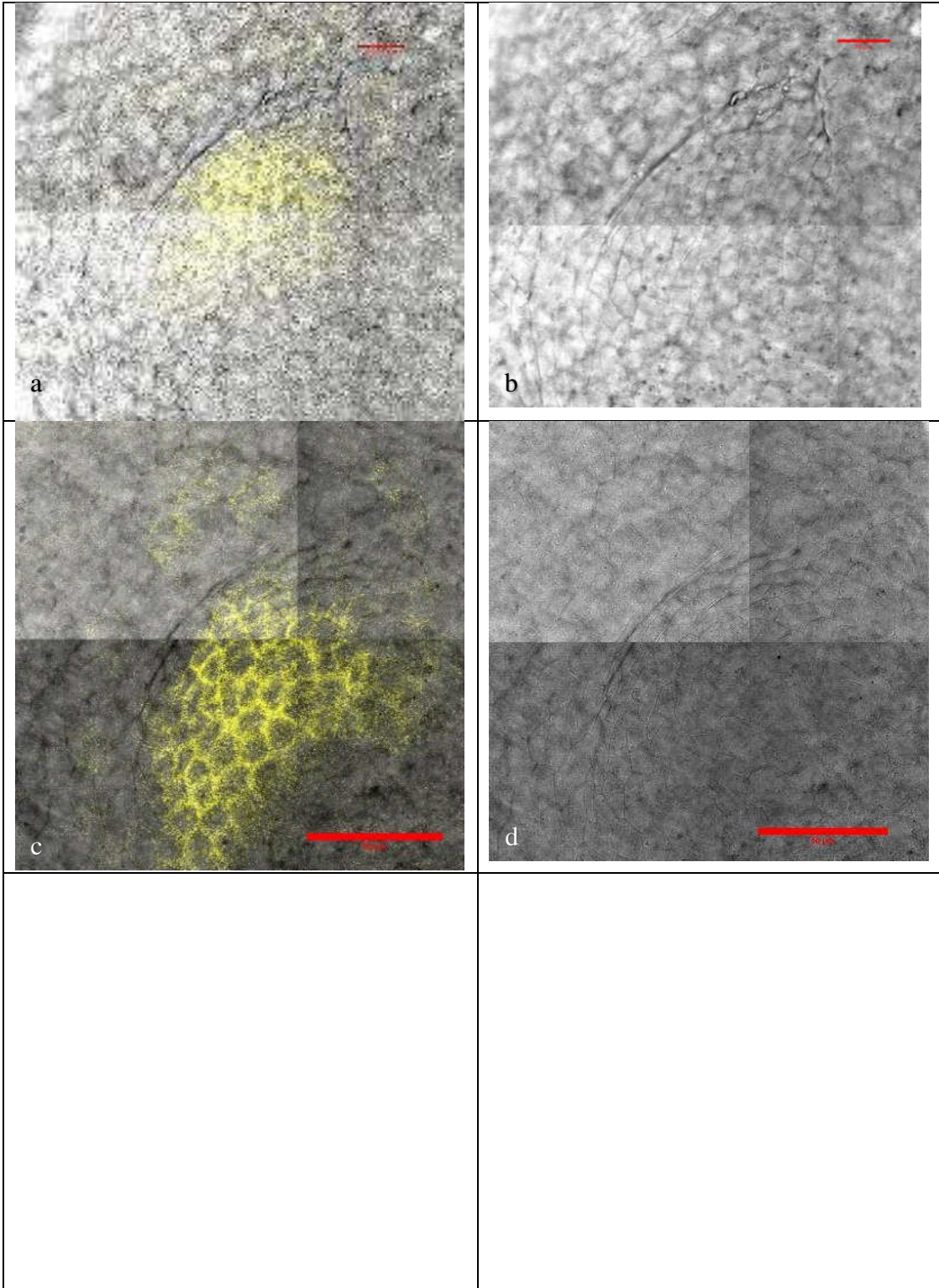
Figure 33. PIN1-YFP expression in normal embryo: PIN1-e8, PIN1-e9. Transition stage to coleoptilar stage, 40x, 2x2 tile, surface of embryo zoomed to formation of coleoptilar ring. Embryo PIN1-e8, (a) brightfield with signal and (b) brightfield only, 20µm bar; Embryo PIN1-e9, (c) brightfield with signal and (d) brightfield only, 100 µm bar.
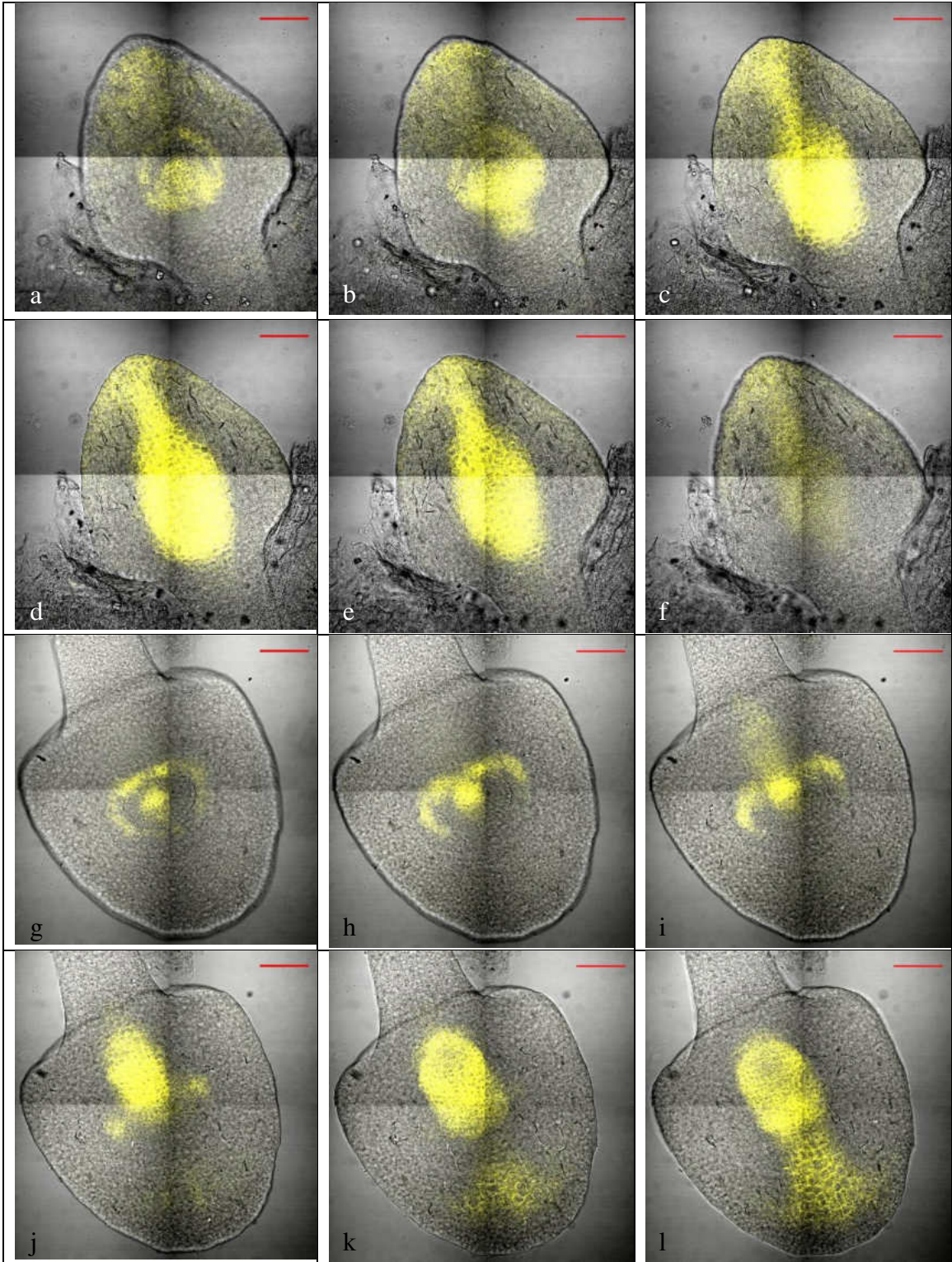
Figure 34. PIN1-YFP expression in normal embryo: PIN1-e10, PIN1-e11. Transition to coleoptilar stage, 40x, 2x2 tile (a-f) PIN1-e10, 0.9µm slice, 12.1µm interval, 60.49 µm range; (g-l) PIN1-e11,1.8µm slice, 9.67µm interval, 48.33µm range. All images have 100 µm bar.
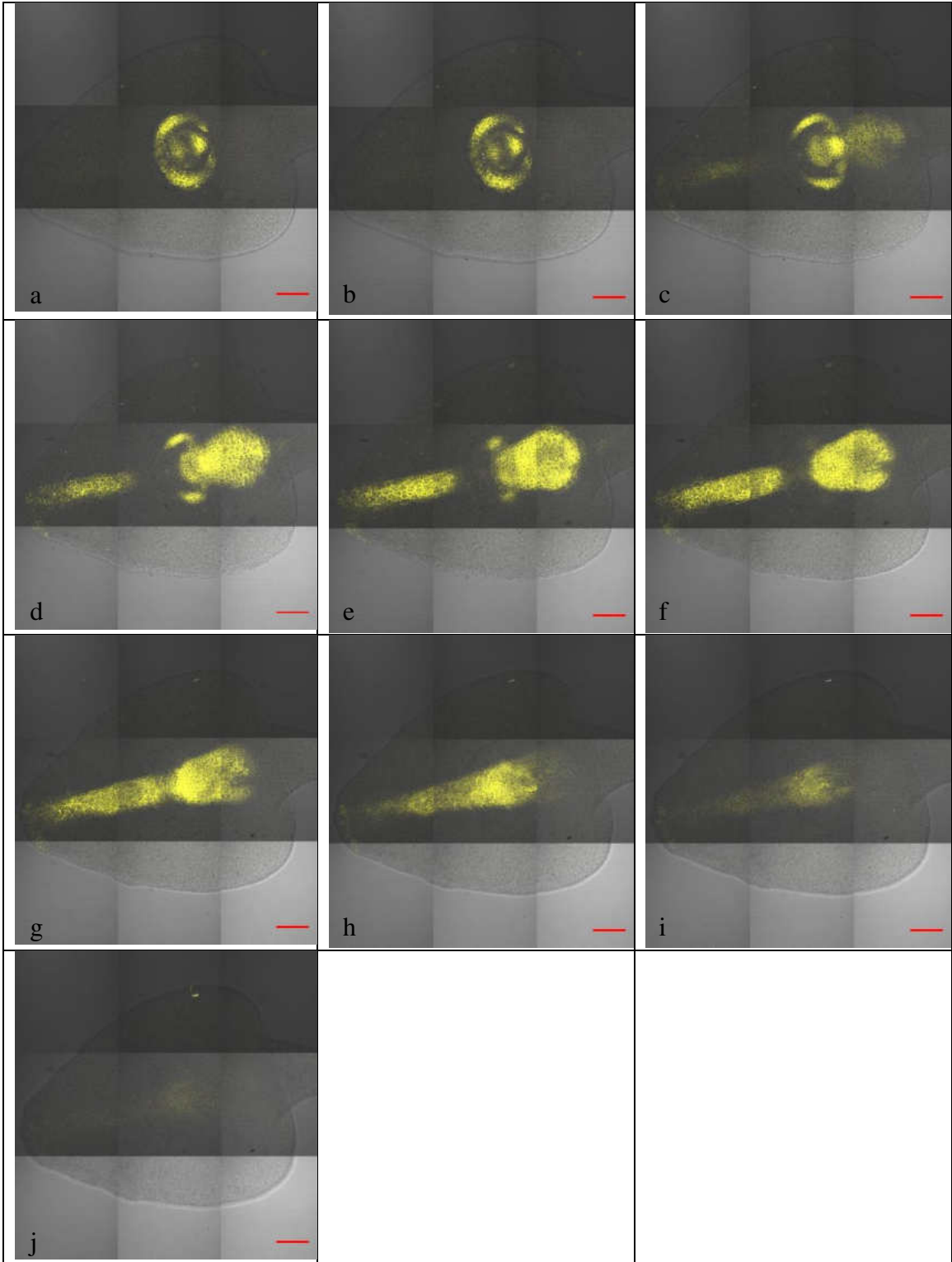
Figure 35. PIN1-YFP expression in normal embryo: PIN1-e12. Coleoptilar stage, 40x, 3x3 tile, 0.9µm slice, 7.11µm interval, 64.00µm range; (a-b) expression at coleoptilar ring and SAM; (c-e) expression in RAM, SAM, scutellar midline and coleoptilar ring; (f-j) expression only in scutellar midline and RAM which weakens in each successive slice. All bars are 100 µm.
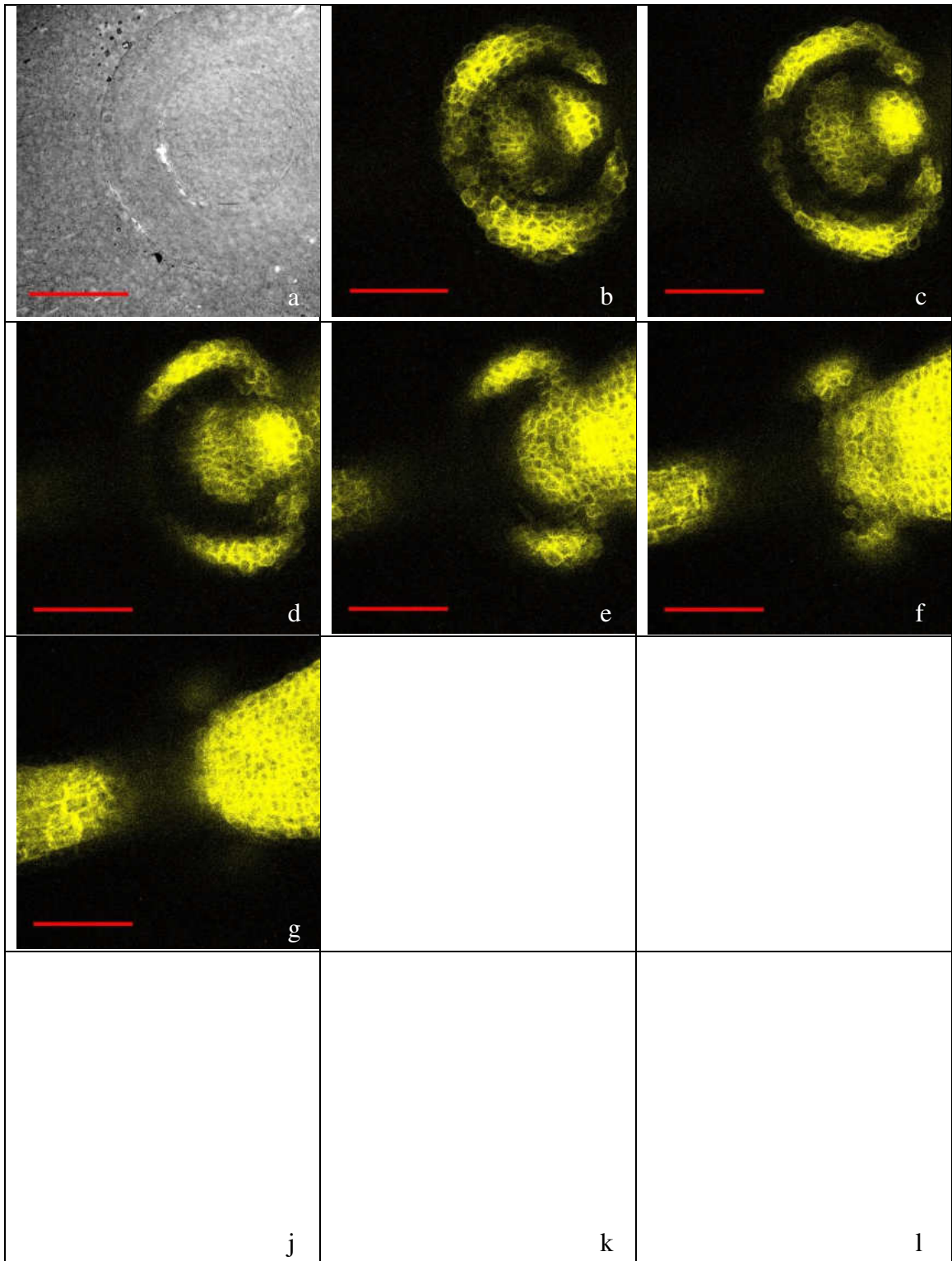
Figure 36. PIN1-YFP expression in normal embryo: PIN1-e12 continued. Coleoptilar stage, 40x, 3x3 tile, 0.9µm slice, 10.04µm interval, 110.45µm range; (a-e) expression seen in SAM and coleoptilar ring which weakens the deeper the slice; (g) expression begins in RAM; (f-k) Ram still show expression with scutellar midline expressing (l) 40x, 0.9µm slice showing expression at the tip scutellum between images h to k. 100um scale bar.
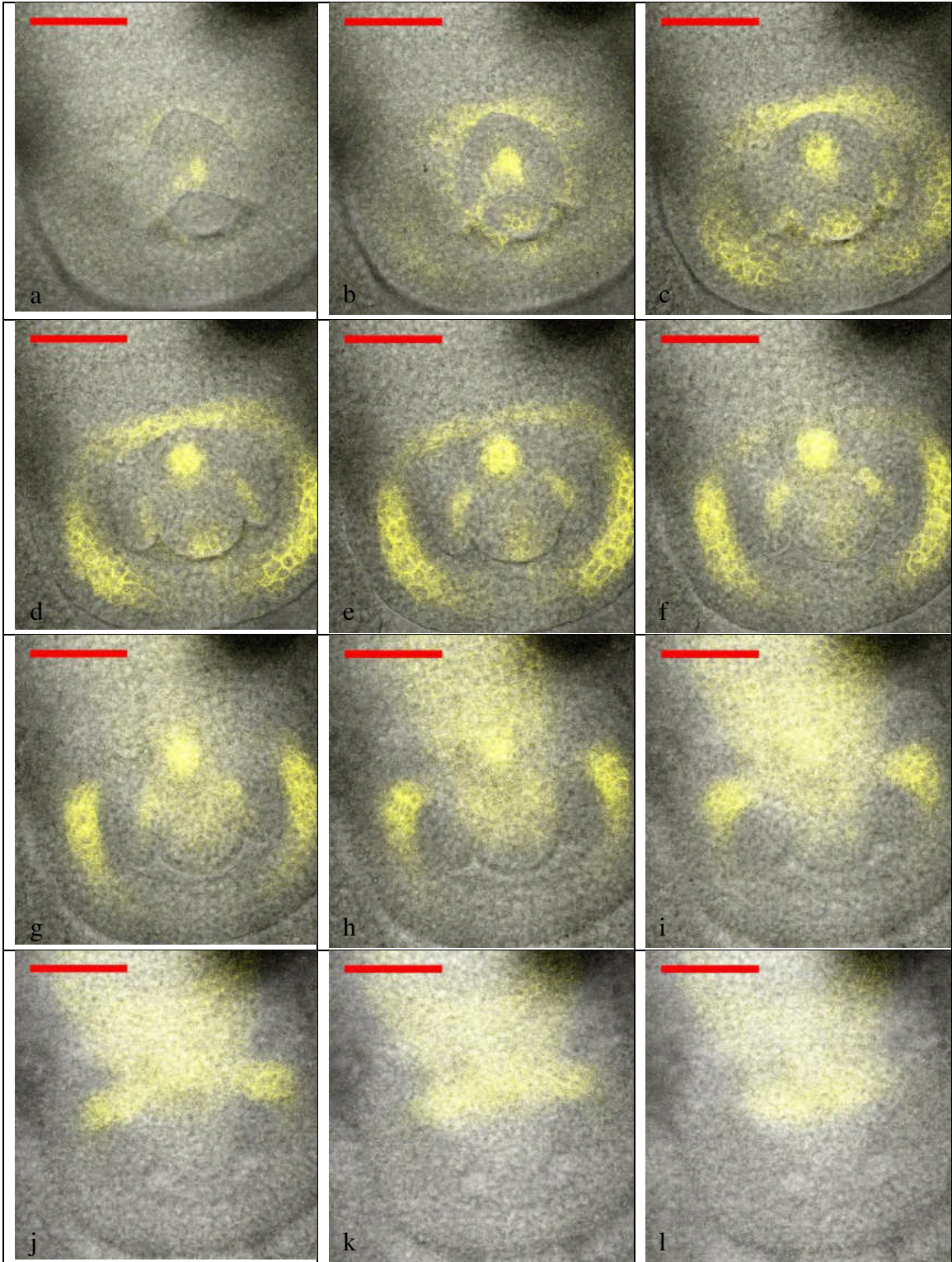
Figure 37. PIN1-YFP expression in normal embryo: PIN1-e13. Stage 1, 40x, 0.9µm slice, 10.04µm interval, 110.45µm range; (a-f) expression seen in first SAM, coleoptilar ring and first leaf primordium; (g-i) expression in RAM begins and not as prominent previous regions; (j-l) expression only in area below SAM and first leaf primordium. All bars 50 µm.
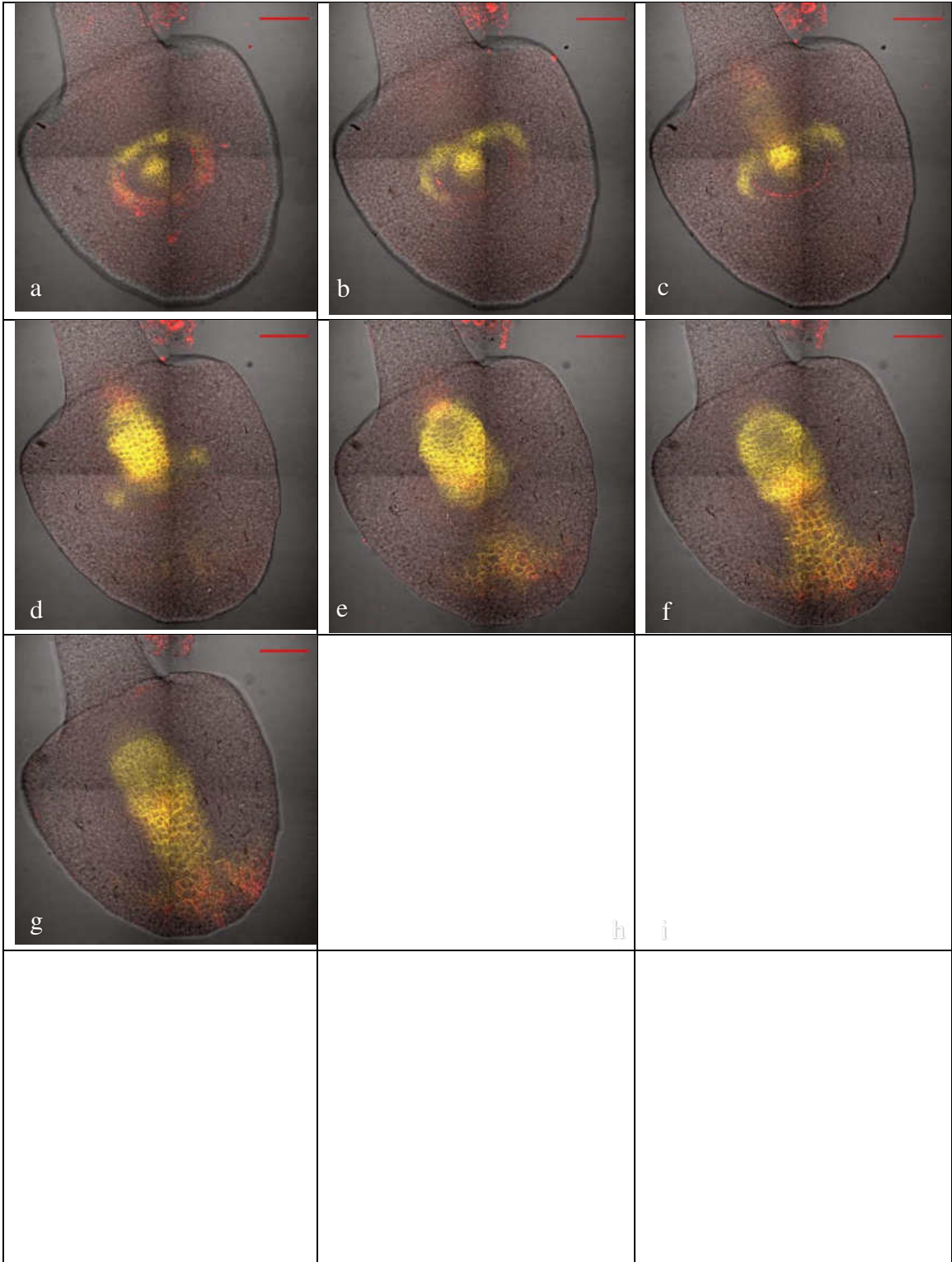
Figure 38. PIN1-YFP and DR5-RF expression in normal embryo. (a-g) coleoptilar stage, 40x, 2x2 tile, 1.8µm slice, 9.67µm interval, 58.0µm range. Individual expression of DR5 and PIN1 in Figures 36 and 50, respectively; (h-i) late coleoptilar stage, 40x, 1.8µm slice (i) at surface; (j) slightly below "i", but unknown depth. All images 100µm bar.

LITERATURE CITED

Abbe, E. C., and O. L. Stein 1954 The growth of the shoot apex in maize: embryogeny. Am. J. Bot. 41: 285-293.

Altun C. 2007 Maize Mre11 DNA repair and recombination complex. PhD thesis. Purdue University, West Lafayette, IN, USA. http://docs.lib.purdue.edu/dissertations/AAI3343976/.

Becraft P.W., K. Li, N. Dey, and Y. Asuncion-Crabb 2002 The maize *dek1* gene functions in embryonic pattern formation and cell fate specification. Development 129: 5127-5225.

Bhuina, T. and J. K. Roy 2014 Rab proteins: The key regulators of intracellular vesicle transport. Experimental Cell Research 328: 1-19.

Borde, V. 2007 The multiple roles of the Mre11 complex for meiotic recombination. Chromosome Research 15: 551–563.

Brunelle, D. C., J. K. Clark, and W. F. Sheridan 2017 Genetic Screening for EMS-Induced Maize Embryo-Specific Mutants Altered in Embryo Morphogenesis. Genes Genomes Genetics 7: 3559-3570.

Busch, W., A. Miotk, F.D. Ariel, *et al.* 2010 Transcriptional control of a plant stem cell niche. Dev. Cell 18: 841-853.

Carraro, N., C. Forestan, S. Canova, *et al.* 2006 ZmPIN1a and ZmPIN1b Encode Two Novel Putative Candidates for Polar Auxin Transport and Plant Architecture Determination of Maize. Plant Physiology 142: 254–264.

Chen, J., A. Lausser, and T. Dresselhaus 2014 Hormonal responses during early embryogenesis in maize. Biochem. Soc. Trans. 42: 325-331.

Chen, X., F. Feng, W. Qi, *et al.* 2017 Dek35 Encodes a PPR Protein that Affects cis-Splicing of Mitochondrial nad4 Intron 1 and Seed Development in Maize. Molecular Plant 10: 427–441.

Chettoor, A. M., G. Yi, E. Gomez, *et al.* 2015 A putative plant organelle RNA recognition protein gene is essential for maize kernel development. JIPB 57(3): 236-246.

Chettoor, A. M. and M. M. S. Evans 2015 Correlation between a loss of auxin signaling and a loss of proliferation n maize antipodal cells. Front. in Plant Sci. V6, Article187:1-14.

Chuang, C., M. P. Running, R. W. Williams, *et al.* 1999 The PERIANTHIA gene encodes a bZIP protein involved in the determination of floral organ number in Arabidopsis thaliana. Genes and Development 13: 334–344.

Clark, J. K. 1996 Maize embryogenesis mutants, pp. 89–112 in Embryogenesis: The Generation of a Plant, edited by Wang, T., and A. C. Cuming. Bios Scientific Publishers, Oxford.

Clark, J. K., and W. F. Sheridan 1986 Development profiles of the maize embryo-lethal mutants *dek* 22 and dek23. J. of Hered. 77(2): 83-92.

Clark, J. K., and W. F. Sheridan 1988 characterization of the two maize embryo-lethal defective kernel mutants *rgh*-1210* and *fl*-1253B*: effects on embryo and gametophyte development. Genetics 120: 279-290.

Clark, J. K., and W. F. Sheridan 1991 Isolation and Characterization of 51 *embryospecific* mutations in maize. The Plant Cell 3: 935-951.

Consonni, G., C. Aspesi, A. Barbante, *et al.* 2003 Analysis of four maize mutants arrested in early embryogenesis reveals an irregular pattern of cell division. Sex Plant Reproduction 15: 281–290.

Demerec, M. 1923 Heritable characters of maize. XV-germless seeds. J. Hered. 14: 297-300.

Doebley, J. F., A. Stec, J. Wendel, and M. Edwards 1990. Genetic and morphological analysis of a maize-teosinte F2 population: implications for the origin of maize. Proc. Natl. Acad. Sci. USA 87: 9888-9892.

Elster, R., P. Bommert, W. F. Sheridan, *et al.* 2000 Analysis of four embryo-specific mutants in Zea mays reveals that incomplete radial organization of the proembryo interferes with subsequent development. Dev Genes Evol 210: 300–310.

Flint-Garcia, S.A. 2017 Kernel Evolution: From Teosinte to Maize, pp1-15 in *Maize Kernel Development*, edited by Brian A. Larkins. CPI Group (UK) Ltd, Croydon, UK.

Forestan, C., S. Meda, and S. Varotto 2010 ZmPIN1-Mediated Auxin Transport Is Related to Cellular Differentiation during Maize Embryogenesis and Endosperm Development. Plant Physiology 152: 1373–1390.

Gallavotti, A., Y. Yang, R. J. Schmidt, *et al.* 2008 The Relationship between Auxin Transport and Maize Branching. Plant Physiology 147: 1913–1923.

Giuliani C., G. Consonni, G. Gavazzi, M. Colombo, S. Dolfini 2002 Programmed cell death during embryogenesis in maize. Ann Bot 90:1–6.

Giulini, A., J. Wang and D. Jackson 2004 Control of phyllotaxy by the cytokinin-inducible response regulator homologue ABPHYL1. Nature 430: 1031-1034.

Goday, A., A. B. Jensen, F. A. Culiáííez-Macia, *et al.* 1994 The Maize Abscisic Acid-Responsive Protein Rabl7 1s Located in the Nucleus and lnteracts with Nuclear Localization Signals. The Plant Cell 6: 351-360.

Gutierrez-Marcos, J. F., M. D. Pra, A. Giulini, *et al.* 2007 Empty pericarp4 Encodes a Mitochondrion-Targeted Pentatricopeptide Repeat Protein Necessary for Seed Development and Plant Growth in Maize. The Plant Cell 19: 196–210.

Hariharan, T., P. J. Johnson, and R. A. Cattolico 1998 Purification and Characterization of Phosphoribulokinase from the Marine Chromophytic Alga Heterosigma carterae. Plant Physiol. 117: 321–329.

Hattori, M., M. Hasebe, and M. Sugita 2004 Identification and characterization of cDNAs encoding pentatricopeptide repeat proteins in the basal land plant, the moss Physcomitrella patens. Gene 343: 305–311.

Heckel T., K. Werner, W. F. Sheridan, *et al.* 1999 Novel phenotypes and developmental arrest in early embryo speci®c mutants of maize. Planta 210: 1-8.

Hertel, T. W., A. A. Golub, A. D. Jones, *et al.* 2010 Gas Emissions: Estimating Market-mediated Responses. BioScience 60: 223-231.

Jackson, D., and S. Hake 1999 Control of phyllotaxy in maize by the abphyl1 gene. Development 126: 315-323.

Jones, D. G. 1920 Heritable characters of maize. IV. A lethal factor – defective seeds. J. Hered. 11: 161-167.

Juarez, M. T., R. W. Twigg, and M. C. P. Timmermans 2004 Specification of adaxial cell fate during maize leaf development. Development 131: 4533-4544.

Kiesselbach, T. A. 1949 *The Structure and Reproduction of Corn.* University of Nebraska Press, Lincoln, Nebraska.

Kir, G., H. Ye, H. Nelissen, *et al.* 2015 RNA Interference Knockdown of BRASSINOSTEROID INSENSITIVE1 in Maize Reveals Novel Functions for Brassinosteroid Signaling in Controlling Plant Architecture. Plant Physiology 169: 826–839.

Kotliński, M., K. Rutowicz, Ł. Kniżewski, *et al.,* 2016 Histone H1 Variants in Arabidopsis Are Subject to Numerous Post-Translational Modifications, Both Conserved and Previously Unknown in Histones, Suggesting Complex Functions of H1 in Plants. PLoS ONE 11(1): e0147908. doi:10.1371/journal. pone.0147908.

Li, C., Y. Shen, R. Meeley, *et al.* 2015 Embryo defective 14 encodes a plastid-targeted cGTPase essential for embryogenesis in maize. The Plant Journal 84: 785–799.

Li1, X., Y. Zhang, M. Hou, *et al.* 2014 Small kernel 1 encodes a pentatricopeptide repeat protein required for mitochondrial nad7 transcript editing and seed development in maize (Zea mays) and rice (Oryza sativa). The Plant Journal 79: 797–809.

Lid, S.E., D. Gruis, R. Jung, J. A. Lorentzen, *et al.* 2002 The defective kernel 1(*dek1*) gene required for aleurone cell development in the endosperm of maize grains encodes a membrane protein of the calpain gene superfamily. PNAS 99: 5460-5465.

Liu, Y., Z. Xiu, R. Meeley, *et al.* 2013 Empty Pericarp5 Encodes a Pentatricopeptide Repeat Protein That Is Required for Mitochondrial RNA Editing and Seed Development in Maize. The Plant Cell 25: 868–883.

Liu, Z. B., T. Ulmasov, X. Shi, G. Hagen, *et al.* 1994 The soybean GH3 promoter contains multiple auxin-inducible elements. Plant Cell 6: 645-657.

Lurin, C., C. Andres, S. Aubourg, *et al.* 2004 Genome-wide analysis of Arabidopsis pentatricopeptide repeat proteins reveals their essential role in organelle biogenesis. Plant Cell 16: 2089–2103.

Lutcke, A., S. Jansson, R. G. Parton, *et al.* 1993 Rab17, a novel small GTPase, is specific for epithelial cells and is induced during cell polarization. J. of Cell Biol. 121(3): 553-564.

Magnard, J., T. Heckel, A. Massonneau, *et al.* 2004 Morphogenesis of Maize Embryos Requires ZmPRPL35-1 Encoding a Plastid Ribosomal Protein. Plant Physiology 134: 649–663.

Manglesdorf, P. C. 1923 The inheritance of defective seeds in maize. J. Hered. 14: 119-125.

Manglesdorf, P. C. 1926 The genetics and morphology of some endosperm characters in maize. Conn. Agric. Exp. Stn. Bull. 179: 509-614.

Marri, L., F. Sparla, P. Pupillo, *et al.* 2005 Co-ordinated gene expression of photosynthetic glyceraldehyde-3-phosphate dehydrogenase, phosphoribulokinase, and CP12 in Arabidopsis thaliana. Journal of Experimental Botany 409: 73–80.

Mayer, K. F. X., H. Schoof, A. Haecker, *et al.* 1998 Role of WUSCHEL in Regulating Stem Cell Fate in the Arabidopsis Shoot Meristem. Cell 95: 805–815.

Mohanty, A., A. Luo, S. DeBlasio, *et al.* 2009 Advancing Cell Biology and Functional Genomics in Maize Using Fluorescent Protein-Tagged Lines. Plant Physiology 149: 601–605.

Muller B., and J. Sheen 2008 Cytokinin and auxin interaction in root stem-cell specification during early embryogenesis. Nature 453: 1094-1098.

Muller J., C. González-Martínez, and A. Chiralt 2017 Combination of Poly(lactic) Acid and Starch for Biodegradable Food Packaging. Materials 10(952): 1-22.

Nardmann J., and W. Werr 2006 The Shoot Stem Cell Niche in Angiosperms: Expression Patterns of WUS Orthologues in Rice and Maize Imply Major Modifications in the Course of Mono- and Dicot Evolution. Mol. Biol. Evol. 23:2492–2504.

Neuffer, M. G. and W. F. Sheridan 1980 Defective kernel mutants of maize I. genetic and lethality study. Genetics 95: 929-944.

Neuffer, M. G. 1994 Mutagenesis, pp. 212–218 in The Maize Handbook, edited by Freeling, M., and V. Walbot. Springer-Verlag, New York.

Qi, W., Y. Yang, X. Feng, *et al.* 2017 Mitochondrial Function and Maize Kernel Development Requires Dek2, a Pentatricopeptide Repeat Protein Involved in nad1 mRNA Splicing. Genetics 205: 239–249.

Ramirez-Cabral N. Y. Z., L. Kumar, and F. Shabani 2017 Global alterations in areas of suitability for maize production from climate change and using a mechanistic species distribution model (CLIMEX). Scientific Report 7(5910): 1-13.

Randolph, L. F. 1936 Developmental morphology of the caryopsis in maize. J. of Agric. Research 53: 881-916.

Razafimahatratra, P., N. Chaubet, G. Philipps, *et al.* 1991 Nucleotide sequence and expression of a maize Hi histone cDNA. Nucleic Acids Research 19: 1491-1496.

Robertson, D. S. 1978 Characterization of a mutator system in maize. Mutat. Res. 51**:** 21-28.

Šamanić, I., J. Simunić, K. Riha, *et al.* 2013 Evidence for Distinct Functions of MRE11 in Arabidopsis Meiosis. PLoS ONE 8: e78760. doi: 10.1371/journal.pone.0078760.

Sawers, R.J.H., P. Liu, K. Anufrikova, *et al.* 2007 A multi-treatment experimental system to examine photosynthetic differentiation in the maize leaf. BMC Genomics 8: 1-13.

Scanlon, Micheal J., P. S. Stinard, M.B. James *et al.* 1994 Genetic Analysis of 63 mutations affecting maize kernel development isolated from *Mutator* stock. Genetics 136: 2812-294.

Schnable P. S., D. Ware, R. S. Fulton, *et al.* 2009 The B73 Maize Genome: Complexity, Diversity, and Dynamics. Science 326(5956): 1112-1115.

Sedbrook J. C., K. L. Carroll, K. F. Hung, P. H. Masson, *et al.* 2002 The Arabidopsis SKU5 gene encodes an extracellular glycosyl phosphatidylinositol-anchored glycoprotein involved in directional root growth. Plant Cell 14: 1635–1648.

Shen, Y., C. Li1, D. R. McCarty, *et al.* 2013 Embryo defective12 encodes the plastid initiation factor 3 and is essential for embryogenesis in maize. The Plant Journal 74: 792–804.

Sheridan, W. F. and M. G. Neuffer 1980 Defective kernel mutants of maize II. Morphological and embryo culture studies. Genetics 95: 945-960.

Sheridan, W. F., and J. K. Clark 2017 Embryo Development, pp81-94 in *Maize Kernel Development*, edited by Brian A. Larkins. CPI Group (UK) Ltd, Croydon, UK.

Sheridan, W. F., and Y. R. Thorstenson 1986 Developmental Profiles of Three Embryo-lethal maize mutants lacking leaf primordia: *ptd*-1130, cp*-1418,* and *bno*-747B*. Developmental Genetics 7:35-49.

Sheridan, W.F, and J. K. Clark 1987 Maize embryogeny: a promising experimental system. Trends Genet. 3: 3-6.

Sheridan, W.F, and J. K. Clark 1993 Mutational analysis of morphogenesis of the maize embryo. The Plant Journal 3(2): 347-358.

Sidhu, G. K., T. Warzecha, and W. P. Pawlowski 2017 Evolution of meiotic recombination genes in maize and teosinte. BMC Genomics 18: 1-17.

Small, I.D., and N. Peeters 2000 The PPR motif—A TPR-related motif prevalent in plant organellar proteins. Trends Biochem. Sci. 25: 46–47.

Sosso, D., M. Canut, G. Gendrot, *et al.* 2012 PPR8522 encodes a chloroplast-targeted pentatricopeptide repeat protein necessary for maize embryogenesis and vegetative development. Journal of Experimental Botany 63: 695–709.

Springer, N.M., S.N. Anderson, C.M. Andorf, *et al.* 2018 The maize W22 genome provides a foundation for functional genomics and transposon biology. Nature Genetics 50:1282-1288.

Sun, F., X. Wang, G. Bonnard, *et al.* 2015 Empty pericarp7 encodes a mitochondrial E–subgroup pentatricopeptide repeat protein that is required for $ccmF_N$ editing, mitochondrial function and seed development in maize. The Plant Journal 84: 283–295.

Thompson, C.J., N.R. Movva, R. Tizard, *et al.* 1987 Characterization of the herbicid-resistance gene *bar* from *Streptomyces hybroscopicus*. The EMBO Journal 6(9): 2519-2523.

Tian, G., A. Mohanty, S. N. Chary, *et al.* 2004 High-Throughput Fluorescent Tagging of Full-Length Arabidopsis Gene Products in Planta. Plant Physiology 135: 25–38.

Tigchelaara M., D. S. Battistia, R. L. Naylor, *et al.* 2018 Future warming increases probability of globally synchronized maize production shocks. PNAS 115(26): 6644-6649.

Ulmasov, T., J. Murfett, G. Hagen, *et al.* 1997 Aux/IAA Proteins Repress Expression of Reporter Genes Containing Natural and Highly Active Synthetic Auxin Response Elements. The Plant Cell 9: 1963-1971.

Ulmasov, T., Z. B. Liu, G. Hagen, *et al.* 1995 Composite structure of auxin response elements. Plant Cell 7: 1611-1623.

Vernoud, V., M. Hajduch, A. S. Khaled, N. Depege, P. M. Rogowsky 2005 Maize Embryogenesis. Maydica 50: 469-483.

Wang, Z., T. Nakano, J. Gendron, *et al.* 2002 Nuclear-Localized BZR1 Mediates Brassinosteroid-Induced Growth and Feedback Suppression of Brassinosteroid Biosynthesis. Developmental Cell 2: 505–513.

Waterworth, W. M., C. Altun, S. J. Armstrong, *et al.* 2007 NBS1 is involved in DNA repair and plays a synergistic role with ATM in mediating meiotic homologous recombination in plants. The Plant Journal 52: 41–52.

Xiu, Z., F. Sun, Y. Shen, *et al.* 2016 EMPTY PERICARP16 is required for mitochondrial nad2 intron 4 cis-splicing, complex I assembly and seed development in maize. The Plant Journal 85: 507–519.

Yang, Y., S. Ding, H. Wang, *et al.* 2017 The pentatricopeptide repeat protein EMP9 is required for mitochondrial ccmB and rps4 transcript editing, mitochondrial complex biogenesis and seed development in maize. New Phytologist 214: 782–795.

Yin, Y., Z. Wang, S. Mora-garcia *et al.* 2002 BES1 accumulates in the nucleus in response to brassinosteroids to regulate gene expression oand promote stem elongation. Cell 109: 181-191.

Zhang, Y., M. Hou, and B. Tan 2013 The Requirement of WHIRLY1 for Embryogenesis Is Dependent on Genetic Background in Maize. PLoS ONE 8(6): e67369. doi:10.1371/journal.pone.0067369.